Analyzing the function of a peroxisomal NAD carrier in Arabidopsis and yeast

Inaugural-Dissertation

zur Erlangung des Doktorgrades
der Mathematisch-Naturwissenschaftlichen Fakultät
der Heinrich-Heine-Universität Düsseldorf

vorgelegt von

Martin Gard Schroers

aus Viersen

Willich, März 2015

aus dem Institut für Biochemie der Pflanzen
der Heinrich-Heine-Universität Düsseldorf

Gedruckt mit der Genehmigung der
Mathematisch-Naturwissenschaftlichen Fakultät
der Heinrich-Heine-Universität Düsseldorf

Betreuerin: PD Dr. Nicole Linka
Referent: Prof. Dr. Andreas P. M. Weber
Korreferent: apl. Prof. Dr. Peter Jahns

Tag der mündlichen Prüfung:

Erklärung

Ich versichere an Eides Statt, dass ich die vorliegende Dissertation eigenständig und ohne unerlaubte Hilfe unter Beachtung der „Grundsätze zur Sicherung guter wissenschaftlicher Praxis“ an der Heinrich-Heine-Universität Düsseldorf angefertigt habe. Die Dissertation habe ich in dieser oder in ähnlicher Form noch bei keiner anderen Institution eingereicht. Ich habe bisher keine erfolglosen Promotionsversuche unternommen.

Willich, den 30.03.2015

_____

Martin Schroers

Contents

I. Preface

The present thesis has been divided into independent sections, written as manuscripts. *Manuscript 1* elucidates the *in vivo* function of the Arabidopsis peroxisomal NAD carrier (PXN). This manuscript is an advanced draft and will be submitted to the *Journal of Biological Chemistry* in its final version. *Manuscript 2* provides first insights in posttranslational regulation of PXN transport activity by phosphorylation. The involvement of peroxisomal metabolism in breakdown of branched-chain amino acids and small carboxylic acids is depicted in *Manuscript 3*. *Manuscript 4* deals with the use of plant peroxisomes in biotechnological applications and was published in *Plant Science* (Kessel-Vigelius et al., 2013).

References

Kessel-Vigelius, S.K., Wiese, J., Schroers, M.G., Wrobel, T.J., Hahn, F. and Linka, N. (2013) An engineered plant peroxisome and its application in biotechnology. *Plant science : an international journal of experimental plant biology*, **210**, 232-240.

II.1 Summary

Eukaryotic cells contain different highly specialized cell organelles which are encased by at least one lipid bilayer membrane. These membranes are impermeable for most metabolites without assistance of specific solute transport proteins. These proteins are also called carriers and enable to maintain a functional metabolic network extending over different organelles inside the cell (Linka and Weber, 2010). This thesis contributes to the knowledge of peroxisomal transport proteins in plants. The main focus of this thesis was to extend the knowledge of the Peroxisomal NAD Carrier (PXN) of the model plant *Arabidopsis thaliana.* The peroxisomal metabolism depends on the import of substrates and cofactors, but our knowledge of the transporters involved is very limited.

PXN mutants exhibit a slowed mobilization of storage oils, linking PXN function to the peroxisomal β-oxidation of fatty acids (Bernhardt et al., 2012). *In vitro* studies showed PXN to be able to transport e.g., NAD, NADH, AMP, and CoA (Agrimi et al., 2012; Bernhardt et al., 2012). In our experiments we could confirm that PXN imports AMP into liposomes preloaded with CoA at a concentration of 10 mM, but also showed that it does not mediate the transport of CoA on lower concentrations (*Manuscript 1*). Based on these findings CoA import is unlikely to be the *in vivo* role of PXN. Phenotype suppression studies of yeast mutants impaired in peroxisomal β-oxidation were used to get additional results. We could demonstrate the ability of PXN to suppress the phenotype of *mdh3Δ* mutants. Mdh3p is part of the malate/oxaloacetate redox shuttle in yeast, which regenerates NAD in the peroxisomal matrix (van Roermund et al., 1995). Yeast cells deficient in Mdh3p function showed a β-oxidation activity of about 30% compared to wild-type cells when grown on oleate as sole carbon source. Expression of PXN in the *mdh3Δ* background raised this activity significantly to 73% of wild-type levels (*Manuscript 1*). Thereby we showed PXN to be able to supply peroxisomal β-oxidation with NAD independently of the malate/oxaloacetate shuttle. To identify the counter exchange substrate which is exported from the peroxisome upon NAD import we analyzed an *mdh3Δ/npy1Δ* double mutant. Npy1p is a peroxisomal NADH pyrophosphatase catalyzing the hydrolysis of NADH to AMP and NMNH (AbdelRaheim et al., 2001). PXN accepts both NADH and AMP as substrates *in vitro* and loss of Npy1p function results in higher intraperoxisomal NADH levels and less AMP. Expression of PXN in the yeast double mutant did not restore β-oxidation activity, making AMP the most

likely counter substrate for NAD uptake *in vivo*. To verify these findings we targeted PXN to the mitochondria of *ndt1Δ/ndt2Δ* yeast cells. This mutant lacks the activity of both mitochondrial NAD carriers which import NAD against AMP and is unable to grow on ethanol as sole carbon source (Todisco et al., 2006). Expression of mitochondrial-targeted PXN in the *ndt1Δ/ndt2Δ* mutant partly suppressed the growth phenotype on ethanol. Thus the import of NAD against AMP is likely to be the *in vivo* function of PXN.

In *Manuscript 2* we investigated how the PXN-mediated import of NAD into plant peroxisomes is regulated. Thus we studied if PXN activity is regulated by phosphorylation of the serine residue at position 155 (S155) of the polypeptide chain. This phosphorylation site is located in an elongated hydrophilic loop region which is unique among MCF transporters but conserved in PXN homologues in different higher plant and algae species. Phosphorylation of S155 enhanced the speed of PXN mediated NAD/AMP exchange without altering the proteins affinity to NAD.

Manuscript 3 elucidated the involvement of peroxisomal metabolism during the breakdown of small-chain fatty acids which for example arise from the catabolism of branched-chain amino acids (BCAAs). BCAA breakdown is important during different stress conditions, where these amino acids serve as alternative energy source (Araujo et al., 2011). Based on our results peroxisomal metabolism is involved in BCAA degradation as well as in breakdown of exogenously supplied BCAA catabolites like propionate, isobutyrate, and acrylate. PXA1 activity is essential for the import of propionyl-CoA, isobutyryl-CoA, and possibly 2-methylbutyryl-CoA into peroxisomes during BCAA breakdown. Intraperoxisomal ATP provided by PNC1 and PNC2 is mandatory during these processes, while the role of PXN is less distinct.

References

AbdelRaheim, S.R., Cartwright, J.L., Gasmi, L. and McLennan, A.G. (2001) The NADH diphosphatase encoded by the Saccharomyces cerevisiae NPY1 nudix hydrolase gene is located in peroxisomes. *Arch Biochem Biophys*, **388**, 18-24.

Agrimi, G., Russo, A., Pierri, C.L. and Palmieri, F. (2012) The peroxisomal NAD+ carrier of Arabidopsis thaliana transports coenzyme A and its derivatives. *J Bioenerg Biomembr*, **44**, 333-340.

Araujo, W.L., Tohge, T., Ishizaki, K., Leaver, C.J. and Fernie, A.R. (2011) Protein degradation - an alternative respiratory substrate for stressed plants. *Trends Plant Sci*, **16**, 489-498.

Bernhardt, K., Wilkinson, S., Weber, A.P. and Linka, N. (2012) A peroxisomal carrier delivers NAD(+) and contributes to optimal fatty acid degradation during storage oil mobilization. *Plant J*, **69**, 1-13.

Linka, N. and Weber, A.P.M. (2010) Intracellular metabolite transporters in plants. *Molecular plant*, **3**, 21-53.

Todisco, S., Agrimi, G., Castegna, A. and Palmieri, F. (2006) Identification of the mitochondrial NAD+ transporter in Saccharomyces cerevisiae. *J Biol Chem*, **281**, 1524-1531.

van Roermund, C.W., Elgersma, Y., Singh, N., Wanders, R.J. and Tabak, H.F. (1995) The membrane of peroxisomes in Saccharomyces cerevisiae is impermeable to NAD(H) and acetyl-CoA under in vivo conditions. *EMBO J*, **14**, 3480-3486.

II.2 Zusammenfassung

Eukaryotische Zellen beinhalten verschiedene hochspezialisierte Zellorganellen, welche von mindestens einer Lipiddoppelschicht-Membran umgeben sind. Diese Membranen sind für die meisten Metaboliten ohne die Hilfe spezifischer Transportproteine impermeabel. Die Aufrechterhaltung eines funktionellen metabolischen Netzwerkes, welches sich über verschiedene Zellorganellen in der Zelle erstreckt, wird von diesen Transportern ermöglicht (Linka und Weber, 2010).
Diese Arbeit trägt zum Wissen über peroxisomale Transportproteine der Pflanzen bei. Der Hauptschwerpunkt der Arbeit lag darauf, das Wissen über den peroxisomalen NAD Transporter (PXN) der Modellpflanze *Arabidopsis thaliana* zu vergrößern. Der peroxisomale Metabolismus ist vom Import von Substraten und Cofaktoren abhängig, aber unser Wissen über die beteiligten Transporter ist stark limitiert.

PXN Mutanten zeigen eine verlangsamte Mobilisierung von Speicherölen, was die Funktion von PXN mit der peroxisomalen β-Oxidation von Fettsäuren verbindet (Bernhardt et al., 2012). *In vitro* Untersuchungen haben gezeigt, dass PXN unter anderem NAD, NADH, AMP und CoA transportieren kann (Agrimi et al., 2012; Bernhardt et al., 2012). In unseren Experimenten konnten wir bestätigen, dass PXN AMP in Liposomen importiert, die mit 10 mM CoA vorbeladen waren. Einen Transport von CoA bei niedrigeren Konzentrationen wurde dagegen nicht festgestellt (*Manuskript 1*). Basierend auf diesen Erkenntnissen ist der Transport von CoA wahrscheinlich nicht die *in vivo* Funktion von PXN. Experimente, bei denen der Phänotyp von Hefemutanten unterdrückt wird, wurden durchgeführt um zusätzliche Ergebnisse zu erhalten. Wir konnten zeigen, dass PXN den Phänotyp von *mdh3Δ* Mutanten unterdrückt. Mdh3p ist Teil des sogenannten Malat/Oxalacetat Redoxshuttles in der Hefe, welches NAD in der peroxisomalen Matrix regeneriert (van Roermund et al., 1995). Hefezellen mit fehlerhafter Funktion von Mdh3p zeigten eine β-Oxidation Aktivität von etwa 30% verglichen mit wildtypischen Zellen, wenn sie auf Oleat als einziger Kohlenstoffquelle wuchsen. Die Expression von PXN in *mdh3Δ* Zellen erhöhte diese Aktivität signifikant auf 73% des wildtypischen Levels (*Manuskript 1*). Damit haben wir gezeigt, dass PXN fähig ist die peroxisomale β-Oxidation unabhängig vom Malat/Oxalacetat Shuttles mit NAD zu versorgen. Um das Austauschsubstrat zu identifizieren, welches aus den Peroxisomen während der NAD-Aufnahme exportiert wird, wurde eine *mdh3Δ/npy1Δ* Doppelmutante analysiert.

Npy1p ist eine peroxisomale NADH Pyrophosphatase, welche die Hydrolyse von NADH zu AMP und NMNH katalysiert (AbdelRaheim et al., 2001). PXN akzeptiert sowohl NADH als auch AMP als Substrat und der Verlust von Npy1p führt zu erhöhter intraperoxisomaler NADH und zu verringerter AMP Konzentration. Die Expression von PXN in der Hefe-Doppelmutante stellte die β-Oxidationsaktivität nicht wieder her, was AMP zum wahrscheinlichsten Austauschsubstrat für NAD Aufnahme in *vivo* macht. Um diese Erkenntnisse zu verifizieren exprimierten wir eine PXN Variante in *ndt1Δ/ndt2Δ* Hefezellen, die in die Mitochondrien transportiert wird (mt-PXN). Dieser Mutante fehlen beide mitochondriale NAD Transporter, welche NAD gegen AMP importieren. Dadurch ist sie unfähig zu wachsen, wenn Ethanol als einzige Kohlenstoffquelle vorliegt (Todisco et al., 2006). Expression von mt-PXN in der *ndt1Δ/ndt2Δ* Mutante unterdrückt diesen Wachstumsphänotyp teilweise. Daher ist der Import von NAD gegen AMP wahrscheinlich die *in vivo* Funktion von PXN.

In *Manuskript* 2 untersuchten wir, wie der von PXN durchgeführte Import von NAD in Pflanzenperoxisomen reguliert wird. Wir überprüften, ob die Aktivität von PXN durch Phosphorylierung des Serinrestes an Position 155 (S155) der Polypeptidkette reguliert wird. Diese Phosphorylierungsstelle befindet sich in einer verlängerten hydrophilen Schleifenregion, welche einzigartig in MCF Transportern ist, aber in Homologen von PXN in verschiedenen höheren Pflanzen- und Algenspezies konserviert ist. Phosphorylierung von S155 erhöht die Geschwindigkeit von NAD/AMP Austausch durch PXN, ohne dabei die Affinität des Proteins zu NAD zu verändern.

Manuskript 3 untersucht die Beteiligung des peroxisomalen Metabolismus beim Abbau kurzkettiger Fettsäuren, welche unter anderem beim Abbau verzweigtkettiger Aminosäuren (BCAAs) entstehen. BCAA Abbau ist während verschiedener Stressbedingungen wichtig, bei denen diese Aminosäuren als alternative Energiequellen dienen (Araujo et al., 2011). Basierend auf unseren Ergebnissen ist der peroxisomale Metabolismus sowohl am Abbau von BCAAs, als auch von exogen dargereichten BCAA Katabolіten, wie Propionat, Isobutyrat und Acrylat, beteiligt. Während des BCAA Katabolismuses ist die Aktivität von PXA1 essentiell für den Import von Propionyl-CoA, Isobutyryl-CoA und vermutlich 2-Methylbutyryl-CoA in die Peroxisomen. Intraperoxisomales ATP, welches von PNC1 und PNC2 zur Verfügung gestellt wird, ist für diese Prozesse ebenfalls unabdingbar, wogegen die Beteiligung von PXN weniger deutlich ist.

Referenzen

AbdelRaheim, S.R., Cartwright, J.L., Gasmi, L. and McLennan, A.G. (2001) The NADH diphosphatase encoded by the Saccharomyces cerevisiae NPY1 nudix hydrolase gene is located in peroxisomes. *Arch Biochem Biophys*, **388**, 18-24.

Agrimi, G., Russo, A., Pierri, C.L. and Palmieri, F. (2012) The peroxisomal NAD+ carrier of Arabidopsis thaliana transports coenzyme A and its derivatives. *J Bioenerg Biomembr*, **44**, 333-340.

Araujo, W.L., Tohge, T., Ishizaki, K., Leaver, C.J. and Fernie, A.R. (2011) Protein degradation - an alternative respiratory substrate for stressed plants. *Trends Plant Sci*, **16**, 489-498.

Bernhardt, K., Wilkinson, S., Weber, A.P. and Linka, N. (2012) A peroxisomal carrier delivers NAD(+) and contributes to optimal fatty acid degradation during storage oil mobilization. *Plant J*, **69**, 1-13.

Linka, N. and Weber, A.P.M. (2010) Intracellular metabolite transporters in plants. *Molecular plant*, **3**, 21-53.

Todisco, S., Agrimi, G., Castegna, A. and Palmieri, F. (2006) Identification of the mitochondrial NAD+ transporter in Saccharomyces cerevisiae. *J Biol Chem*, **281**, 1524-1531.

van Roermund, C.W., Elgersma, Y., Singh, N., Wanders, R.J. and Tabak, H.F. (1995) The membrane of peroxisomes in Saccharomyces cerevisiae is impermeable to NAD(H) and acetyl-CoA under in vivo conditions. *EMBO J*, **14**, 3480-3486.

III. Introduction

Plant peroxisomes – a short introduction

Peroxisomes are small organelles of 0.2 to 4 µm in diameter, depending on cell and tissue type (Huang et al., 1983). They are specialized compartments in almost all eukaryotic cells and surrounded by a single lipid-bilayer membrane. The most well-known peroxisomal function in plants is the β-oxidation of fatty acids. β-oxidation fuels the seedling establishment of oilseed plants, like *Arabidopsis thaliana*, by providing energy and carbon skeletons for carbohydrate synthesis. Additionally, β-oxidation is important during conditions where photoautotrophic growth is not possible such as periods of extended darkness. Other peroxisomal functions include photorespiration, hormone biosynthesis, and pathogen defense (Hu et al., 2012).

Peroxisomal transport proteins

The peroxisomal membrane is impermeable for bulky solutes, therefore substrates and co-factors of the various metabolic pathways need to be imported or exported via transport proteins (Linka and Weber, 2010). This work addresses the role of the peroxisomal NAD carrier PXN from *Arabidopsis thaliana* – a transporter of the Mitochondrial Carrier Family.

The Mitochondrial Carrier Family

Three identified peroxisomal transporters from Arabidopsis PXN, PNC1, and PNC2 belong to the same family of transport proteins: the Mitochondrial Carrier Family (MCF). This thesis focuses on peroxisomal MCF transporters in *Arabidopsis thaliana*. The Mitochondrial Carrier Family is labeled TC 2.A.29 in the Transporter Classification Database (Saier et al., 2006). Transporters of the MC family are exclusive to eukaryotic cells and are encoded in the nucleus. Despite their name MCF carriers localize to mitochondria, peroxisomes, plastids, the endoplasmic reticulum, and the plasma membrane (Bedhomme et al., 2005; Thuswaldner et al., 2007; Leroch et al., 2008; Linka et al., 2008; Rieder and Neuhaus, 2011; Bernhardt et al., 2012). To date, 58 MCF transporters have been identified in Arabidopsis, 50 in humans and 35 in *S. cerevisiae.* These different MCF carriers mediate the transport of a broad spectrum of substrates, which are highly variable in size and structure. Most substrates are negatively charged, but there are also positively charged or zwitterions. Transported by MCF transporters are e.g., nucleotides, carboxylic acids,

amino acids, keto acids, phosphate, protons, and Coenzyme A (CoA; Palmieri et al., 2011). According to the substrate, MCF mediated transport can either be electrogenic by transferring a net charge or electroneutral. Most MCF proteins mediate a strict antiport of two different substrates in a 1:1 stoichiometry. Unidirectional substrate transport (uniport) and H^+-compensated anion symport are also mediated by specific MCF proteins (Kunji and Robinson, 2010; Palmieri et al., 2011).

MCF carriers are commonly 30 – 40 kDa in size and share characteristic structural features: three repetitive structures of about 100 amino acids, each composed of two α-helical transmembrane spans, connected by hydrophilic loops. A conserved so called mitochondrial energy transfer signature (or MCF motif; Pfam PF00153) directly follows each odd-numbered transmembrane span. The six transmembrane helices form a barrel-like three-dimensional (3D) structure, which stretches through the membrane and is open towards one side and closed to the other. This 3D-structure of a MCF transporter has been solved to a resolution of 2.2 Å by X-ray crystallography of the bovine ADP/ATP carrier 1 and has greatly improved our understanding of the MCF transporter function (Pebay-Peyroula et al., 2003). Briefly, the transport mechanism is thought to be facilitated by two salt bridge networks, which form gates on both membrane sides. Interaction with the correct substrate leads to conformation changes inside the protein, resulting in closing of the substrate entry gate and opening of the opposed gate, thereby releasing the substrate molecule on the other side of the transport protein (Robinson et al., 2008; Palmieri et al., 2011).

It was previously thought that MCF transporters function exclusively as homodimers. However, more recent studies confirmed the carriers to be able to form homodimers, but also to be fully functional as monomers (Robinson et al., 2008; Kunji and Crichton, 2010; Palmieri et al., 2011).

The peroxisomal NAD transporter PXN

The peroxisomal NAD carrier PXN from Arabidopsis is encoded by At2G39970. The protein was originally identified in multiple independent proteome analyses as Peroxisomal Membrane Protein of 38 kDa (PMP38; Fukao et al., 2001; Reumann et al., 2007; Eubel et al., 2008; Reumann et al., 2009). It possesses all MCF specific features described above. A more recent study showed PXN mutants to exhibit

enlarged peroxisomes and speculated on a possible role of PXN during peroxisome proliferation through division of existing peroxisomes (Mano et al., 2011). Bernhardt et al. (2012) were able to show that PXN mutants (*pxn*) suffer from a delayed and slowed mobilization of storage oils during germination. These findings suggested a role of PXN in peroxisomal β-oxidation. Previously, impaired β-oxidation has been shown to result in enlarged peroxisomes, possibly through intraperoxisomal accumulation of acyl-CoA, which explains the observation of enlarged peroxisomes in PXN mutants (Germain et al., 2001; Graham et al., 2002; Rylott et al., 2006; Mano et al., 2011). Loss of PXN function has a mild effect on seedling establishment. *pxn-1* mutants display a delay and not a block in storage oil mobilization and grow as fast as the wild type (Bernhardt et al., 2012). In contrast RNAi suppressor lines of the two other identified peroxisomal MCF transporters, the peroxisomal ATP carriers PNC1 and PNC2, are strictly “sucrose-dependent” (Linka et al., 2008; Kessel-Vigelius et al., unpublished). *pxn-1* also only showed a mild resistance to root growth inhibition by 2,4-DB compared to PNC1/2 suppressors (Linka et al., 2008; Bernhardt et al., 2012). It was therefore assumed that there is a redundant system for PXN function.

In vitro uptake experiments performed with recombinant protein showed PXN to transport NAD, AMP, NADH, and ADP in antiport mode (Bernhardt et al., 2012). The ability to mediate NAD/NADH exchange is unique among NAD transporters characterized so far in plants, yeast, and human (Todisco et al., 2006; Palmieri et al., 2009; Agrimi et al., 2012b; Bernhardt et al., 2012). An independent study confirmed these substrates to be accepted by PXN, but also added CoA as *in vitro* substrate. The authors hypothesized PXN to be a peroxisomal CoA transporter (Agrimi et al., 2012a). The present thesis provides new insights that the actual *in vivo* function of PXN does not include the transport of CoA (*Manuscript 1*) and features first results on posttranslational regulation of PXN activity (*Manuscript 2*).

NAD in plant cells

The peroxisomal NAD carrier PXN is able to transport nicotinamide adenine dinucleotide (NAD) in its oxidized and also in its reduced form (NADH) *in vitro*. The oxidized form is often referred to as NAD^+, because of the positive charge on the nitrogen atom inside the nicotinamide ring. This term is somehow misleading, because NAD has a net charge of -1 at physiological pH values. This study will therefore refer to oxidized nicotinamide adenine dinucleotide as NAD.

NAD and NADH form a ubiquitous redox pair and are essential cofactors for different metabolic reactions. NAD is highly oxidized in plants so that NAD concentrations are in the millimolar range, while NADH concentrations are estimated in the lower micromolar range (ca. 1 µM; Heineke et al., 1991). NAD(H) concentrations differ between cell organelles and range from 0.4 mM in chloroplasts over 0.6 mM in the cytosol to 2 mM in mitochondria (Takahama et al., 1981; Igamberdiev and Gardestrom, 2003). Up to now there is no data available regarding the peroxisomal NAD(H) concentrations. However, most of the NAD(H) present in cells is not 'free' but enzyme bound and current methods are unable to differentiate between these two states.

NAD *de novo* synthesis consists of five steps which take place in chloroplasts and the cytosol. The individual steps, as well as the involved enzymes are presented in Figure 1A.

Generally NAD is involved in catabolic reactions, where it is used to oxidize substrates by accepting two electrons and one proton. It also serves as the substrate for poly-ADP-ribose polymerases (PARPs) which facilitate the poly ADP-ribosylation of specific glutamate residues of proteins. PARPs and thereby NAD are involved in essential processes including DNA repair, cell cycle regulation, apoptosis, and regulation of telomere length (Burkle, 2001). Additionally NAD is the precursor of cyclic ADP-ribose which is involved in Ca^{2+}-release based signaling pathways, which are important for e.g., stomatal closure (Leckie et al., 1998).

In respect to peroxisomal metabolism both the reduced and the oxidized form of NAD are used as cofactors. NADH is needed during photorespiration and H_2O_2 degradation via the peroxisomal glutathione-ascorbate cycle. NAD on the other hand is an essential cofactor of the multifunctional protein (MFP) during peroxisomal β-oxidation of fatty acids. Involvements of NAD(H) in peroxisomal metabolism are presented in Figure 1B.

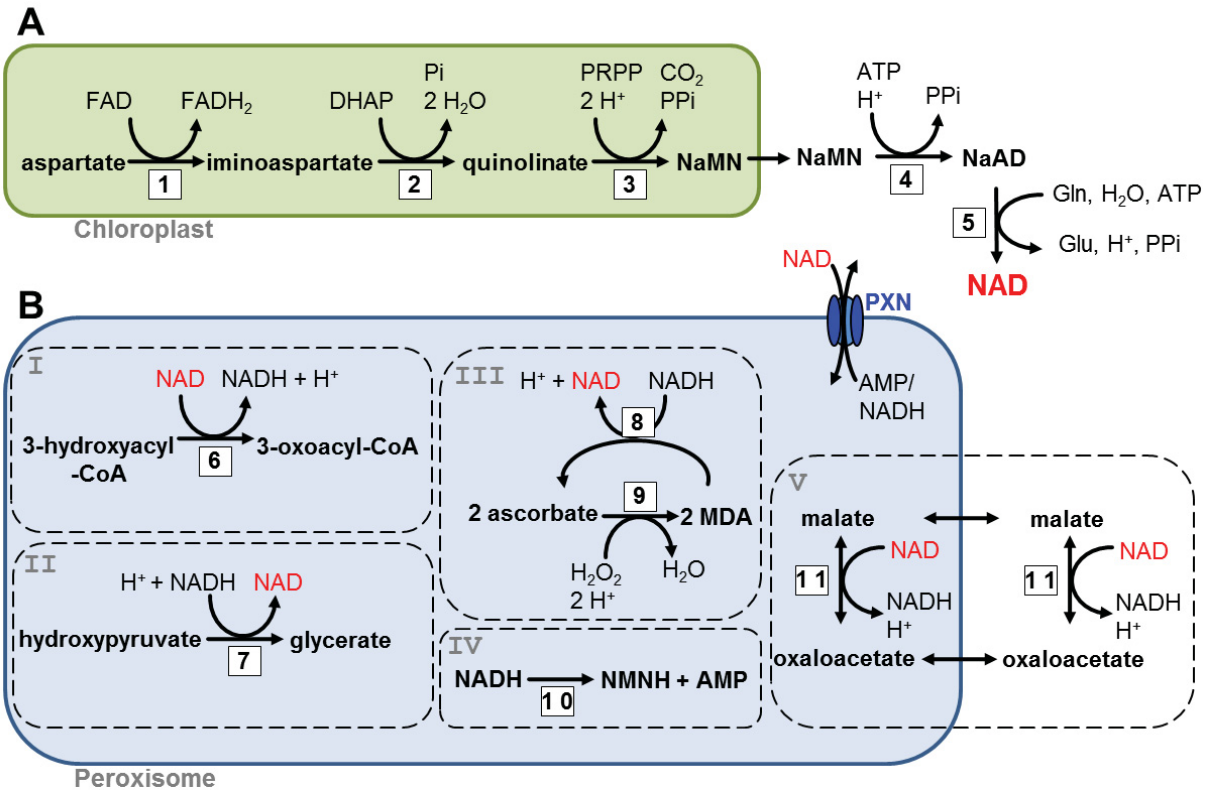

Figure 1: *De novo* biosynthesis of NAD (A) and NAD(H) involving peroxisomal reactions (B).
A: The scheme shows the 5-step *de novo* synthesis of NAD from aspartate in the chloroplast (green) and the cytosol. Enzymes involved in NAD synthesis are **1**: aspartate oxidase, **2**: quinolinate synthase, **3**: quinolinate phosphoribosyltransferase, **4**: nicotinamide-nucleotide adenylyl-transferase, and **5**: NAD synthase. FAD(H_2): flavin adenine dinucleotide, DHAP: dihydroxyacetone phosphate, PRPP: 5-phospho-α-D-ribose 1-diphosphate, NaMN: nicotinate mononuleotide, NaAD: nicotinate adenine dinucleotide, Gln: glutamine, Glu: glutamate.
B: I-V represent NAD(H) involving reactions inside the peroxisome (blue). Dashed lines are for clarity and separation and do not represent membranes or otherwise differentiated compartments. **I**: Conversion of a 3-hydroxyacyl-CoA to a 3-oxoacyl-CoA by Multifunctional Protein 2 (**6**) during β-oxidation. **II**: Conversion of hydroxypyruvate to glycerate by peroxisomal Hydroxypyruvate Reductase 1 (**7**) during photorespiration. **III**: Part of H_2O_2 detoxification via the peroxisomal glutathione-ascorbate cycle; MDA: monodehydroascorbate, **8**: MDA reductase, **9**: ascorbate peroxidase. **IV**: Degradation of excessive NADH to reduced nicotinamide mononucleotide (NMNH) and AMP by peroxisomal Nudix Hydrolase 19 (**10**). **V**: Conversion of NAD to NADH et vice versa via the malate/oxaloacetate shuttle; **11**: peroxisomal and cytosolic malate dehydrogenases.

References

Agrimi, G., Russo, A., Pierri, C.L. and Palmieri, F. (2012a) The peroxisomal NAD+ carrier of Arabidopsis thaliana transports coenzyme A and its derivatives. *J Bioenerg Biomembr*, **44**, 333-340.

Agrimi, G., Russo, A., Scarcia, P. and Palmieri, F. (2012b) The human gene SLC25A17 encodes a peroxisomal transporter of coenzyme A, FAD and NAD+. *Biochem J*, **443**, 241-247.

Bedhomme, M., Hoffmann, M., McCarthy, E.A., Gambonnet, B., Moran, R.G., Rebeille, F. and Ravanel, S. (2005) Folate metabolism in plants: an Arabidopsis homolog of the mammalian mitochondrial folate transporter mediates folate import into chloroplasts. *J Biol Chem*, **280**, 34823-34831.

Bernhardt, K., Wilkinson, S., Weber, A.P. and Linka, N. (2012) A peroxisomal carrier delivers NAD(+) and contributes to optimal fatty acid degradation during storage oil mobilization. *Plant J*, **69**, 1-13.

Burkle, A. (2001) Physiology and pathophysiology of poly(ADP-ribosyl)ation. *BioEssays : news and reviews in molecular, cellular and developmental biology*, **23**, 795-806.

Eubel, H., Meyer, E.H., Taylor, N.L., Bussell, J.D., O'Toole, N., Heazlewood, J.L., Castleden, I., Small, I.D., Smith, S.M. and Millar, A.H. (2008) Novel proteins, putative membrane transporters, and an integrated metabolic network are revealed by quantitative proteomic analysis of Arabidopsis cell culture peroxisomes. *Plant Physiol*, **148**, 1809-1829.

Fukao, Y., Hayashi, Y., Mano, S., Hayashi, M. and Nishimura, M. (2001) Developmental analysis of a putative ATP/ADP carrier protein localized on glyoxysomal membranes during the peroxisome transition in pumpkin cotyledons. *Plant Cell Physiol*, **42**, 835-841.

Germain, V., Rylott, E.L., Larson, T.R., Sherson, S.M., Bechtold, N., Carde, J.P., Bryce, J.H., Graham, I.A. and Smith, S.M. (2001) Requirement for 3-ketoacyl-CoA thiolase-2 in peroxisome development, fatty acid beta-oxidation and breakdown of triacylglycerol in lipid bodies of Arabidopsis seedlings. *Plant J*, **28**, 1-12.

Graham, I.A., Li, Y. and Larson, T.R. (2002) Acyl-CoA measurements in plants suggest a role in regulating various cellular processes. *Biochem Soc Trans*, **30**, 1095-1099.

Heineke, D., Riens, B., Grosse, H., Hoferichter, P., Peter, U., Flugge, U.I. and Heldt, H.W. (1991) Redox Transfer across the Inner Chloroplast Envelope Membrane. *Plant Physiol*, **95**, 1131-1137.

Hu, J., Baker, A., Bartel, B., Linka, N., Mullen, R.T., Reumann, S. and Zolman, B.K. (2012) Plant peroxisomes: biogenesis and function. *Plant Cell*, **24**, 2279-2303.

Huang, A.H.C., Trelease, R.N. and Moore, T.S. (1983) Plant Peroxisomes: Academic Press.

Igamberdiev, A.U. and Gardestrom, P. (2003) Regulation of NAD- and NADP-dependent isocitrate dehydrogenases by reduction levels of pyridine nucleotides in mitochondria and cytosol of pea leaves. *Biochim Biophys Acta*, **1606**, 117-125.

Kunji, E.R. and Crichton, P.G. (2010) Mitochondrial carriers function as monomers. *Biochim Biophys Acta*, **1797**, 817-831.

Kunji, E.R. and Robinson, A.J. (2010) Coupling of proton and substrate translocation in the transport cycle of mitochondrial carriers. *Current opinion in structural biology*, **20**, 440-447.

Leckie, C.P., McAinsh, M.R., Allen, G.J., Sanders, D. and Hetherington, A.M. (1998) Abscisic acid-induced stomatal closure mediated by cyclic ADP-ribose. *Proc Natl Acad Sci U S A*, **95**, 15837-15842.

Leroch, M., Neuhaus, H.E., Kirchberger, S., Zimmermann, S., Melzer, M., Gerhold, J. and Tjaden, J. (2008) Identification of a novel adenine nucleotide transporter in the endoplasmic reticulum of Arabidopsis. *Plant Cell*, **20**, 438-451.

Linka, N., Theodoulou, F.L., Haslam, R.P., Linka, M., Napier, J.A., Neuhaus, H.E. and Weber, A.P. (2008) Peroxisomal ATP import is essential for seedling development in Arabidopsis thaliana. *Plant Cell*, **20**, 3241-3257.

Linka, N. and Weber, A.P.M. (2010) Intracellular metabolite transporters in plants. *Molecular plant*, **3**, 21-53.

Mano, S., Nakamori, C., Fukao, Y., Araki, M., Matsuda, A., Kondo, M. and Nishimura, M. (2011) A defect of peroxisomal membrane protein 38 causes enlargement of peroxisomes. *Plant Cell Physiol*, **52**, 2157-2172.

Palmieri, F., Pierri, C.L., De Grassi, A., Nunes-Nesi, A. and Fernie, A.R. (2011) Evolution, structure and function of mitochondrial carriers: a review with new insights. *Plant J*, **66**, 161-181.

Palmieri, F., Rieder, B., Ventrella, A., Blanco, E., Do, P.T., Nunes-Nesi, A., Trauth, A.U., Fiermonte, G., Tjaden, J., Agrimi, G., Kirchberger, S., Paradies, E., Fernie, A.R. and Neuhaus, H.E. (2009) Molecular identification and functional characterization of Arabidopsis thaliana mitochondrial and chloroplastic NAD+ carrier proteins. *J Biol Chem*, **284**, 31249-31259.

Pebay-Peyroula, E., Dahout-Gonzalez, C., Kahn, R., Trezeguet, V., Lauquin, G.J. and Brandolin, G. (2003) Structure of mitochondrial ADP/ATP carrier in complex with carboxyatractyloside. *Nature*, **426**, 39-44.

Reumann, S., Babujee, L., Ma, C., Wienkoop, S., Siemsen, T., Antonicelli, G.E., Rasche, N., Luder, F., Weckwerth, W. and Jahn, O. (2007) Proteome analysis of Arabidopsis leaf peroxisomes reveals novel targeting peptides, metabolic pathways, and defense mechanisms. *Plant Cell*, **19**, 3170-3193.

Reumann, S., Quan, S., Aung, K., Yang, P., Manandhar-Shrestha, K., Holbrook, D., Linka, N., Switzenberg, R., Wilkerson, C.G., Weber, A.P., Olsen, L.J. and Hu, J. (2009) In-depth proteome analysis of Arabidopsis leaf peroxisomes combined with in vivo subcellular targeting verification indicates novel metabolic and regulatory functions of peroxisomes. *Plant Physiol*, **150**, 125-143.

Rieder, B. and Neuhaus, H.E. (2011) Identification of an Arabidopsis plasma membrane-located ATP transporter important for anther development. *Plant Cell*, **23**, 1932-1944.

Robinson, A.J., Overy, C. and Kunji, E.R. (2008) The mechanism of transport by mitochondrial carriers based on analysis of symmetry. *Proc Natl Acad Sci U S A*, **105**, 17766-17771.

Rylott, E.L., Eastmond, P.J., Gilday, A.D., Slocombe, S.P., Larson, T.R., Baker, A. and Graham, I.A. (2006) The Arabidopsis thaliana multifunctional protein gene (MFP2) of peroxisomal beta-oxidation is essential for seedling establishment. *Plant J*, **45**, 930-941.

Saier, M.H., Jr., Tran, C.V. and Barabote, R.D. (2006) TCDB: the Transporter Classification Database for membrane transport protein analyses and information. *Nucleic Acids Res*, **34**, D181-186.

Takahama, U., Shimizu-Takahama, M. and Heber, U. (1981) The redox state of the NADP system in illuminated chloroplasts. *Biochimica et Biophysica Acta*, **637**, 530-539.

Thuswaldner, S., Lagerstedt, J.O., Rojas-Stutz, M., Bouhidel, K., Der, C., Leborgne-Castel, N., Mishra, A., Marty, F., Schoefs, B., Adamska, I., Persson, B.L. and Spetea, C. (2007) Identification, expression, and functional analyses of a thylakoid ATP/ADP carrier from Arabidopsis. *J Biol Chem*, **282**, 8848-8859.

Todisco, S., Agrimi, G., Castegna, A. and Palmieri, F. (2006) Identification of the mitochondrial NAD+ transporter in Saccharomyces cerevisiae. *J Biol Chem*, **281**, 1524-1531.

IV.1 *Manuscript 1*

Elucidating the *in vivo* function of the Arabidopsis peroxisomal NAD carrier in yeast

Martin G. Schroers[1,2], Carlo W.T. van Roermund[1,3], Jan Wiese[2], Samantha Kurz[2], Sabrina Wilkinson, Lennart Charton[2], Ronald J.A. Wanders[3], Hans R. Waterham[3], Andreas P.M. Weber[2], and Nicole Linka[2,4]

[1] These authors contributed equally to this work.

[2] Institute for Plant Biochemistry and Cluster of Excellence on Plant Sciences (CEPLAS), Heinrich Heine University, Universitaetsstrasse 1, 40225 Duesseldorf, Germany.

[3] Laboratory Genetic Metabolic Diseases, Laboratory Division, Academic Medical Center, University of Amsterdam, the Netherlands.

[4] To whom correspondence should be addressed. E-mail Nicole.Linka@hhu.de.

ABSTRACT

Cofactors such as nicotinamide adenine dinucleotide (NAD), AMP or CoA, are essential for a diverse set of reactions and pathways in the cell. In plants, NAD synthesis takes place in the cytosol, after which it is distributed to different cell compartments, including peroxisomes, which requires efficient transport across the cellular membranes. We previously identified a novel transport protein in Arabidopsis called PXN (peroxisomal NAD carrier) that resides in the peroxisomal membrane. *In vitro* uptake studies using recombinant PXN protein provided evidence that this carrier exhibits versatile transport functions, *e.g.*, catalyzing the import of NAD and CoA against AMP, and the exchange of NAD against NADH. This observation raises the question about the biological function of PXN in plants, since the peroxisomal fatty acid oxidation demands NAD, CoA and a link with the cytosolic NADH pool via a redox shuttle. To address this question, we used *Saccharomyces cerevisiae* deletion mutants to elucidate the *in vivo* role of PXN. To this end, we expressed PXN in the mutant strains and investigated the suppression of the mutant phenotype. Our study provides strong evidence that PXN supplies peroxisomes with NAD by importing NAD in exchange with AMP.

INTRODUCTION

Nicotinamide adenine dinucleotide (NAD) is a ubiquitous biological molecule, which participates in many fundamental processes within the living cell (Pollak et al., 2007; Houtkooper et al., 2010) acting as an electron acceptor in numerous redox reactions. In addition to a role as metabolic cofactor, NAD has critical regulatory functions in other cellular processes. For example, its phosphorylated form is involved in the generation and scavenging of reactive oxygen species that serve as signaling molecules (Droge, 2002; Mittler, 2002). Furthermore, NAD is also a precursor for cyclic ADP-ribose, which modulates the release of calcium as a second messenger (Pollak et al., 2007; Houtkooper et al., 2010). Moreover, it also plays a role in transcription and posttranslational modification through histone deacetylation and ADP ribosylation of proteins (Chambon et al., 1963; Imai et al., 2000; Landry et al., 2000).

Since NAD has multiple essential functions, its cellular levels need to be maintained either through *de novo* synthesis or salvage which involves recycling of NAD degradation products. In eukaryotic cells both pathways take place in the cytosol and thus NAD has to be distributed to diverse cell compartments. As a consequence, transport proteins are required to shuttle NAD across the intracellular membranes. In plants, humans, and fungi, members of the mitochondrial carrier family (MCF) mediate the import of NAD into mitochondria, plastids, and peroxisomes (Todisco et al., 2006; Palmieri et al., 2009; Agrimi et al., 2011; Agrimi et al., 2012a; Bernhardt et al., 2012). These transporters have been characterized by *in vitro* uptake assays using recombinant protein reconstituted into lipid vesicles (liposomes). Based on these biochemical data, the NAD carriers function as antiporters, importing NAD in a strict counter-exchange with another substrate (Todisco et al., 2006; Palmieri et al., 2009; Agrimi et al., 2011; Agrimi et al., 2012a; Bernhardt et al., 2012).

In case of plastids and mitochondria, the carriers catalyze the uptake of NAD in counter-exchange with AMP or ADP (Todisco et al., 2006; Palmieri et al., 2009). The efflux of adenine nucleotides is compensated by their *de novo* synthesis in the stroma or unidirectional uptake into the matrix (Todisco et al., 2006; Palmieri et al., 2008; Palmieri et al., 2009). The importance of such an NAD import system has been established in the yeast *Saccharomyces cerevisiae* (Todisco et al., 2006; Agrimi et al., 2011). Yeast cells lacking the mitochondrial NAD carrier proteins Ndt1p and

Ndt2p were unable to grow on non-fermentable carbon sources, such as ethanol (Todisco et al., 2006). The utilization of ethanol requires the operation of the NAD-dependent tricarboxylic acid (Krebs) cycle and respiration. The *ndt1Δ/ndt2Δ* double mutant lacks mitochondrial NAD, hence both pathways were inhibited, causing the mutant growth phenotype (Todisco et al., 2006; Agrimi et al., 2011). This finding indicates that mitochondrial NAD transport proteins are essential for providing NAD to mitochondria.

A peroxisomal NAD transporter from *Arabidopsis thaliana*, called PXN, has been previously identified (Agrimi et al., 2012a; Bernhardt et al., 2012). In comparison to the plastidial and mitochondrial NAD carriers, PXN exhibits unique transport properties. The recombinant PXN protein accepts NADH and coenzyme A (CoA) as suitable substrates in addition to NAD, AMP, and ADP (Agrimi et al., 2012a; Bernhardt et al., 2012). Based on its broad substrate spectrum, three transport functions can be postulated for PXN in plants (Fig. 1).

In plants, NAD-dependent processes play fundamental roles in the peroxisomal metabolism. For example, fatty acid degradation via β-oxidation requires NAD as cofactor (Graham, 2008). But before fatty acids can enter β-oxidation they need to be activated to the corresponding acyl-CoA esters, which occurs both in the extra- and intra-peroxisomal spaces depending upon the fatty acid chain length (Fulda et al., 2004). Therefore, a specific transport protein is required to import CoA into plant peroxisomes. PXN might be a good candidate for catalyzing this transport step, since it accepts CoA as a substrate *in vitro* (Fig. 1A).

Alternatively, PXN might import NAD in exchange with an adenine nucleotide to feed plant peroxisomes with NAD, as known for the plastidial and mitochondrial NAD transporters (Fig. 1B). During β-oxidation, NAD is reduced to NADH. To maintain the flux through this pathway NAD is regenerated via the reversible reduction of oxaloacetate. The resulting malate is exported to the cytosol, where it is re-oxidized to oxaloacetate, which in return is imported into peroxisomes (Fig. 1). Such a malate/oxaloacetate shuttle allows the exchange of the oxidized and reduced forms of NAD with the cytosol (Mettler and Beevers, 1980; Pracharoenwattana et al., 2007). As a redundant system, PXN might catalyze the import of NAD in exchange with NADH. This leads to the transfer of reducing equivalents across the peroxisomal membrane (Fig. 1C). These predicted transport modes raise the question: what is the physiological function of PXN in intact cells?

In this work, we used different deletion mutants from *Saccharomyces cerevisiae* to explore the *in vivo* role of PXN in plants. To this end, we functionally expressed the *Arabidopsis* carrier protein in yeast mutant strains and investigated the suppression of the mutant yeast phenotypes in the presence of recombinant PXN. Our study supports the hypothesis that PXN is required to supply peroxisomes with NAD by importing NAD in exchange with AMP.

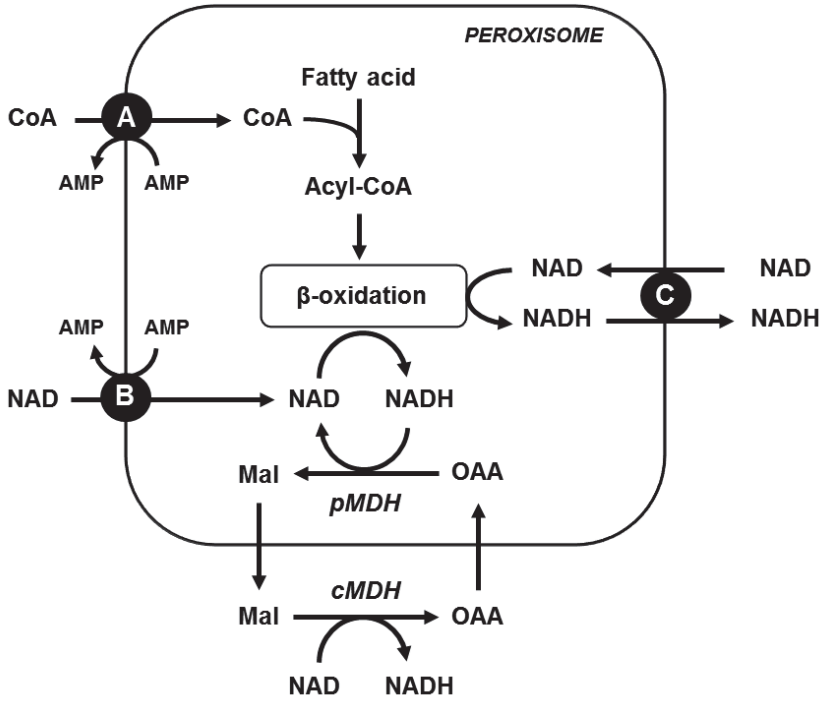

Figure 1: Possible transport functions for the peroxisomal NAD carrier (PXN) in plants with respect to fatty acid degradation via β-oxidation.
PXN exhibits unique transport properties *in vitro*, accepting NADH and CoA as suitable substrates in addition to NAD and adenine nucleotides. This variety of transport substrates raises the question: which of the three following transport functions is the physiological role of PXN *in vivo*? **(A)** PXN imports CoA against AMP to fuel fatty acid activation required for β-oxidation. **(B)** PXN mediates the NAD uptake in exchange with AMP to provide β-oxidation with its cofactor.
(C) PXN functions as redox shuttle by transferring NAD versus NADH across the peroxisomal membrane to regenerate NAD for β-oxidation, redundant to the malate/oxaloacetate shuttle via the peroxisomal and cytosolic malate dehydrogenases (pMDH and cMDH). Mal, malate; OAA, oxaloacetate.

RESULTS

PXN protein is functional when expressed in yeast

In this study we used several deletion mutants from *S. cerevisiae* to dissect the physiological transport function of PXN. Our approach was to express PXN in the corresponding yeast mutant and to analyze the suppression of the respective yeast mutant phenotype. In order to establish the feasibility of this approach we first expressed recombinant PXN and assessed its functionality by analyzing the NAD uptake rates in yeast. Therefore, we expressed PXN with a C-terminal histidine affinity tag (His) in the *S. cerevisiae* wild-type strain FGY217 (Kota et al., 2007). We extracted membranes from yeast cells expressing PXN-His or transformed with the empty vector and separated the membrane proteins by SDS-PAGE (Fig. 2A). Proper expression of PXN-His, which has a calculated molecular mass of 38.3 kDa, was checked by immunoblot analysis with an anti-His antibody (Fig. 2B). Total yeast membranes containing recombinant PXN-His protein was reconstituted into lipid vesicles. The uptake of radioactively labeled [α-^{32}P]-NAD into these liposomes was measured in the presence or absence of 10 mM NAD as counter-exchange substrate. We used total membrane fractions from yeast cells transformed with the empty vector as controls, to estimate the background activity of yeast endogenous NAD carriers. NAD import into liposomes reconstituted with yeast membranes from control cells was below the detection limit of the assay system employed (Fig. 2C). In contrast, reconstituted PXN-His protein mediated rapid uptake of NAD into liposomes, but only when they were preloaded with NAD (Fig. 2D). The NAD/NAD exchange mediated by PXN-His followed first order kinetics and reached a maximum uptake rate of 0.79 µmol/mg protein per minute. This finding confirmed that PXN functions as an antiporter, as we demonstrated in our previous work (Bernhardt et al., 2012).Taken together, our *in vitro* activity experiments showed that PXN is functionally expressed in yeast cells.

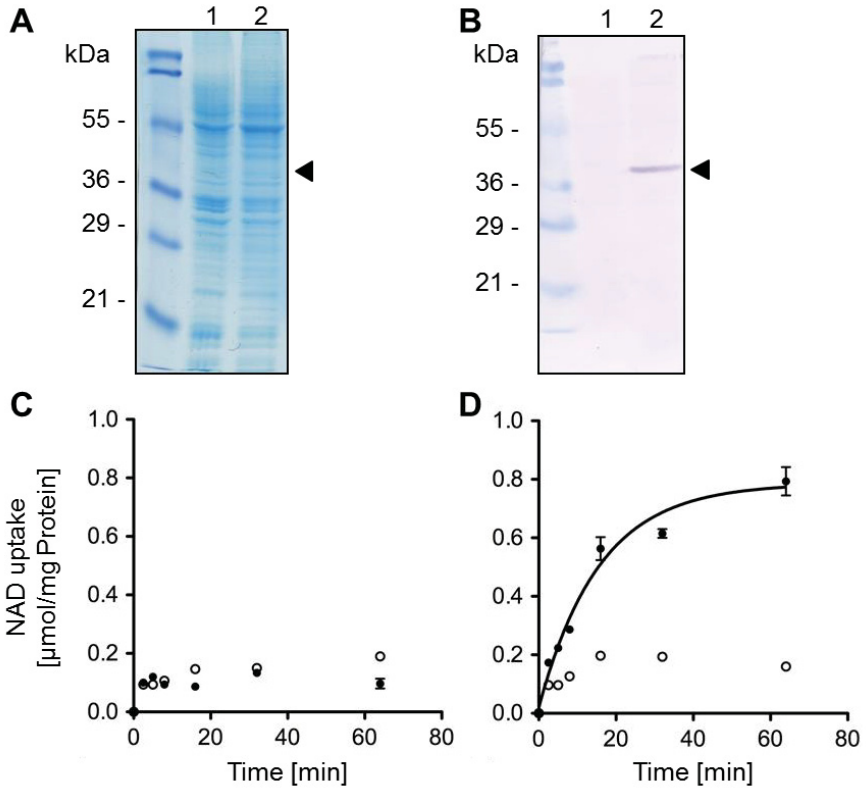

Figure 2. Recombinant His-tagged PXN protein is functionally expressed in yeast.
(**A**) Coomassie-stained SDS-PAGE gel showing total yeast membrane proteins isolated from yeast cells containing pYES vector (lane 1) and from yeast cells expressing PXN-His (lane 2). (**B**) Detection of PXN-His with a calculated molecular mass of 38.3 kDa (lane 2; arrowhead) by immunoblot analysis using His-tag antibody.
Time-dependent uptake of radioactively labeled [α-32P]-NAD (0.2 mM) was measured into liposomes reconstituted with total yeast membranes in the absence (**C**) or presence (**D**) of PXN-His. The proteoliposomes were preloaded internally with 10 mM NAD (closed symbols) or in the absence of NAD as counter-exchange substrate (open symbols). All graphs represent the arithmetic mean ±SE of three independent experiments.

Analysis of the PXN-mediated CoA transport function

To confirm that PXN protein indeed has CoA transport activity, we conducted *in vitro* uptake assays into liposomes with yeast expressed PXN-His protein, as described above. We measured the uptake of radioactively labeled [^{3}H]-CoA (0.2 mM) or [α-^{32}P]-AMP (0.2 mM) into lipid vesicles reconstituted with yeast membranes in the presence or absence of recombinant PXN-His, respectively (Fig. 3A-C). The liposomes used in this study contained 10 mM CoA, 10 mM AMP or no internal substrate. In the absence of PXN-His protein, we did not measure any AMP uptake into CoA-preloaded liposomes (Fig. 3A), which indicates that the activity of endogenous yeast carriers could not be detected under the experimental conditions used. Once recombinant PXN-His was incorporated in the liposomal membrane,

substantial AMP transport rates were observed, but only in exchange with internal CoA (Fig. 3B). This result confirmed our conclusion that PXN is able to mediate an AMP/CoA antiport. In an independent experiment, we used radioactively labeled CoA (0.2 mM) as external substrate and preloaded the liposomes either with AMP or CoA (10 mM) as counter-exchange substrates. The control assays did not reveal any background activities for CoA import in exchange with the tested internal substrates (Fig. 3C and E). However, the same results were found when PXN-His was reconstituted into liposomes. We did not detect uptake of labeled CoA into PXN-containing liposomes loaded with either CoA or AMP (Fig. 3D and F). Based on our findings we conclude that PXN is only able to transport CoA under certain conditions: a high CoA concentration and a low concentration of a different counter-exchange substrate (here: AMP) on the opposite membrane side. Based on our results PXN does not mediate CoA/CoA homoexchange, despite the high concentration gradient of 50-fold (in/out) present in our experiment.

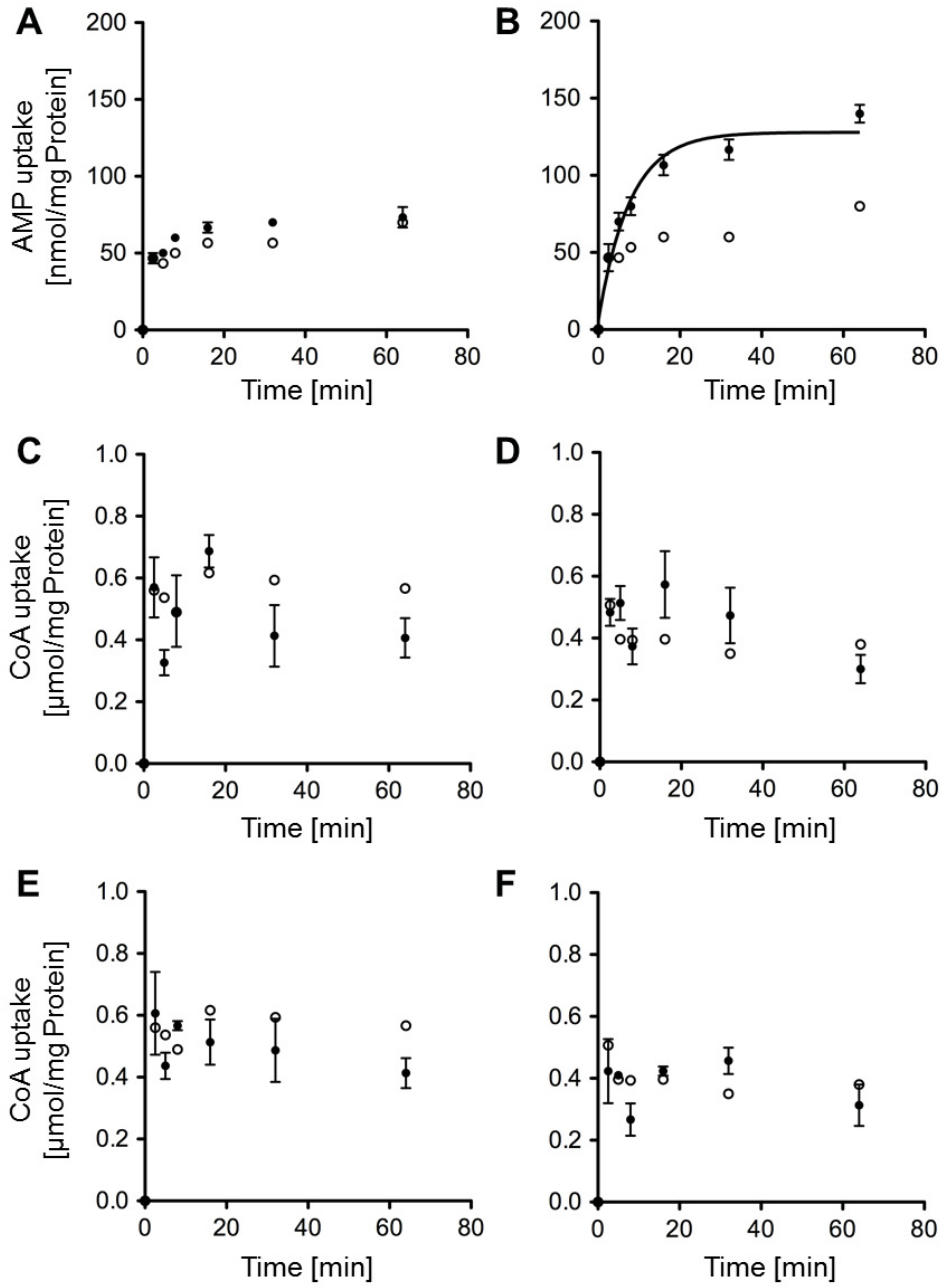

Figure 3: PXN expressed in yeast exhibits low CoA transport activity *in vitro.*
Total membranes isolated form yeast cells transformed with empty vector pYES2 (**A**, **C**, and **E**) or containing PXN-His (**B**, **D**, and **F**) were reconstituted into lipid vesicles. **A** and **B**: Uptake of radioactively labeled [α-^{32}P]-AMP (0.2 mM) into proteoliposomes preloaded with CoA (10 mM) (closed symbols) or in the absence of internal substrate (open symbols) in nmol/mg protein. **C** and **D**: Uptake of radioactively labeled [^{3}H]-CoA (0.2 mM) into proteoliposomes preloaded with AMP (10 mM) (closed symbols) or in the absence of internal substrate (open symbols) in µmol/mg protein. **E** and **F**: Uptake of radioactively labeled [^{3}H]-CoA (10 mM) into proteoliposomes preloaded with CoA (10 mM) (closed symbols) or in the absence of internal substrate (open symbols) in µmol/mg protein. All graphs represent the arithmetic mean ±SE of three independent experiments.

PXN partially restores the *mdh3Δ* mutant phenotype

Based on biochemical data PXN is able to catalyze an NAD/NADH exchange (Agrimi et al., 2012a; Bernhardt et al., 2012). Thus, we hypothesized that PXN transfers reducing equivalents across the peroxisomal membrane in addition to the peroxisomal malate/oxaloacetate shuttle (Pracharoenwattana et al., 2007; Fig. 1). To test this hypothesis, we used a yeast mutant deficient for the peroxisomal malate dehydrogenase 3 (Mdh3p) (van Roermund et al., 1995). This enzyme is part of the peroxisomal malate/oxaloacetate redox shuttle, which regenerates NAD in the peroxisomal matrix. NAD is required for fatty acid breakdown via peroxisomal β-oxidation. The loss of Mdh3p led to a yeast mutant unable to metabolize fatty acids as sole carbon source (van Roermund et al., 1995).

We expressed the Arabidopsis PXN protein in the *mdh3Δ* yeast mutant under the control of a catalase promoter to investigate if PXN represents an alternative route for supplying peroxisomal β-oxidation with NAD. Since the yeast mutant successfully expressed PXN (Fig. 4A), we analyzed the growth of *mdh3Δ* cells transformed with *MDH3*, *PXN* or an empty vector in oleate rich medium to induce the expression of genes required for β-oxidation. In addition, we used *fox1Δ* cells as control, a yeast mutant in which the acyl-CoA oxidase, the first enzyme in peroxisomal β-oxidation, is deficient (Hiltunen et al., 1992). As expected, the *mdh3Δ* cells transformed with the empty vector did not grow on oleate, whereas the complementation of *mdh3Δ* mutant with Mdh3p led to fully restored growth (van Roermund et al., 1995). Expression of PXN in *mdh3Δ* mutant cells partially suppressed the mutant phenotype (Fig. 4B).

To examine whether the partial suppression of the *mdh3Δ* mutant by PXN is associated with an increase rate of β-oxidation, we measured the rate of fatty acid oxidation (FAO) using octanoate (C8:0) as substrate for different yeast mutants. Fig. 4C shows the relative rates for C8:0 β-oxidation of mutant cells compared to the wild type, which was set to 100%. In *fox1Δ* the β-oxidation of C8:0 was completely deficient, whereas deletion of the *MDH3* gene resulted in a decreased FAO rate of 31%, in line with earlier results (van Roermund et al., 1995). Complementation with the endogenous *MDH3* gene led to a full recovery of β-oxidation function (94%). When PXN was expressed in the *mdh3Δ* cells, we determined 73% of the wild-type FAO rates and in comparison with β-oxidation activities in *mdh3Δ* we measured a significant increase of 2.4-fold. These data indicate that PXN is able to exchange

NAD for NADH *in vivo*, which is required to suppress the *mdh3Δ* growth defect and restore FAO function.

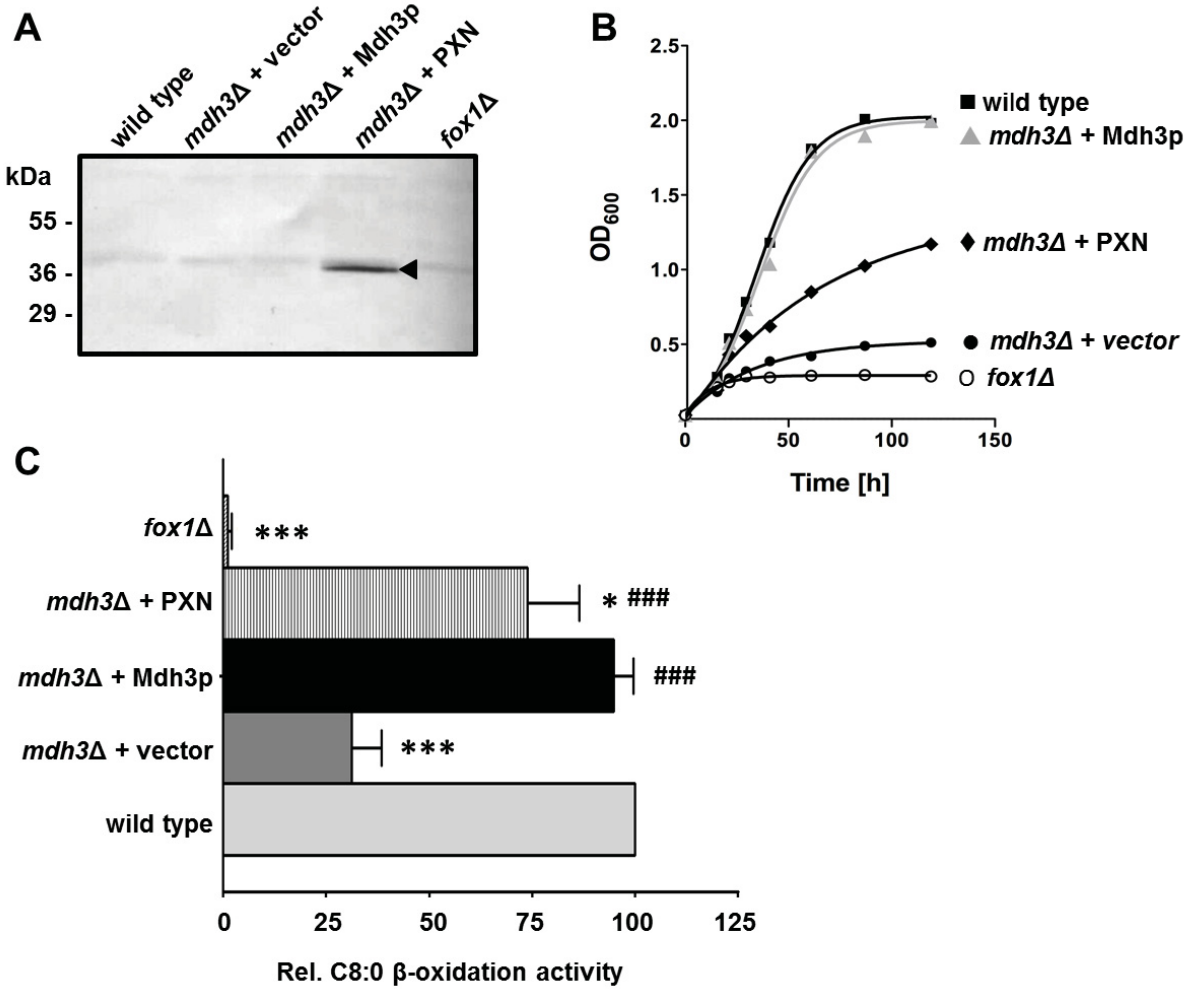

Figure 4: PXN is able to partially rescue the *mdh3Δ* mutant phenotype.
(A) Constitutive expression of PXN in the *mdh3Δ* mutant background was confirmed by immunoblot using PXN-specific antibody. Arrowhead indicates the detected protein band for the recombinant PXN. **(B)** Growth curves of wild type and mutant strains on oleate rich medium. The strains shown are: wild type (■), *mdh3Δ* cells transformed with empty vector (●), *mdh3Δ* cells expressing Mdh3p (▲), *mdh3Δ* cells expressing PXN (♦). As negative control *fox1Δ* cells (O) were used. **(C)** Wild type, and *mdh3Δ* cells transformed with the empty vector or expressing PXN or Mdh3p, grown on oleate medium were incubated with [1-^{14}C]-octanoate and β-oxidation activity was measured. The β-oxidation activity of wild type cells was taken as reference (100%). Data represent arithmetic means ±SD of 2-5 independent experiments. Asterisks indicate statistical differences to wild type cells as significant (*: P<0.05 or ***: P<0.001. Number signs indicate statistical differences to *mdh3Δ* cells as significant (###: P<0.001).

Further suppressor analysis to confirm PXN as redox shuttle candidate

We performed an additional phenotype suppression analysis in yeast, to investigate the NAD/NADH exchange function of PXN. *S. cerevisiae* peroxisomes contain an NADH pyrophosphatase, called Npy1p, which catalyzes the hydrolysis of NADH to AMP (AbdelRaheim et al., 2001). Npy1p regulates NADH homeostasis, in particular when reducing equivalents accumulate inside the peroxisomal matrix (AbdelRaheim et al., 2001).

Loss of Mdh3p likely leads to heightened levels of NADH inside peroxisomes under oleate conditions, because the NAD regeneration is blocked. As a consequence, we expect Npy1p to be active to reduce the peroxisomal NADH levels by converting it to AMP in the *mdh3Δ* mutant. As a consequence, higher amounts of AMP might be available in peroxisomes of Mdh3p deficient cells compared to the wild type. To elucidate whether AMP or NADH is more likely the counter-exchange substrate for PXN mediated NAD import, we deleted the *NPY1* gene in the *mdh3Δ* mutant background by PCR-mediated gene replacement. For the FAO analyses we compared wild type with the *mdh3Δ, npy1Δ* and *mdh3Δ/npy1Δ* mutants, which were transformed either with the empty vector or with the PXN expression construct. Expression of PXN in the mutants was verified by immunodetection using PXN-specific antibody (Fig. 5A; Bernhardt et al., 2012). We then grew the cells on oleate and measured octanoate FAO rates (Fig. 5B).

The loss of Npy1p did not affect β-oxidation activities (96%; Fig. 5B). We also measured octanoate oxidation activities comparable to the wild type in *npy1Δ* cells when PXN was expressed (97%). In the *mdh3Δ/npy1Δ* double mutant, we expected decreased activities, similar as in the *mdh3Δ* single mutant. Indeed, we observed reduced rates of octanoate oxidation in *mdh3Δ* and *mdh3Δ/npy1Δ* mutants of about 30% (Fig. 5B). To verify if PXN functions as NAD/NADH antiporter, we transformed *mdh3Δ/npy1Δ* cells with PXN and measured octanoate β-oxidation. We observed that FAO activity was not restored to the same extend by expression of PXN when Npy1p was absent. The octanoate oxidation activities of the double mutant with PXN were significantly decreased compared to *mdh3Δ* expressing PXN.

Peroxisomes of the *mdh3Δ* single mutant likely contain less NADH and more AMP when compared to *mdh3Δ/npy1Δ* cells. Taken together our results suggest that the increased NADH levels in the peroxisomal matrix of *mdh3Δ/npy1Δ* cells did not drive (stimulate) the NAD import required for FAO under these conditions. Thus we

hypothesize that PXN does not function as redox shuttle by exchanging NAD for NADH across the peroxisomal membrane in intact yeast cells, but is rather catalyzing the exchange of NAD with AMP.

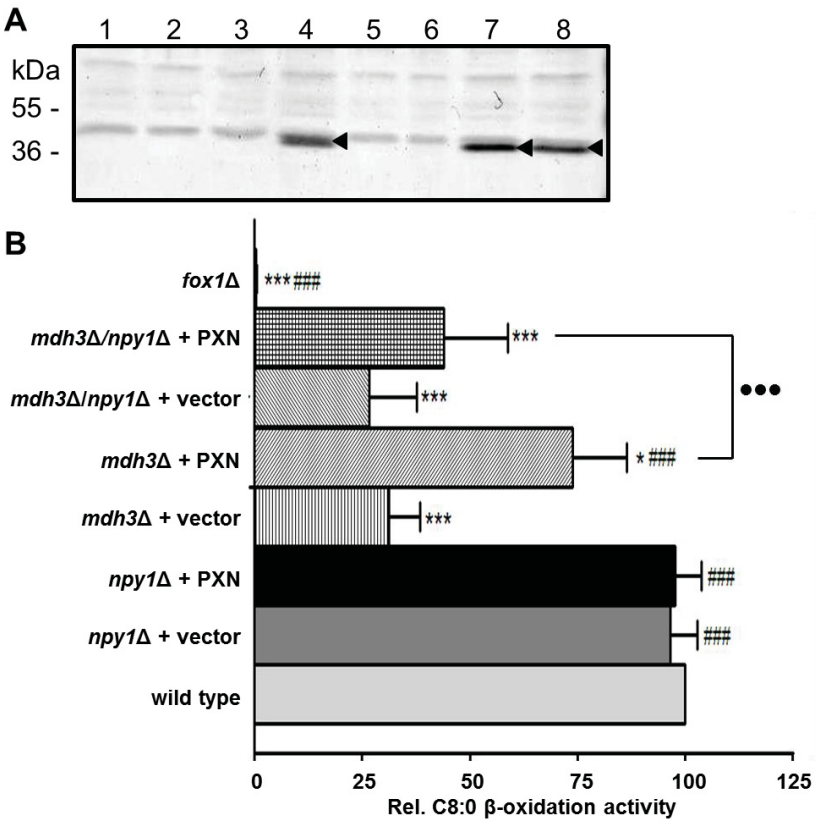

Figure 5: AMP derived from Npy1p mediated NADH degradation likely drives PXN mediated NAD import in *mdh3Δ* cells.

(A) Constitutive expression of PXN in the *mdh3Δ* and *mdh3Δ/npy1Δ* mutants was confirmed by immunodetection using PXN-specific antibody. Arrowheads indicate the detected protein bands for recombinant PXN. Lanes correspond to 1: wild type cells, 2: *fox1Δ*, 3: *mdh3Δ*, 4: *mdh3Δ* + PXN, 5: *npy1Δ*, 6: *mdh3Δ/npy1Δ*, 7: *npy1Δ* + PXN, 8: *mdh3Δ/npy1Δ* + PXN.

(B) Octanoic acid β-oxidation activity in oleate-induced yeast wild-type and mutant cells. The strains shown are: wild type, *mdh3Δ*, *npy1Δ* and *mdh3Δ/npy1Δ* transformed with or without PXN expression construct. Relative FAO rates were calculated, in which the activities in wild type cells were taken as reference (100%). Data represent arithmetic means ±SD of 3 independent experiments. Asterisks indicate statistical differences to wild type cells as significant (*: P<0.05 or ***: P<0.001. Number signs indicate statistical differences to *mdh3Δ* cells as significant (###: P<0.001). Filled circles indicate the statistical difference between *mdh3Δ* + PXN and *mdh3Δ/npy1Δ* + PXN as significant (●●●: P <0.001).

PXN likely catalyzes NAD/AMP exchange *in vivo*

We used a yeast mutant lacking both mitochondrial NAD carriers Ndt1p and Ndt2p (Todisco et al., 2006) to verify the NAD/AMP exchange function of PXN *in vivo*. This double mutant displays a growth delay when ethanol is used as non-fermentable sole carbon source (Todisco et al., 2006). In this *ndt1Δ*/*ndt2Δ* double mutant, the TCA cycle and mitochondrial respiration are inhibited due to the lack of mitochondrial NAD, which normally is imported by Ndt proteins in exchange for AMP (Todisco et al., 2006).

To be able to restore the impaired NAD uptake into the mitochondria of the *ndt1Δ*/*ndt2Δ* double mutant, the peroxisomal PXN was targeted to mitochondria. To this end, the mitochondrial target peptide (mt) of the mitochondrial succinate/fumarate translocator from Arabidopsis was fused to the N-terminus of PXN (Catoni et al., 2003). In addition mt-PXN was tagged at the C-terminus with the enhanced yellow fluorescent protein (EYFP). This reporter allows visualization of the subcellular localization of the fusion protein by fluorescence microscopy. We expressed mt-PXN-EYFP in yeast cells, which were stained with the mitochondria-specific dye MitoTracker Orange. Confocal microscopy revealed that the fluorescence pattern of EYFP matched with the distribution of the MitoTracker signal (Fig. 6) confirming that PXN fused with a mitochondrial target signal is effectively localized to mitochondria in yeast.

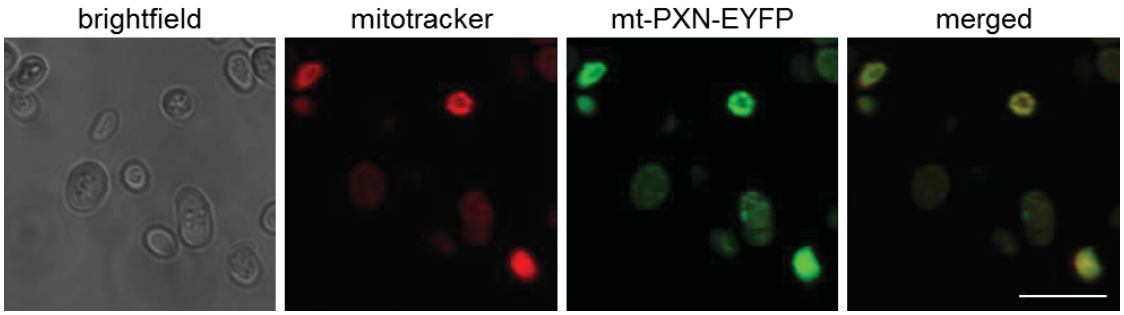

Figure 6: Fusion with a mitochondrial target signal allows the localization of PXN to yeast mitochondria. Co-localization study in yeast was analyzed by fluorescence microscopy. Confocal images were taken from yeast cells expressing the mt-PXN-EYFP fusion protein (green). Yeast mitochondria were stained with MitoTracker Orange (red). The merged image represents an overlay of MitoTracker and EYFP signals (yellow). Bar = 10 µm.

To show that the fusion with the mitochondrial target peptide did not affect the transport function of PXN, we expressed the mt-PXN in yeast and performed *in vitro* uptake studies using yeast membranes reconstituted with liposomes (Fig. 7). Expression of mt-PXN with an expected calculated mass of 39 kDa was checked by

immunoblot analysis using PXN-specific antibody (Fig. 7A+B; Bernhardt et al., 2012). We reconstituted lipid vesicles with yeast membranes with and without mt-PXN fusion protein and measured the uptake of radioactively labeled [α-^{32}P]-NAD dependent on internal NAD. In the absence of mt-PXN, no significant NAD uptake rates were measured into liposomes with internal NAD (Fig. 7C). Reconstituted mt-PXN protein mediated high NAD transport activities when counter-exchange substrate was present (Fig. 7D), indicating that the recombinant fusion protein was active.

The *ndt1Δ/ndt2Δ* double mutant permits testing the hypothesis that mt-PXN imports NAD into mitochondria in counter-exchange with AMP, as it has been previously described for the yeast Ndt carriers (Todisco et al., 2006). Therefore, we grew the double mutant carrying either the empty vector or the mt-PXN expression plasmid on glucose or ethanol as sole carbon source at 28°C. Over time we monitored the growth of liquid yeast cultures by measuring the optical density at 600 nm (OD_{600}) using a spectrophotometer. In the presence of glucose no large growth difference of wild type, *ndt1Δ*/*ndt2Δ* and *ndt1Δ*/*ndt2Δ* expressing mt-PXN was observed (Fig. 7E). In contrast, growth on the non-fermentable carbon source ethanol was severely slowed in the *ndt1Δ*/*ndt2Δ* double mutant compared to wild type (Fig. 7F), as described by Todisco et al. (2006). Expression of mt-PXN in this mutant background partially suppressed the growth defect on ethanol. From the resulting growth curves shown in Figure 7F we calculated the growth rates. Compared to the exponential growth phase of wild type with a doubling time of 121 h, *ndt1Δ*/*ndt2Δ* cells were unable to grow on ethanol, indicated by the doubling time of 566 h. This severe phenotype was partially suppressed by the expression of mt-PXN, represented by the doubling time of 182 h. Based on this data mt-PXN is able to partly compensate the loss of both mitochondrial Ndt carriers. Since these transporters import NAD against AMP and to not accept NADH as a substrate (Todisco et al., 2006), we suggest PXN to mediate the same exchange.

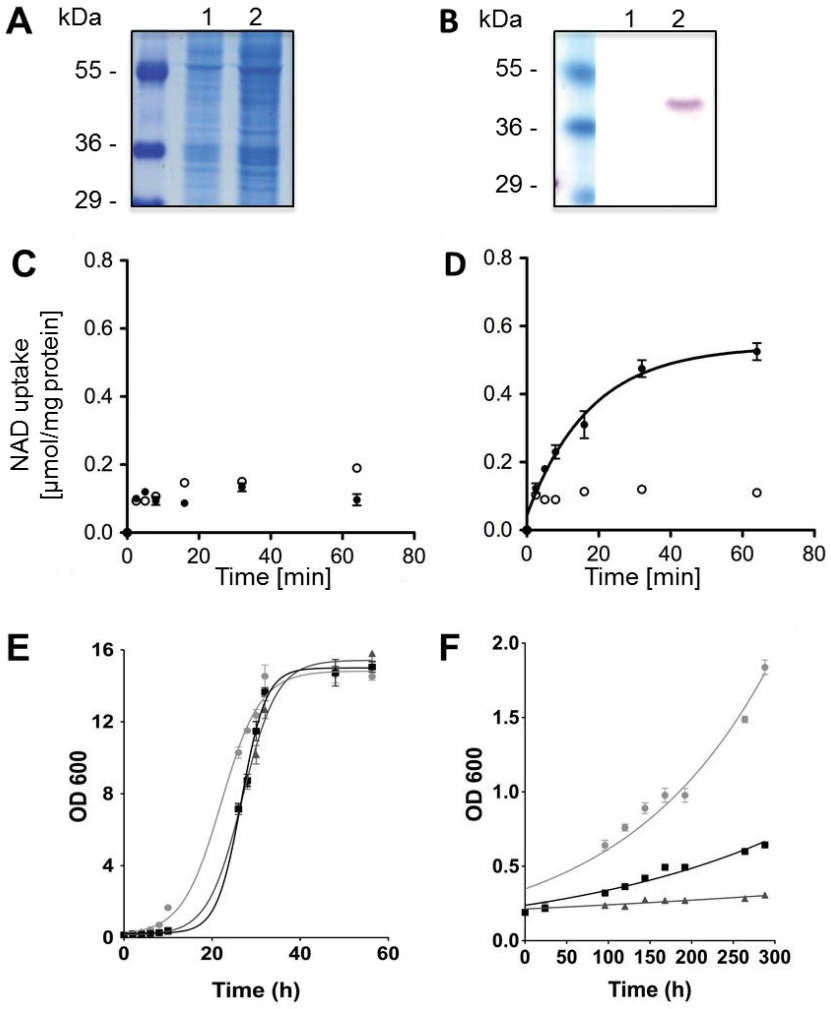

Figure 7: Mitochondrial targeted PXN (mt-PXN) protein partly suppresses the *ndt1Δ*/*ndt2Δ* double mutant phenotype by importing NAD into yeast mitochondria.

(**A**+**B**) Constitutive expression of mt-PXN in the *ndt1Δ*/*ndt2Δ* double mutant was verified by immunodetection: coomassie stained protein gel **(A)** and western blot **(B)** using PXN-specific antibody; 1: *ndt1Δ*/*ndt2Δ*, 2: *ndt1Δ*/*ndt2Δ* + PXN.

(**C**+**D**) Time-dependent uptake of radioactively labeled [α-^{32}P]-NAD (150 µM) was measured in liposomes reconstituted with total yeast membranes in the absence **(C)** and presence of mt-PXN-His **(D).** The proteoliposomes were preloaded internally with 20 mM NAD (closed symbols) or lack NAD as counter-exchange substrate (open symbols). Graphs represent the arithmetic means ±SE of three independent experiments.

(**E**+**F**) Suppression of the *ndt1Δ*/*ndt2Δ* growth phenotype by mt-PXN: wild type (●), *ndt1Δ*/*ndt2Δ* transformed with the empty vector pDR195 (▲) and *ndt1Δ*/*ndt2Δ* expressing mt-PXN (■) were inoculated in SM medium supplemented with 2% (w/v) glucose **(E)** or 2% (v/v) ethanol **(F)**. Optical densities of liquid cultures were measured at 600 nm (OD_{600}) using a spectrophotometer. Data from a representative experiment are shown. Graphs represent the arithmetic mean ±SD of three technical replicates. Similar results were obtained in three independent experiments.

DISCUSSION

Our knowledge of how peroxisomes are supplied with essential cofactors is still incomplete. In this study we elucidated the potential routes by which peroxisomes acquire NAD(H) and/or CoA. Like plastids and mitochondria, peroxisomes are absolutely dependent on supply with these cofactors from the cytoplasm (Linka and Esser, 2012). Since the last steps of NAD and CoA biosynthesis take place in the cytosol, these molecules must enter peroxisomes by specific transport proteins. The peroxisomal NAD carrier from *Arabidopsis thaliana* (PXN) has been previously characterized (Agrimi et al., 2012a; Bernhardt et al., 2012) and it was found that loss of PXN compromises seedling growth. This phenotype was explained by a delayed storage oil mobilization due to inefficient degradation of fatty acids via peroxisomal β-oxidation (Bernhardt et al., 2012). This previous work raised the question: how does PXN support fatty acid oxidation? Previous *in vitro* studies using artificial liposomes provided evidence that PXN is able to catalyze the exchange of NAD/AMP, NAD/NADH, and AMP/CoA (Agrimi et al., 2012a; Bernhardt et al., 2012). Consequently, three transport scenarios for a role of PXN in β-oxidation can be postulated (Fig. 1): (A) PXN imports CoA into peroxisomes required to activate fatty acids for β-oxidation. (B) PXN provides peroxisomes with NAD, which is needed as electron acceptor for the fatty acid oxidation. (C) PXN functions as redox shuttle by exchanging NAD against NADH, allowing the re-oxidation of NADH outside the peroxisomes and therefore maintaining the flux through β-oxidation.

Here, we performed analyses using baker's yeast to elucidate PXN function in a living system. First, we confirmed that PXN expression in yeast led to functional protein. We analyzed the transport activity in the reconstituted system, measuring the uptake of labeled substrate against a counter-exchange substrate. The reconstitution of yeast expressed PXN into liposomes led to high NAD exchange activities against NAD (Fig. 2D). In the same experimental set-up we confirmed that PXN imports AMP against CoA, as it has been previously described by Agrimi et al. (2012). Here, we also tested the opposite transport mode and externally offered labelled CoA for exchange with preloaded AMP or CoA. However, we did not detect substantial CoA uptake rates when PXN was reconstituted (Fig. 3D+F). Based on these results we assume that PXN has a very low affinity to CoA and thus CoA cannot be efficiently transported by PXN at low CoA concentrations. In animal tissue the cytosolic CoA concentration is estimated between 0.02 – 0.14 mM and the peroxisomal levels of

free CoA are approximately 0.7 mM (Leonardi et al., 2005). Since the intracellular concentration of CoA in plants is also very low compared to acetyl-CoA amounts (Tumaney et al., 2004), we do not expect a physiological (*in vivo*) role of PXN in supplying peroxisomes with CoA.

To address the *in vivo* transport function of PXN, we used different *S. cerevisiae* mutant strains. First, we analyzed a yeast strain deficient in the malate/oxaloacetate redox shuttle due to deletion of the peroxisomal malate dehydrogenase Mdh3p. This mutant is unable to metabolize fatty acids, because NAD required for β-oxidation cannot be regenerated (van Roermund et al., 1995). Our complementation assay revealed that the growth on oleate and the activity of octanoate oxidation were partially restored in the presence of PXN (Fig. 4B+C), indicating that PXN might catalyze a NAD/NADH exchange.

When the peroxisomal enzyme Npy1p, which degrades NADH to AMP to prevent NADH accumulation (AbdelRaheim et al., 2001), was deleted in the *mdh3Δ* mutant, PXN was unable to suppress the β-oxidation phenotype of the corresponding double mutant (Fig. 5B). From this result we conclude that PXN substitutes the loss of *MDH3* via the import of cytosolic NAD in exchange with peroxisomal AMP, the latter being generated by Npy1p-mediated NADH degradation. This PXN-catalyzed transport mode supplies β-oxidation with NAD even when the redox shuttle is compromised. We confirmed this hypothesis with an independent phenotype suppression experiment. We artificially targeted PXN to yeast mitochondria (Fig. 6) and demonstrated that mitochondrially targeted PXN was able to partly replace the endogenous mitochondrial NAD carriers Ndt1p and Ndt2p, which catalyze NAD/AMP exchange and do not accept NADH as substrate (Todisco et al., 2006; Fig. 7F). The successful suppression of the *ndt1Δ/ndt2Δ* mutant phenotype by PXN indicated this carrier to catalyze NAD/AMP exchange under *in vivo* conditions.

Our work provides strong evidence that the main function of PXN is to supply peroxisomes with NAD. In other eukaryotic organisms an analogous peroxisomal NAD import system has not yet been identified (Visser et al., 2007; Linka and Theodoulou, 2013). However, the loss of the *MDH3* gene in *S. cerevisiae* did not fully abolish fatty acid oxidation activity. We still observed in the *mdh3Δ* mutant residual fatty acid oxidation activities of 31% compared to the wild type (Fig. 4C). Thus, we assume that the impaired redox shuttle across the peroxisomal membrane is partially compensated by an endogenous NAD carrier of yeast peroxisomes, but the

abundance of these proteins is lower than the constitutively expressed PXN in the yeast mutant background. The higher import activity of the recombinant PXN protein led to a significant restoration of the phenotype (Fig. 4C). One prime candidate for mediating the NAD import into yeast peroxisomes is the peroxisomal ATP carrier Ant1p (Palmieri et al., 2001; van Roermund et al., 2001), which is the closest relative of PXN in yeast. Uptake studies using recombinant protein confined the substrate specificity of Ant1p to ATP, ADP, and AMP (Palmieri et al., 2001). However, in this study only (desoxy) nucleotides were tested. Thus, we investigated if cell-free expressed Ant1p has a larger substrate spectrum (Fig. S1). Based on this first analysis Ant1p is unable to transport NAD, implying that other putative carrier proteins are involved in the uptake of NAD into yeast peroxisomes. Further yeast candidates for peroxisomal NAD import are the two mitochondrial Ndt proteins (Todisco et al., 2006). These carriers are able to specifically import NAD and might be dual-targeted to yeast peroxisomes, since several mitochondrial proteins have been found in peroxisomes as well (Carrie et al., 2009; Yogev and Pines, 2011; Ast et al., 2013). Ndt1p has been demonstrated by GFP fusion to be located to mitochondria (Todisco et al., 2006), whereas the mitochondrial localization of Ndt2p has not been experimentally validated. A putative alternative route for supplying yeast peroxisomes with NAD is via vesicular traffic from the ER, but up to now there is no evidence for this route (Hoepfner et al., 2005).

In this work we showed that PXN likely acts as NAD/AMP transporter *in vivo* and excluded other postulated transport functions. Consequently, additional transport systems in the peroxisomal membrane must exist to mediate CoA uptake or the redox shuttle in plants. In humans a peroxisomal CoA carrier has been identified, which belongs to the mitochondrial carrier family, as is the case for PXN (Agrimi et al., 2012b). Thus, one of the 58 members of this protein family encoded by the Arabidopsis genome might provide the peroxisomal β-oxidation with CoA (Haferkamp and Schmitz-Esser, 2012). An independent uptake route for this cofactor might be the peroxisomal fatty acid transporter, called PXA1 (also known as AtABCD1, CTS, PED3, ACN2; Zolman et al., 2001). It has been shown that this membrane protein has an additional intrinsic thioesterase function (De Marcos Lousa et al., 2013). During the import of acyl-CoAs into plant peroxisomes, this enzymatic activity of PXA1 releases the CoA moiety likely on the luminal side of the peroxisome membrane, resulting in a net CoA uptake (De Marcos Lousa et al., 2013). A

peroxisomal pore-forming channel (porin) has been proposed to mediate the exchange of malate and oxaloacetate, which acts as a redox shuttle that connects the cytosolic and peroxisomal NAD/NADH pools (Linka and Theodoulou, 2013). Such a porin has been characterized by electrophysiological experiments using spinach leaf peroxisomes and castor bean glyoxysomes (Reumann et al., 1995; Reumann et al., 1996; Reumann et al., 1997), but the identity of the corresponding proteins remains elusive. In mammals Pxmp2 has been characterized as a channel-forming peroxisomal protein (Rokka et al., 2009). The respective Arabidopsis ortholog might represent a candidate protein for linking the peroxisomal and cytosolic pools of NADH in plants (Linka and Theodoulou, 2013). A major challenge for the future will be to identify the genes responsible for the transport processes mentioned above, which are required to execute the great diversity of peroxisomal functions in plants.

MATERIAL AND METHODS

Materials

Chemicals were purchased from Sigma-Aldrich (www.sigmaaldrich.com). Reagents and enzymes for recombinant DNA techniques were obtained from Invitrogen (www.invitrogen.com), New England Biolabs (www.neb.com), Qiagen (www.qiagen.com), Thermo Scientific (www.thermoscintificbio.com) and Promega (www.promega.com). Anion exchange resin was purchased from Bio-Rad Laboratories (www.bio-rad.com). Radiochemical [α-^{32}P]-AMP, [α-^{32}P]-NAD, and [^{3}H]-CoA were obtained from Hartmann Analytic (www.hartmann-analytic.de) and Perkin Elmer (www.perkinelmer.de).

Cloning procedures

In silico DNA sequences for cloning were retrieved from the Aramemnon database (aramemnon.uni-koeln.de) and the Saccharomyces Genome database (www.yeastgenome.org). Cloning was performed according to standard molecular techniques (Sambrook et al., 1989). Sequences were verified by DNA sequencing (Macrogen, dna.macrogen.com). Primers were synthesized by Sigma-Aldrich. The oligonucleotide sequences used in this study are listed in the supplementary data table S1.

The coding sequence (CDS) of PXN (At2g39970) was amplified via PCR using the cDNA clone pda.00682 provided by Riken BioResource Center as a template. For the yeast expression, PXN was fused at the C-terminus with a His-tag under the control of the galactose-inducible promoter pGAL1. The pYES2 vector was chosen, in which a linker sequence (NL230/NL231) encoding for 6 histidine residues was introduced via BamHI and XbaI, yielding pNL14. The gene-specific primers NL33 (HindIII) and NL34 (BamHI) were used to clone the PXN open reading frame (ORF) into the pNL14 expression vector, resulting in pMSU219. The mitochondrial target sequence from the mitochondrial succinate/fumarate carrier (At5g01340) was introduced into pNL14 via the corresponding linker sequence (P75/P76). The obtained vector was named pNL33. The PXN CDS amplified by NL335/NL34 was then inserted into pNL33 vector via BamHI. The resulted pMSU237 construct was used for the inducible expression of mt-PXN-His fusion protein in yeast.

For the complementation studies of the *ndt1Δ/ndt2Δ* yeast mutant the constitutive promoter of the plasma membrane H^{+}-ATPase (pPMA1) from *S.*

cerevisiae (Rentsch et al., 1995) was cloned into pNL33, in which the pGAL1 promoter was removed. The resulting pNL24 vector was then used to introduce the enhanced yellow fluorescent protein (EYFP) via BamHI and XbaI. To this end, a PCR product encoding for EYFP was generated by PCR using the NL350/351 primer pair. The obtained vector was named pNL34. The PXN CDS amplified by NL335/NL34 was then inserted into pNL24 and pNL34 vector via BamHI, resulting in the constructs pMSU377 and pMSU388, respectively. The *mdh3Δ* and *mdh3Δ/nyp1Δ* mutant were transformed with the yeast expression vector pEL30 containing the PXN coding sequence. The expression of PXN was under the control of the oleate-inducible promoter pCTA1 (Elgersma et al., 1993).

Yeast strains and culture conditions

The *S. cerevisiae* strain FGY217 (MATα ura3-52 lys2Δ201 pep4Δ) was used for PXN uptake studies (Kota et al., 2007). For complementing the *mdh3Δ and mdh3/npy1Δ* mutant phenotype the BJ1991 yeast cells (Mat-α, *leu2,trp1,ura3-251,prb1-1122,pep4-3,gal2*) were used as wild type strain. The following derivatives of this strain, all impaired in β-oxidation, were used: *fox1Δ* and *mdh3Δ* (carrying a deletion of the acyl-CoA oxidase or peroxisomal malate dehydrogenase, respectively). These mutants were constructed from BJ1991 as described by (van Roermund et al., 1995). The *mdh3Δ/npy1Δ* double mutant was created by replacing the whole *NPY1* ORF from the *mdh3Δ*::LEU mutant by the *BLE* gene conferring resistance to phleomycin. The *NPY1* deletion construct was made by PCR using the pUG66 plasmid (Gueldener et al., 2002) as a template and the CVR1 and CVR2 primers. BLE+ transformants were selected for integration in the *NPY1* gene by PCR analysis.

BY4741 (*MATa, his3*Δ1, *leu2*Δ0, *met15*Δ0, *ura3*Δ0) was used for subcellular localization of mt-PXN-EYFP. For the generation of the *ndt1*Δ/*ndt2*Δ double mutant, the *ndt1Δ* single mutant (BY4741; Mat a; his3D1; leu2D0; met15D0; ura3D0; YIL006w::kanMX4) was obtained from the EUROSCARF collection (http://web.uni-frankfurt.de/fb15/mikro/euroscarf). The *NDT2* gene in *ndt1Δ* single mutant was disrupted by PCR-mediated gene replacement using the *LEU2* cassette, amplified from pUG73 (Gueldener et al., 2002) with the primer set NL352/353. Transformed yeast cells that were able to grow in the absence of leucine were selected and the presence of the *LEU2* cassette was verified by PCR analysis.

Yeast cells were transformed according to standard protocols for lithium acetate/PEG transformation (Gietz and Schiestl, 2007). Yeast cells were selected on synthetic complete medium (SC; 0.67% (w/v) YNB supplemented with appropriate amino acids and bases for auxotrophy and a carbon source).

Heterologous protein expression in yeast for uptake studies

For the heterologous expression, the FGY217 strain was transformed with the empty vectors pNL14 and pNL33 or the expression constructs pMSU219 (PXN-His) and pMSU237 (mt-PXN-His). 50 ml of SC-U medium containing 2% (w/v) glucose were inoculated with an overnight culture and cultured to an OD_{600} of 0.4. The yeast cells were aerobically grown for 6 h at 30°C. Control cultures with the empty vectors were processed in parallel. Harvest and enrichment of total yeast membranes without and with heterologously expressed PXN protein were achieved according to (Linka et al., 2008).

Protein biochemistry

SDS-PAGE and immunoblot analyses were conducted as described in Sambrook et al. (1989). For immunodetection, either α-polyhistidine HPR-conjugated mouse IgG1 antibody (MACS molecular, http://www.miltenyibiotec.com) or the PXN-specific antibody (Bernhardt et al., 2012) was used. None tagged PXN-variants were visualized using anti-PXN-specific serum (Bernhardt et al., 2012) and AP-conjugated anti-rabbit IgG (Promega). PageRuler Prestained Protein Ladder (New England Biolabs) was used to estimate molecular masses. Protein concentrations were determined using a bicinchoninic acid assay (ThermoScientific).

Reconstitution of transport activities into liposomes

Yeast membranes were reconstituted into 3% (w/v) L-α-phosphatidylcholine by a freeze-thaw-sonication procedure for *in vitro* uptake studies, as described in (Linka et al., 2008). Proteoliposomes were either preloaded with 10 mM NAD, AMP, CoA or produced without pre-loading (negative control). Counter-exchange substrate, which was not incorporated into proteoliposomes, was removed via gel filtration on Sephadex G-25M columns (GE Healthcare, www.gehealthcare.com).

Transport assays were started via addition of 0.2 mM [α-^{32}P]-AMP, [α-^{32}P]-NAD or [^{3}H]-CoA. The uptake reaction was terminated via passing proteoliposomes

over Dowex AG1-X8 anion-exchange columns. The incorporated radiolabeled compounds were analyzed by liquid scintillation counting. Time-dependent uptake data were fitted using nonlinear regression analysis based on one-phase exponential association using GraphPad Prism 5.0 software (GraphPad, www.graphpad.com).

Suppression analysis of the *ndt1Δ*/*ndt2Δ* double mutant

Wild type strain BY4741 and *ndt1Δ*/*ndt2Δ* double mutant was transformed with the empty vector pNL24 and pMSU377 expressing mt-PXN-His. Yeast cells were grown on YNB-uracil supplemented with either 2% (w/v) glucose or 2% (v/v) ethanol, as described in (Todisco et al., 2006)

β-oxidation activity measurements

β-oxidation assays in intact yeast cells were performed as described previously by (van Roermund et al., 1995). Cells were grown 17 h in media containing oleate to induce β-oxidation. The β-oxidation activity was measured in 200 µl of 50 mM MES (pH 6.0) and 0.9% (w/v) NaCl supplemented with 10 µM [1-^{14}C]-octanoate. Subsequently, [1-^{14}C]-CO_2 was trapped with 2 M NaOH and used to quantify the rate of fatty acid oxidation. Results are presented as percentage relative activity to the rate of oxidation of wild type cells. In wild-type cells the rates of octanoate oxidation is 7.84+/- 1.09 nmol * min^{-1} * OD cells^{-1}.

Fluorescence microscopy

BY4741 cells transformed with pMSU388 for expression of the mt-PXN-EYFP fusion protein were grown in liquid culture overnight in SC-Ura with 2% (w/v) glucose. Yeast cells were harvested by centrifugation for 5 min at 3,000 g, washed with 25 mM Hepes-KOH (pH 7.3) and 10 mM $MgCl_2$ and then stained with 50 µM MitoTracker ORANGE CMTMRos (Life Technologies) for 10 min at room temperature. Residual Mito Tracker dye was removed by washing with wash buffer twice. Yeast cells were immobilized on poly-L-Lysine coated microscope slides for confocal microscopy. Analysis of yeast cells was performed with a confocal laser scanning microscope LSM 510 Meta (Carl Zeiss). MitoTracker fluorescence was excited at 561 nm, fluorescence emission was detected with a 575 nm to 615 nm band pass filter. EYFP fluorescence was excited at 514 nm and the emission was recorded with a 530 nm to 600 nm band-pass filter.

ACKNOWLEDGEMENTS

This work was supported by DFG-grant 1781/2-1 (to NL), GRK 1525 (to NL), and EXC1028 (to APMW). Authors thank Jeanine Schlebusch and Daniel Wrobel for assistance with obtaining yeast growth curves. For technical assistance the authors acknowledge Kirsten Abel. We thank Dr. R. van der Bend from Saxion Hogeschool (Life Science, Engineering and Design) in Deventer for assistance in creating the *npy1Δ* and *mdh3Δ/npy1Δ* double mutants and are grateful to Lodewijk IJlst for stimulating discussion.

AUTHOR CONTRIBUTIONS

Martin Schroers, Nicole Linka and Carlo van Roermund designed the experiments. Nicole Linka and Martin Schroers wrote the manuscript. Martin Schroers established the assay for measuring uptake of ^{3}H-CoA. Uptake data presented in the manuscript was generated by Martin Schroers, Nicole Linka, and Samantha Kurz. The supplemented Ant1p substrate specificity test was performed by Lennart Charton. Jan Wiese provided localization data for mt-PXN-EYFP. Sabrina Wilkinson generated the *ndt* yeast mutants and cloned the first mt-PXN constructs for complementation. Growth curves of the *mdh3Δ* mutant and respective complementants were performed by Carlo van Roermund. Growth curves with *ndt1Δ/ndt2Δ* mutants and respective complementants were generated by Martin Schroers, Nicole Linka, and Sabrina Wilkinson. Fatty acid oxidation activity measurements were done by Carlo van Roermund. Ronald Wanders, Hans Waterham, and Andreas Weber provided lab space and helpful discussions.

SUPPLEMENTAL DATA

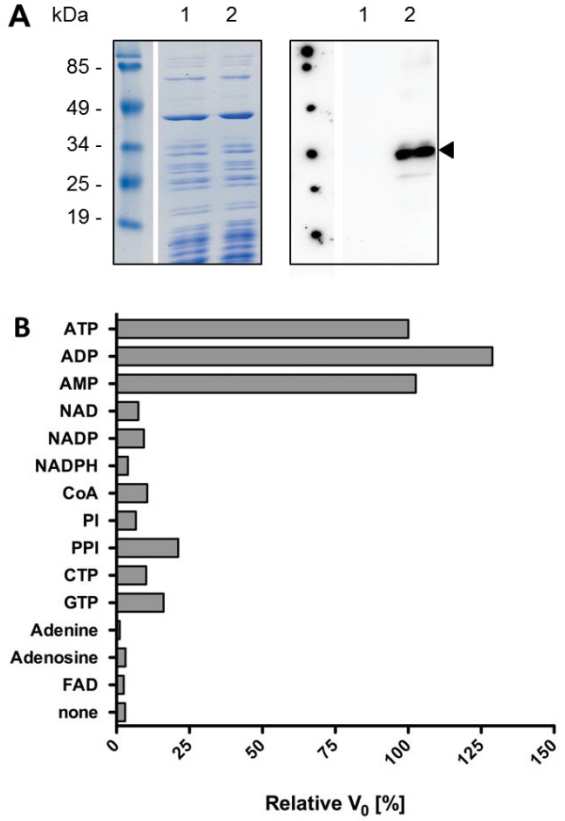

Supplemented figure S1: **Substrate specificity of the peroxisomal ATP carrier Ant1p from *S. cerevisiae*.**
(**A**) Expression of Ant1p-HA fusion protein in a cell-free *E.coli*-based system, was verified by immunodetection: shown are a coomassie stained protein gel and a western blot using HA-specific antibody; 1: negative control, 2: Ant1p-HA (arrowhead).
(**B**) We reconstituted the recombinant Ant1p-HA into liposomes. To test which substrates can be handled by Ant1p, vesicles were preloaded with saturating concentrations (i.e. 20 mM) of various potential counter-exchange substrates and the initial rates of [α-^{32}P]-ATP uptake (100 µM) were determined. Relative uptake activities were compared with the ATP/ATP homo-exchange experiment, which was set to 100%.

Table S1. Primer used in this study. Restriction sites (RS) are underlined

Name	RS	Sequence in 5' – 3' orientation
NL33	HindIII	cacacaagcttaccatggcggacgct
NL34	BamHI	cacacggatccgctagaggtagcgt
NL230		gatcccatcatcatcatcattgat
NL231		ctagatcaatgatgatgatgatgg
NL335	BamHI	cacacggatcctcggacgctttgatcaatg
NL350	BamHI	cacacggatccatggtgagcaagggcgag
NL351	XbaI	cacactctagattacttgtacagctcgtccatgc
NL352		tcattgtttgatgaaaagcggaatatacatcacggctatataatgcagctgaagcttcgtacgc
NL353		tacgaccctcagcttgtgtcatgtacatttttctgtttcactttagcataggccactagtggatctg
P75		agcttaccatggcgacgagaacggaatcgaagaagcagattccgccggagct
P76		ccggcggaatctgcttcttcgattccgttctcgtcgccatggaa
CVR1		gcccaccaaccataagaataaagaacaagagcaggagcgaaacgaaagagcagctgaagcttcgtacgc
CVR2		tatccatatgctgaagcacgcctatttatcaatgtttattatattaaaaagcataggccactagtggatctg

REFERENCES

AbdelRaheim, S.R., Cartwright, J.L., Gasmi, L. and McLennan, A.G. (2001) The NADH diphosphatase encoded by the Saccharomyces cerevisiae NPY1 nudix hydrolase gene is located in peroxisomes. *Arch Biochem Biophys*, **388**, 18-24.

Agrimi, G., Brambilla, L., Frascotti, G., Pisano, I., Porro, D., Vai, M. and Palmieri, L. (2011) Deletion or overexpression of mitochondrial NAD+ carriers in Saccharomyces cerevisiae alters cellular NAD and ATP contents and affects mitochondrial metabolism and the rate of glycolysis. *Appl Environ Microbiol*, **77**, 2239-2246.

Agrimi, G., Russo, A., Pierri, C.L. and Palmieri, F. (2012a) The peroxisomal NAD+ carrier of Arabidopsis thaliana transports coenzyme A and its derivatives. *J Bioenerg Biomembr*, **44**, 333-340.

Agrimi, G., Russo, A., Scarcia, P. and Palmieri, F. (2012b) The human gene SLC25A17 encodes a peroxisomal transporter of coenzyme A, FAD and NAD+. *Biochem J*, **443**, 241-247.

Ast, J., Stiebler, A.C., Freitag, J. and Bolker, M. (2013) Dual targeting of peroxisomal proteins. *Front Physiol*, **4**, 297.

Bernhardt, K., Wilkinson, S., Weber, A.P. and Linka, N. (2012) A peroxisomal carrier delivers NAD(+) and contributes to optimal fatty acid degradation during storage oil mobilization. *Plant J*, **69**, 1-13.

Carrie, C., Kuhn, K., Murcha, M.W., Duncan, O., Small, I.D., O'Toole, N. and Whelan, J. (2009) Approaches to defining dual-targeted proteins in Arabidopsis. *Plant J*, **57**, 1128-1139.

Catoni, E., Schwab, R., Hilpert, M., Desimone, M., Schwacke, R., Flugge, U.I., Schumacher, K. and Frommer, W.B. (2003) Identification of an Arabidopsis mitochondrial succinate-fumarate translocator. *FEBS Lett*, **534**, 87-92.

Chambon, P., Weill, J.D. and Mandel, P. (1963) Nicotinamide mononucleotide activation of new DNA-dependent polyadenylic acid synthesizing nuclear enzyme. *Biochem Biophys Res Commun*, **11**, 39-43.

De Marcos Lousa, C., van Roermund, C.W., Postis, V.L., Dietrich, D., Kerr, I.D., Wanders, R.J., Baldwin, S.A., Baker, A. and Theodoulou, F.L. (2013) Intrinsic acyl-CoA thioesterase activity of a peroxisomal ATP binding cassette transporter is required for transport and metabolism of fatty acids. *Proc Natl Acad Sci U S A*.

Droge, W. (2002) Free radicals in the physiological control of cell function. *Physiological reviews*, **82**, 47-95.

Elgersma, Y., van den Berg, M., Tabak, H.F. and Distel, B. (1993) An efficient positive selection procedure for the isolation of peroxisomal import and peroxisome assembly mutants of Saccharomyces cerevisiae. *Genetics*, **135**, 731-740.

Fulda, M., Schnurr, J., Abbadi, A., Heinz, E. and Browse, J. (2004) Peroxisomal Acyl-CoA synthetase activity is essential for seedling development in Arabidopsis thaliana. *Plant Cell*, **16**, 394-405.

Gietz, R.D. and Schiestl, R.H. (2007) High-efficiency yeast transformation using the LiAc/SS carrier DNA/PEG method. *Nature protocols*, **2**, 31-34.

Graham, I.A. (2008) Seed storage oil mobilization. *Annu Rev Plant Biol*, **59**, 115-142.

Gueldener, U., Heinisch, J., Koehler, G.J., Voss, D. and Hegemann, J.H. (2002) A second set of loxP marker cassettes for Cre-mediated multiple gene knockouts in budding yeast. *Nucleic Acids Res*, **30**, e23.

Haferkamp, I. and Schmitz-Esser, S. (2012) The plant mitochondrial carrier family: functional and evolutionary aspects. *Frontiers in plant science*, **3**, 2.

Hiltunen, J.K., Wenzel, B., Beyer, A., Erdmann, R., Fossa, A. and Kunau, W.H. (1992) Peroxisomal multifunctional beta-oxidation protein of Saccharomyces cerevisiae. Molecular analysis of the fox2 gene and gene product. *J Biol Chem*, **267**, 6646-6653.

Hoepfner, D., Schildknegt, D., Braakman, I., Philippsen, P. and Tabak, H.F. (2005) Contribution of the endoplasmic reticulum to peroxisome formation. *Cell*, **122**, 85-95.

Houtkooper, R.H., Canto, C., Wanders, R.J. and Auwerx, J. (2010) The secret life of NAD+: an old metabolite controlling new metabolic signaling pathways. *Endocrine reviews*, **31**, 194-223.

Imai, S., Armstrong, C.M., Kaeberlein, M. and Guarente, L. (2000) Transcriptional silencing and longevity protein Sir2 is an NAD-dependent histone deacetylase. *Nature*, **403**, 795-800.

Kota, J., Gilstring, C.F. and Ljungdahl, P.O. (2007) Membrane chaperone Shr3 assists in folding amino acid permeases preventing precocious ERAD. *J Cell Biol*, **176**, 617-628.

Landry, J., Sutton, A., Tafrov, S.T., Heller, R.C., Stebbins, J., Pillus, L. and Sternglanz, R. (2000) The silencing protein SIR2 and its homologs are NAD-dependent protein deacetylases. *Proc Natl Acad Sci U S A*, **97**, 5807-5811.

Leonardi, R., Zhang, Y.M., Rock, C.O. and Jackowski, S. (2005) Coenzyme A: back in action. *Prog Lipid Res*, **44**, 125-153.

Linka, N. and Esser, C. (2012) Transport proteins regulate the flux of metabolites and cofactors across the membrane of plant peroxisomes. *Frontiers in plant science*, **3**, 3.

Linka, N. and Theodoulou, F.L. (2013) Metabolite transporters of the plant peroxisomal membrane: known and unknown. *Sub-cellular biochemistry*, **69**, 169-194.

Linka, N., Theodoulou, F.L., Haslam, R.P., Linka, M., Napier, J.A., Neuhaus, H.E. and Weber, A.P. (2008) Peroxisomal ATP import is essential for seedling development in Arabidopsis thaliana. *Plant Cell*, **20**, 3241-3257.

Mettler, I.J. and Beevers, H. (1980) Oxidation of NADH in Glyoxysomes by a Malate-Aspartate Shuttle. *Plant Physiol*, **66**, 555-560.

Mittler, R. (2002) Oxidative stress, antioxidants and stress tolerance. *Trends Plant Sci*, **7**, 405-410.

Palmieri, F., Rieder, B., Ventrella, A., Blanco, E., Do, P.T., Nunes-Nesi, A., Trauth, A.U., Fiermonte, G., Tjaden, J., Agrimi, G., Kirchberger, S., Paradies, E., Fernie, A.R. and Neuhaus, H.E. (2009) Molecular identification and functional characterization of Arabidopsis thaliana mitochondrial and chloroplastic NAD+ carrier proteins. *J Biol Chem*, **284**, 31249-31259.

Palmieri, L., Rottensteiner, H., Girzalsky, W., Scarcia, P., Palmieri, F. and Erdmann, R. (2001) Identification and functional reconstitution of the yeast peroxisomal adenine nucleotide transporter. *EMBO J*, **20**, 5049-5059.

Palmieri, L., Santoro, A., Carrari, F., Blanco, E., Nunes-Nesi, A., Arrigoni, R., Genchi, F., Fernie, A.R. and Palmieri, F. (2008) Identification and characterization of ADNT1, a novel mitochondrial adenine nucleotide transporter from Arabidopsis. *Plant Physiol*, **148**, 1797-1808.

Pollak, N., Dolle, C. and Ziegler, M. (2007) The power to reduce: pyridine nucleotides--small molecules with a multitude of functions. *Biochem J*, **402**, 205-218.

Pracharoenwattana, I., Cornah, J.E. and Smith, S.M. (2007) Arabidopsis peroxisomal malate dehydrogenase functions in beta-oxidation but not in the glyoxylate cycle. *Plant J*, **50**, 381-390.

Rentsch, D., Laloi, M., Rouhara, I., Schmelzer, E., Delrot, S. and Frommer, W.B. (1995) NTR1 encodes a high affinity oligopeptide transporter in Arabidopsis. *FEBS Lett*, **370**, 264-268.

Reumann, S., Bettermann, M., Benz, R. and Heldt, H.W. (1997) Evidence for the Presence of a Porin in the Membrane of Glyoxysomes of Castor Bean. *Plant Physiol*, **115**, 891-899.

Reumann, S., Maier, E., Benz, R. and Heldt, H.W. (1995) The membrane of leaf peroxisomes contains a porin-like channel. *J Biol Chem*, **270**, 17559-17565.

Reumann, S., Maier, E., Benz, R. and Heldt, H.W. (1996) A specific porin is involved in the malate shuttle of leaf peroxisomes. *Biochem Soc Trans*, **24**, 754-757.

Rokka, A., Antonenkov, V.D., Soininen, R., Immonen, H.L., Pirila, P.L., Bergmann, U., Sormunen, R.T., Weckstrom, M., Benz, R. and Hiltunen, J.K. (2009) Pxmp2 is a channel-forming protein in Mammalian peroxisomal membrane. *PLoS One*, **4**, e5090.

Sambrook, J., Fritsch, E.F. and Maniatis, T. (1989) *Molecular Cloning: A Laboratory Manual*: Cold Spring Harbor Laboratory Press.

Todisco, S., Agrimi, G., Castegna, A. and Palmieri, F. (2006) Identification of the mitochondrial NAD+ transporter in Saccharomyces cerevisiae. *J Biol Chem*, **281**, 1524-1531.

Tumaney, A.W., Ohlrogge, J.B. and Pollard, M. (2004) Acetyl coenzyme A concentrations in plant tissues. *J Plant Physiol*, **161**, 485-488.

van Roermund, C.W., Drissen, R., van Den Berg, M., Ijlst, L., Hettema, E.H., Tabak, H.F., Waterham, H.R. and Wanders, R.J. (2001) Identification of a peroxisomal ATP carrier required for medium-chain fatty acid beta-oxidation and normal peroxisome proliferation in Saccharomyces cerevisiae. *Molecular and cellular biology*, **21**, 4321-4329.

van Roermund, C.W., Elgersma, Y., Singh, N., Wanders, R.J. and Tabak, H.F. (1995) The membrane of peroxisomes in Saccharomyces cerevisiae is impermeable to NAD(H) and acetyl-CoA under in vivo conditions. *EMBO J*, **14**, 3480-3486.

Visser, W.F., van Roermund, C.W., Ijlst, L., Waterham, H.R. and Wanders, R.J. (2007) Metabolite transport across the peroxisomal membrane. *Biochem J*, **401**, 365-375.

Yogev, O. and Pines, O. (2011) Dual targeting of mitochondrial proteins: mechanism, regulation and function. *Biochim Biophys Acta*, **1808**, 1012-1020.

Zolman, B.K., Silva, I.D. and Bartel, B. (2001) The Arabidopsis pxa1 mutant is defective in an ATP-binding cassette transporter-like protein required for peroxisomal fatty acid beta-oxidation. *Plant Physiol*, **127**, 1266-1278.

IV.2 *Manuscript 2*

Regulation of the peroxisomal NAD carrier from Arabidopsis by phosphorylation

Martin G. Schroers[1], Kristin Bernhardt[1], Andreas P. M. Weber[1] and Nicole Linka[1,2]

[1] Institute for Plant Biochemistry and Cluster of Excellence on Plant Sciences (CEPLAS), Heinrich Heine University, Universitaetsstrasse 1, 40225 Duesseldorf, Germany.

[2] To whom correspondence should be addressed. E-Mail: Nicole.Linka@hhu.de.

ABSTRACT

The peroxisomal NAD transporter from Arabidopsis, called PXN, supplies peroxisomes with NAD by mediating the import of cytosolic NAD against AMP. A proteomic approach demonstrated that PXN is *in vivo* phosphorylated at S155. Here we show that this phosphorylation site is located inside an elongated hydrophilic loop region linking the transmembrane spanning domains three and four, which is unique among MCF transporters, but conserved in PXN homologues. Phosphorylation of PXN_S155 enhances the transport activity of NAD against AMP without altering the affinity to NAD.

INTRODUCTION

The *Arabidopsis thaliana* peroxisomal NAD carrier (PXN; At2G39970) belongs to the Mitochondrial Carrier Family (MCF). Despite their name MCF carriers are not exclusively localized to mitochondria but have been identified in various organelles; e.g., peroxisomes, plastids, the endoplasmic reticulum, and the plasma membrane (Bedhomme et al., 2005; Thuswaldner et al., 2007; Leroch et al., 2008; Linka et al., 2008; Rieder and Neuhaus, 2011; Bernhardt et al., 2012). MCF proteins are nuclear encoded transporters of about 30 – 40 kDa in size (PXN: 331 amino acids; 36.2 kDa) and conserved in eukaryotes. They all share common characteristic structural features: three repetitive structures of about 100 amino acids, each composed of two α-helical transmembrane spans, connected by hydrophilic loops. A conserved so called mitochondrial energy transfer signature (or MCF motif; Pfam PF00153) directly follows each odd-numbered transmembrane span. MCF carriers mediate the exchange of different substrates, such as nucleotides, carboxylic acids, amino acids, keto acids, and phosphate (Palmieri et al., 2011).

PXN has been identified to be peroxisomal localized (Bernhardt et al., 2012). *In vitro* uptake studies revealed PXN to be functioning as an antiporter with a rather broad substrate range. Among other substrates PXN is able to transport NAD, NADH, AMP, and CoA (Agrimi et al., 2012; Bernhardt et al., 2012). Recently we were able to identify that the exchange of NAD against AMP is most likely the *in vivo* function of PXN (*Manuscript 1*). The role of PXN is likely to assist the malate/oxaloacetate shuttle by providing sufficient amounts of NAD for peroxisomal β-oxidation or by establishing the peroxisomal NAD-pool in the first place (Bernhardt et al., 2012).

In the present study we elucidate the role of a phosphorylation site contained in a unique elongated hydrophilic loop region, which links PXN's transmembrane spanning domains three and four, in regards of transport activity. This phosphorylation of serine155 was identified by a proteome analysis (Eubel et al., 2008). Phosphorylation of transporter proteins is a known but not well studied method of their regulation. Our knowledge on how transport proteins are regulated is overall very limited. Understanding transporter regulation will help to understand how transport mechanisms are controlled and adapted to environmental changes or stresses. Phosphorylation as posttranslational protein modification can decrease or enhance the transport efficiency of a carrier. The ammonium transporter AMT1;1

from Arabidopsis builds a homotrimer whose transport activity is inactivated by phosphorylation on the C-termini (Lanquar et al., 2009; Lanquar and Frommer, 2010). In contrast activity of the wheat (*Triticum aestivum*) root malate efflux transporter TaALMT1 is increased by phosphorylation (Ligaba et al., 2009). The same is true for the tonoplast monosaccaride transporter (TMT1) from Arabidopsis (Wingenter et al., 2011). At least 28 Arabidopsis tonoplast transporters contain phosphorylation sites, which displays the widespread use of phosphorylation for transporter regulation (Whiteman et al., 2008). How exactly phosphorylation of carrier proteins leads to enhanced or decreased transport is mostly unknown. A recent publication showed the impact of phosphorylation on the Arabidopsis nitrate transporter NRT1.1, where it leads to uncoupling of a homodimer with low substrate affinity into two highly active monomers (Sun et al., 2014). The present study is the first to present a MCF transporter to be regulated by phosphorylation.

RESULTS

PXN is embedded in the peroxisomal membrane by six transmembrane domains. We compared the protein sequences of different known NAD transporters and known peroxisomal transporters via sequence alignment to identify possible reasons for the unique substrate specificity of PXN (see Fig. 1 for more detail). This sequence alignment of different members of the mitochondrial carrier family (MCF) of Arabidopsis, human, and yeast revealed that PXN in contrast to the other MCF transporters possesses a unique elongated hydrophilic loop region between its transmembrane helices three and four (Fig. 1). The alignment revealed a gap in the sequence of other MCF transporters of 14 – 27 amino acids compared to PXN. The total length of the PXN loop region between predicted transmembrane domains is 43 amino acids. It is thereby elongated by 7 - 10 amino acids when compared to other MCF transporters. Interestingly, the serine on position 155 (S155), which is located inside the elongated region, has been shown to be phosphorylated (marked in red in Fig. 1+2; Eubel et al., 2008).

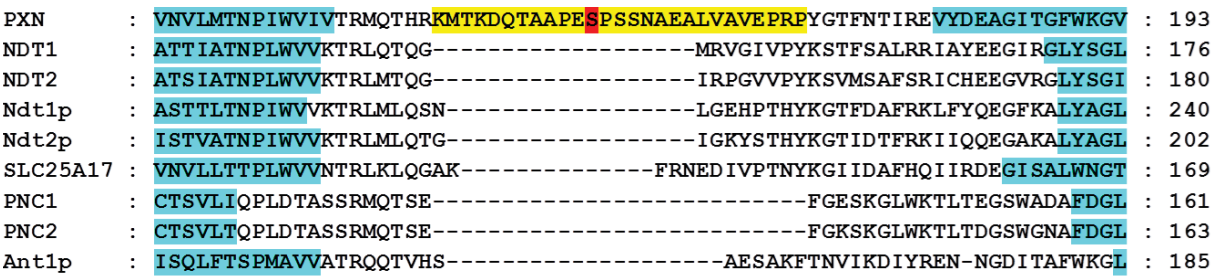

Figure 1: Segment of a protein sequence alignment of PXN and other MCF transporters
The alignment focuses on the unique elongated loop region (yellow) of PXN between its transmembrane helices three and four (marked in blue; positions taken from the UniProt database; (Leinonen et al., 2004). S155 (red) is phosphorylated (Eubel et al., 2008). NAD transporters included are: NDT1 (Arabidopsis; chloroplast), NDT2 (Arabidopsis; mitochondrium), Ndt1p and Ndt2p (yeast; mitochondrium), and SLC25A14 (human; peroxisome). ATP carriers included: PNC1 and PNC2 (Arabidopsis; peroxisome), and Ant1p (yeast; peroxisome).

To elucidate if the unique elongated loop region and the phosphorylation site are conserved in PXN homologues in different species, we aligned their protein sequences with the Arabidopsis PXN protein sequence (Fig. 2). Homologue proteins were identified by protein sequence blast analyses. Since there is no phosphoproteome data available for the PXN homologues shown in Fig. 2 we analyzed the protein sequences for predicted phosphorylation sites, using the NetPhos 2.0 server (Blom et al., 1999). This software also correctly predicts S155 of PXN to be phosphorylated. Predicted phosphorylation sites are marked in green in Fig. 2. All of the PXN homologues presented contain an elongated region similar to that of PXN (marked yellow in Fig. 2), which contrasts to other MCF transporters like PNC1 (Fig. 1+2). However, there is huge variety in the sequence of this region. The exact positions of predicted phosphorylation sites also vary between homologues, but all contain at least one in the specific region, indicating a high possibility for phosphorylation of the elongated loop in PXN homologues.

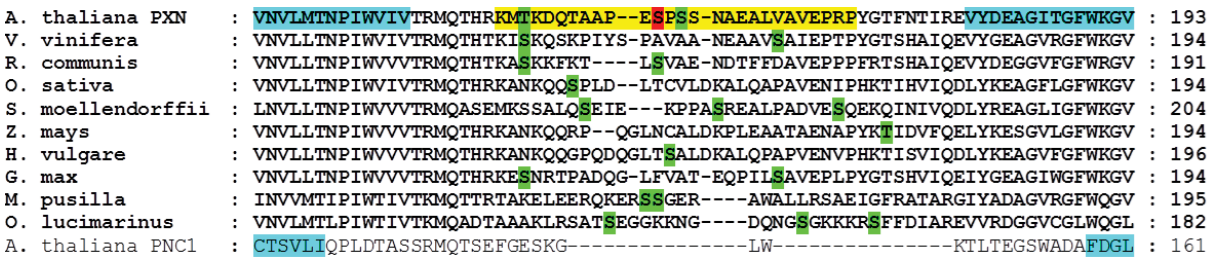

Figure 2: Segment of a protein sequence alignment of PXN and its homologues in different species

Blue: transmembrane domains (positions taken from the UniProt database; (Leinonen et al., 2004)). Yellow: elongated hydrophilic loop region of PXN (see also Fig. 1). Red: phosphorylated S155 (Eubel et al., 2008). Green: phosphorylation sites predicted with the NetPhos 2.0 server (Blom et al., 1999). Proteins included in this figure are: *A. thaliana* PXN (At2G39970), *V. vinifera* (XP_002279488), *R. communis* (XP_002526854), *O. sativa* (NP_001049647), *S. moellendorffii* (XP_002965581), *Z. mays* (NP_001152063), *H. vulgare* (BAK00413), *G. max* (XP_003552504), *M. pusilla* (XP_003059691), *O. lucimarinus* (XP_001422587). *A. thaliana* PNC1 (At3G05290) is shown for visualization of the loop elongation of PXN homologues. Full sequences can be acquired from “www.ncbi.nlm.nih.gov/protein”.

Structure models of the PXN protein were created for better visualization of the elongated loop region. The 2D model nicely showed the localization of the elongated loop in the middle of the protein (Fig. 3A). We also created a 3D model based on the published structure of the bovine ADP/ATP carrier 1 (Fig. 3B+C; (Pebay-Peyroula et al., 2003; Nury et al., 2005). Regarding to this model, the elongated loop region of PXN is indeed easily accessible for post-translational protein modifications.

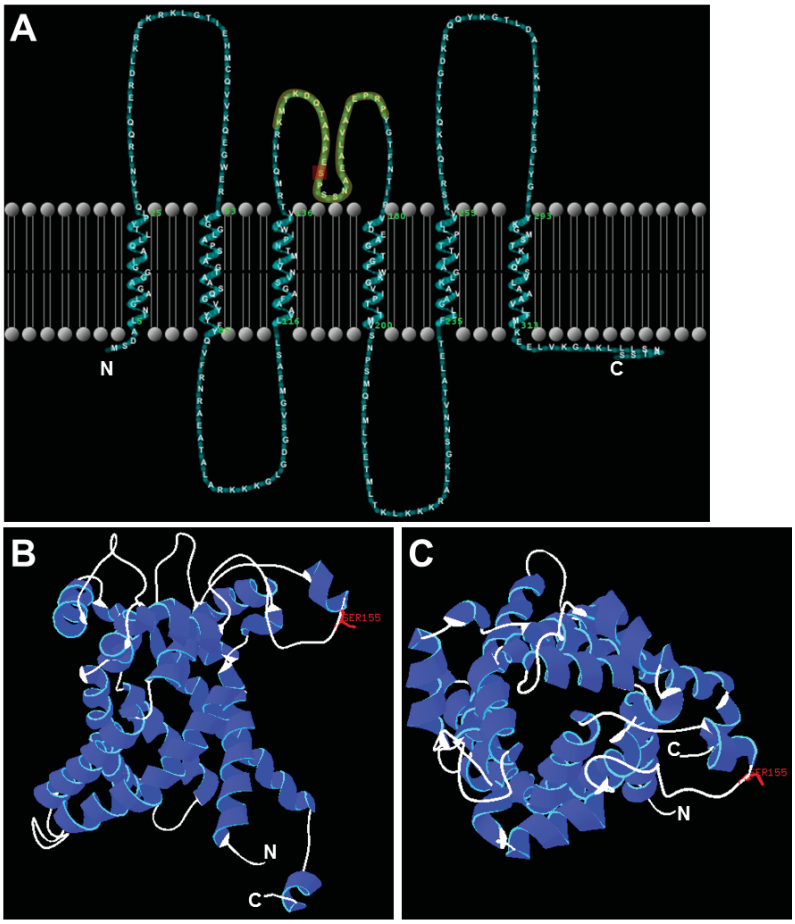

Figure 3: Models of PXN structure
A) 2D model of PXN. Positions of transmembrane domains where taken from the UniProt database (Leinonen et al., 2004) and visualized with TMRPres2D (Spyropoulos et al., 2004). The proteins N- and C-termini are indicated. The elongated loop region is highlighted in yellow, the phosphorylated Serine155 in red.
Side view (**B**) and top view (**C**) of a 3D model of PXN structure. N- and C-termini are indicated. S155 is marked in red. The model was calculated using the I-TASSER server (Zhang, 2008) and is based on the structure of the bovine ADP/ATP carrier 1 (Pebay-Peyroula et al., 2003; Nury et al., 2005). The estimated accuracy of atomic positions is 5.0 ± 3.2 Å (RSMD). The structure was visualized using Swiss-PdbViewer v4.1.0 (Guex and Peitsch, 1997).

Since phosphorylation of carriers has been shown to be a method for regulation of their transport activity (Whiteman et al., 2008; Ligaba et al., 2009; Lanquar and Frommer, 2010; Wingenter et al., 2011), we conducted uptake experiments with different altered versions of PXN. We created constructs with a point mutation on position 155 using site-directed mutagenesis. S155 was changed to cysteine (S155C), which mimics the dephosphorylated state with its sulphur group and to aspartate (S155D) to resemble the phosphorylated state with its negatively charged carboxyl group. A change of S155 to the neutral amino acid alanine (S155A) was

used as control. These different versions of the PXN protein were cell-free expressed in a wheat germ system and reconstituted into liposomes using the freeze-thaw method (Kasahara and Hinkle, 1976). We measured the time dependent uptake of 150 µM [α-$_{32}$P]-NAD into liposomes preloaded either with 5 mM NAD or AMP and reconstituted with one of the three afore mentioned PXN variants. PXN_S155D performed overall better in the [α-$_{32}$P]-NAD uptake studies conducted when compared to the dephosphomimetic variant PXN_S155C (Fig. 4). The uptake rates of the control with an uncharged amino acid (PXN_S155A) were lowest. We calculated the initial transport rates for each combination of protein and preloading from three independent experiments. There was no significant statistical difference detected between PXN_S155D (initial rate of 8.09 ± 1.98 pmol NAD * µg protein^{-1}) and PXN_S155C (2.75 ± 0.27) during NAD homo-exchange experiments due to the enormous variance for PXN_S155D triplicates (t-test: p=0.056). For NAD import in AMP preloaded liposomes the initial rate calculated for the phosphomimetic variant PXN_S155D was significantly higher and with 11.53 ± 0.81 pmol NAD * µg protein^{-1} almost doubled, when compared to PXN_S155C (5.98 ± 0.1; Fig. 4D).

To elucidate if the increased transport rates of the phosphomimetic PXN variant are due to an increased affinity to NAD we determined the Michaelis constant (K_m) for NAD transport of dephosphorylated PXN and PXN_S155D. The published K_m for PXN mediated NAD transport is 246 ± 64 µM (Bernhardt et al., 2012). We calculated a K_m of 289.2 ± 59.7 µM for dephosphorylated PXN and of 374.5 ± 58.77 µM for PXN_S155D from three independent experiments each (Fig. 4E). There was no statistical difference between these K_m values (F-test).

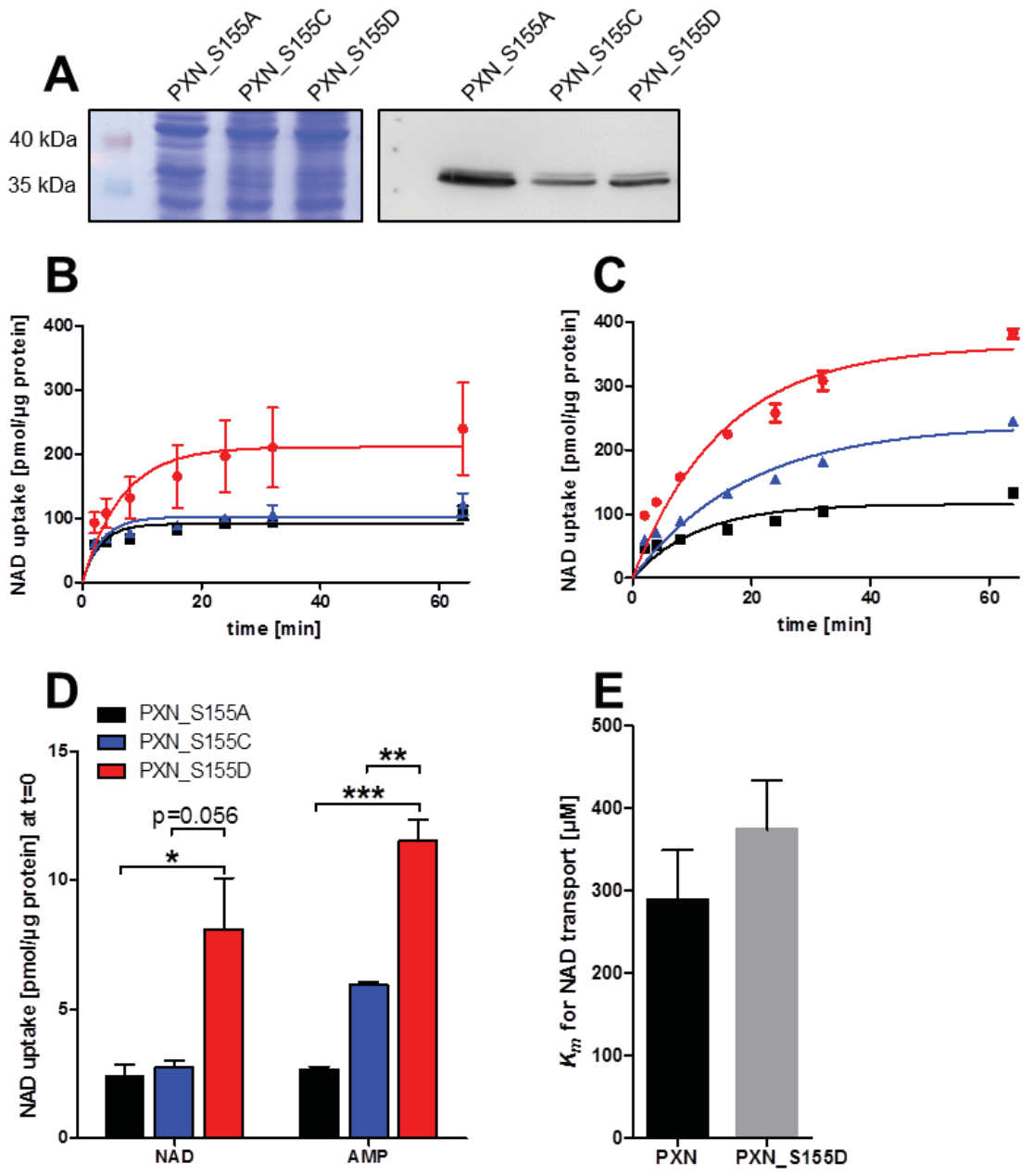

Figure 4: NAD uptake activity of different mutated PXN proteins

Cell free expression of PXN variants with calculated molecular masses of 38 kDa was positively controlled by coomassie staining and αHis immunodetection (**A**). Time dependent uptake of 150 µM [α-$_{32}$P]-NAD was measured with NAD (**B**) and AMP (**C**) preloaded proteoliposomes (5 mM), containing PXN_S155A (black), PXN_S155C (blue), or PXN_S155D (red) protein. Shown are means ± SD of three independent experiments normalized on µg protein. The calculated initial rates for the three PXN versions and the two different preloadings are plotted in graph (**D)** as mean ± SE (* P <0.05, ** P <0.01, *** P <0.001; Student's t-test). **E**: Calculated Michaelis constants (K_m) for NAD transport of dephosphorylated PXN and PXN_S155D (n=3). No statistical difference was detected.

DISCUSSION

Analysis of the PXN protein sequence revealed an elongated hydrophilic loop region to be present between the transmembrane domains three and four. This elongated loop is not common among other MCF transporters (Fig. 1), but conserved in PXN homologues in different higher plant or algae species (Fig. 2). Within this elongated region of PXN resides a phosphorylated serine (S155; marked red in Fig. 1+2). This phosphorylation site has been predicted *in silico* in this study using NetPhos 2.0 server and been shown to be present *in vivo* by a proteome analysis (Eubel et al., 2008). Due to a lack of phosphoproteomic data regarding the PXN homologues presented in Fig. 2, it is not possible to state if this phosphorylation site has been conserved. However, each of the homologues carries at least one predicted phosphorylation site inside its elongated region. Thereby it is reasonable to assume that phosphorylation of the elongated loop occurs in PXN homologues as well.

To elucidate the function of PXN_S155 phosphorylation we conducted uptake experiments with radiolabelled NAD to determine if the phosphorylation state of S155 influences transport rates. Comparison of a phosphomimetic PXN variant (PXN_S155D) with a version mimicking the dephosphorylated state (PXN_S155C) revealed an almost doubled initial uptake rate for NAD/AMP exchange of 11.53 ± 0.81 pmol NAD * µg protein^{-1} (Fig. 4D) for PXN_S155D. Besides the homo-exchange of NAD we choose the uptake of NAD in AMP-preloaded proteoliposomes, because we were recently able to show that this reaction is most likely catalyzed by PXN *in vivo* (*Manuscript 1*). We conclude that phosphorylation of PXN_S155 does increase the uptake rates for NAD in exchange with AMP, although it does not alter the affinity of PXN to NAD, since we found equal K_m values for dephosphorylated PXN and the phosphomimetic PXN_S155D variant (Fig. 4E).

The exact alteration in the PXN structure leading to more efficient uptake when phosphorylated at S155 remains unknown. Generally there is only little known about how phosphorylation of transporters regulates their activity. In case of the MCF family this is the first study to describe a MC family member to be regulated via phosphorylation. The tonoplast monosaccaride transporter from Arabidopsis (TMT1) is like PXN phosphorylated in a loop region and also displays enhanced transport when phosphorylated (Wingenter et al., 2011). How exactly TMT1 is altered by this phosphorylation and how it affects the transport rate is unknown. It has been shown for the Arabidopsis nitrate transporter NRT1.1 that phosphorylation of the single

residue Thr101 uncouples a homodimer with low substrate affinity into two highly active monomers (Sun et al., 2014). Since PXN has been shown to be able to interact with itself (Mano et al., 2011) and MCF transporters in general are able to function as monomers (Kunji and Crichton, 2010), altering the oligomeric state of PXN through phosphorylation could be the regulatory mechanism. Phosphorylation of S155 could also lead to changes in the spatial conformation of PXN and thereby allowing higher transport rates. The S155 phosphorylation site is in close proximity to the mitochondrial energy transfer motif following the third transmembrane helix and could influence formation of the salt bridge network build by the three mitochondrial energy transfer motifs, which shapes one of the two transporter gates (Robinson et al., 2008; Palmieri et al., 2011).

Future experiments will help to understand the role of the phosphorylation of PXN's elongated loop region. For example it will be interesting do determine, whether the loop is located inside or outside the peroxisomal lumen. Since the elongated loop is located on the opposite side of the peroxisomal membrane than the two termini, this question is rather easily addressed (Fig. 3). Addition of a specific tag to the termini of PXN will allow the identification of their position and thereby indirectly the position of the elongated loop. Possible tags would be a redox-sensitive fluorescence protein for microscopic analysis or various standard protein tags coupled with a protease protection assay, performed with isolated intact peroxisomes. Studies of mitochondrial targeted MCF transporters expect the mitochondrial energy transfer motifs to form the gate at the mitochondrial matrix side and thereby the protein termini to be directed to the cytosolic side. Therefore we expect the phosphorylation side of PXN to be localized to the peroxisome matrix. Additionally it is reasonable to regulate PXN activity in direct response to the interperoxisomal NAD or AMP concentration (Robinson et al., 2008).

Following the localization of the loop, the kinase catalyzing the phosphorylation can be identified, e.g., by a pull-down assay. There are three enzymes with serine kinase activity that have been identified as peroxisomal (PK1, PK2, and PK4; Ma and Reumann, 2008) which could phosphorylate PXN inside the peroxisomal lumen. These kinases are good candidates to start interaction studies, using the yeast two-hybrid system or FRET studies (Chien et al., 1991; Kenworthy, 2001). Another candidate is the cytosolic serine kinase encoded by At2g32850, which is co-expressed with PXN (ATTED-II; Obayashi et al., 2007).

Other interesting upcoming experiments can include the suppression of yeast *mdh3Δ* or *ndt1/ndt2Δ* mutant phenotypes with phospho- and dephosphomimetic PXN variants, like it was done with wild-type PXN (*Manuscript 1*). Additionally a complementation of the *pxn-1* mutation in Arabidopsis can be performed with both PXN variants. These experiments will provide *in vivo* results on the impact of PXN_S155 phosphorylation.

In the present study we were able to identify an elongated hydrophilic loop region in the PXN protein, which is not common in MCF transporters. Phosphorylation of S155 localized in this loop positively influences transport speeds without altering the affinity to NAD. Further experiments will help to identify the mechanism of the regulation and the players involved.

MATERIAL AND METHODS

Materials

Chemicals were purchased from Sigma-Aldrich (www.sigmaaldrich.com). Reagents and enzymes for recombinant DNA techniques were obtained from Invitrogen (www.invitrogen.com), New England Biolabs (www.neb.com), Qiagen (www.qiagen.com), Thermo Scientific (www.thermoscintificbio.com) and Promega (www.promega.com). Anion exchange resin was purchased from Bio-Rad Laboratories (www.bio-rad.com). Radiochemical [α-^{32}P]-NAD was obtained from Perkin Elmer (www.perkinelmer.de).

Cloning procedures

In silico DNA sequences for cloning were retrieved from the Aramemnon database (aramemnon.uni-koeln.de). Cloning was performed according to standard molecular techniques (Sambrook et al., 1989). Sequences were verified by DNA sequencing (GATC Biotech, Konstanz, Germany). Primers were synthesized by Sigma-Aldrich.
Site-directed mutagenesis of PXN_S155 was performed using the *in vitro* QuickChange II Site-Directed Mutagenesis system according to the manufacturer's manual (Agilent Technologies). Primers were designed using the QuickChange Primer Design Program (Agilent Technologies). Primers specific for PXN, PXN_S155A, PXN_S155C, and PXN_S155D (KB58 and KB111) were used for PCR based amplification and the coding sequence was introduced into the pIVEX1.3

vector (5Prime) via NcoI/XhoI for C-terminal 6xHis-tag fusion. The sequences of oligonucleotides generated for this study are listed in the supplementary data table S1.

One-step protein expression using wheat germ extract

The *RTS 100 Wheat Germ CECF Kit* (www.5prime.com) was used for cell free expression of different PXN versions. 2900 ng of purified plasmid DNA were used as template for all reactions. Purification was done using the *PureYield Plasmid Miniprep System* (Promega). The expression reaction was prepared according to the manufacturer's manual and run for 24 hours at 24°C with shaking at 900 rpm. The *in vitro* transcription/translation reaction contained 0.04% (w/v) Brij-35 and 1% (w/v) L-α-phosphatidylcholine for better solubilization of expressed proteins (Nozawa et al., 2007). Expressed recombinant proteins were desalted using Sephadex G-25 columns (*illustra NAP-5*, GE Healthcare, www.gelifesciences.com) with 10 mM tricine-KOH (pH 7.5). Expression was controlled by SDS-PAGE and immunoblot analyses conducted as described in Sambrook et al. (1989). For immunodetection, an α-polyhistidine HPR-conjugated mouse IgG1 antibody (MACS molecular, http://www.miltenyibiotec.com) was used. PageRuler Prestained Protein Ladder (New England Biolabs) was used to estimate molecular masses. Protein concentrations were determined using a bicinchoninic acid assay (ThermoScientific).

Reconstitution of transport activities into liposomes

Cell free expressed recombinant proteins were reconstituted into 3% (w/v) L-α-phosphatidylcholine by freeze-thaw-sonication procedure for *in vitro* uptake studies (Kasahara and Hinkle, 1976). Proteoliposomes were either preloaded with 5 mM NAD or AMP. Counter-exchange substrate, which was not incorporated into proteoliposomes, was removed with gel filtration on Sephadex G-25 columns (*illustra NAP-5*, GE Healthcare, www.gelifesciences.com).

Transport assays were started by adding 150 µM [α-^{32}P]-NAD. The uptake reaction was terminated by passing the proteoliposomes over Dowex AG1-X8 anion-exchange columns, binding the non-incorporated radiolabeled substrates by chromatography. The incorporated radiolabeled compounds were analyzed by liquid scintillation counting. Time-dependent uptake data were fitted using nonlinear

regression analysis based on one-phase exponential association using GraphPad Prism 5.0 software (GraphPad, www.graphpad.com).

For K_m measurements proteoliposomes were preloaded with 30 mM NAD and the uptake reaction was started by adding [α-^{32}P]-NAD in the following concentrations: 10 µM, 50 µM, 250 µM, 500 µM, and 1000 µM. The initial rate for the transport of each substrate concentration was determined in triplicates and used to calculate the K_m via the Michaelis-Menten non-linear fit method of GraphPad Prism 5.0.

In silico analyses

MCF protein sequences presented in Fig. 1 were obtained from the Aramemnon database (aramemnon.uni-koeln.de). PXN homologues presented in Fig. 2 were identified via protein sequence blast (blastp; http://blast.ncbi.nlm.nih.gov) using the PXN sequence as query. The full sequences where obtained from www.ncbi.nlm.nih.gov/protein. Protein sequence alignments were created using ClustalW2 (Larkin et al., 2007; Goujon et al., 2010).

ACKNOWLEDGEMENTS

This work was supported by DFG-grant 1781/2-1 (to MGS and NL), EXC1028 (to APMW), and DFG-grant 1781/1-1 (to KB).

AUTHOR CONTRIBUTIONS

Martin Schroers performed the experiments and wrote the manuscript. Kristin Bernhardt provided the PXN_S155 mutation constructs. Andreas Weber and Nicole Linka provided lab space and helpful discussions. Martin Schroers and Nicole Linka designed the experiments.

REFERENCES

Agrimi, G., Russo, A., Pierri, C.L. and Palmieri, F. (2012) The peroxisomal NAD+ carrier of Arabidopsis thaliana transports coenzyme A and its derivatives. *J Bioenerg Biomembr*, **44**, 333-340.

Bedhomme, M., Hoffmann, M., McCarthy, E.A., Gambonnet, B., Moran, R.G., Rebeille, F. and Ravanel, S. (2005) Folate metabolism in plants: an Arabidopsis homolog of the mammalian mitochondrial folate transporter mediates folate import into chloroplasts. *J Biol Chem*, **280**, 34823-34831.

Bernhardt, K., Wilkinson, S., Weber, A.P. and Linka, N. (2012) A peroxisomal carrier delivers NAD(+) and contributes to optimal fatty acid degradation during storage oil mobilization. *Plant J*, **69**, 1-13.

Blom, N., Gammeltoft, S. and Brunak, S. (1999) Sequence and structure-based prediction of eukaryotic protein phosphorylation sites. *J Mol Biol*, **294**, 1351-1362.

Chien, C.T., Bartel, P.L., Sternglanz, R. and Fields, S. (1991) The two-hybrid system: a method to identify and clone genes for proteins that interact with a protein of interest. *Proc Natl Acad Sci U S A*, **88**, 9578-9582.

Eubel, H., Meyer, E.H., Taylor, N.L., Bussell, J.D., O'Toole, N., Heazlewood, J.L., Castleden, I., Small, I.D., Smith, S.M. and Millar, A.H. (2008) Novel proteins, putative membrane transporters, and an integrated metabolic network are revealed by quantitative proteomic analysis of Arabidopsis cell culture peroxisomes. *Plant Physiol*, **148**, 1809-1829.

Goujon, M., McWilliam, H., Li, W., Valentin, F., Squizzato, S., Paern, J. and Lopez, R. (2010) A new bioinformatics analysis tools framework at EMBL-EBI. *Nucleic Acids Res*, **38**, W695-699.

Guex, N. and Peitsch, M.C. (1997) SWISS-MODEL and the Swiss-PdbViewer: an environment for comparative protein modeling. *Electrophoresis*, **18**, 2714-2723.

Kasahara, M. and Hinkle, P.C. (1976) Reconstitution of D-glucose transport catalyzed by a protein fraction from human erythrocytes in sonicated liposomes. *Proc Natl Acad Sci U S A*, **73**, 396-400.

Kenworthy, A.K. (2001) Imaging protein-protein interactions using fluorescence resonance energy transfer microscopy. *Methods*, **24**, 289-296.

Kunji, E.R. and Crichton, P.G. (2010) Mitochondrial carriers function as monomers. *Biochim Biophys Acta*, **1797**, 817-831.

Lanquar, V. and Frommer, W.B. (2010) Adjusting ammonium uptake via phosphorylation. *Plant Signal Behav*, **5**, 736-738.

Lanquar, V., Loque, D., Hormann, F., Yuan, L., Bohner, A., Engelsberger, W.R., Lalonde, S., Schulze, W.X., von Wiren, N. and Frommer, W.B. (2009) Feedback inhibition of ammonium uptake by a phospho-dependent allosteric mechanism in Arabidopsis. *Plant Cell*, **21**, 3610-3622.

Larkin, M.A., Blackshields, G., Brown, N.P., Chenna, R., McGettigan, P.A., McWilliam, H., Valentin, F., Wallace, I.M., Wilm, A., Lopez, R., Thompson, J.D., Gibson, T.J. and Higgins, D.G. (2007) Clustal W and Clustal X version 2.0. *Bioinformatics*, **23**, 2947-2948.

Leinonen, R., Diez, F.G., Binns, D., Fleischmann, W., Lopez, R. and Apweiler, R. (2004) UniProt archive. *Bioinformatics*, **20**, 3236-3237.

Leroch, M., Neuhaus, H.E., Kirchberger, S., Zimmermann, S., Melzer, M., Gerhold, J. and Tjaden, J. (2008) Identification of a novel adenine nucleotide transporter in the endoplasmic reticulum of Arabidopsis. *Plant Cell*, **20**, 438-451.

Ligaba, A., Kochian, L. and Pineros, M. (2009) Phosphorylation at S384 regulates the activity of the TaALMT1 malate transporter that underlies aluminum resistance in wheat. *Plant J*, **60**, 411-423.

Linka, N., Theodoulou, F.L., Haslam, R.P., Linka, M., Napier, J.A., Neuhaus, H.E. and Weber, A.P. (2008) Peroxisomal ATP import is essential for seedling development in Arabidopsis thaliana. *Plant Cell*, **20**, 3241-3257.

Ma, C. and Reumann, S. (2008) Improved prediction of peroxisomal PTS1 proteins from genome sequences based on experimental subcellular targeting analyses as exemplified for protein kinases from Arabidopsis. *J Exp Bot*, **59**, 3767-3779.

Mano, S., Nakamori, C., Fukao, Y., Araki, M., Matsuda, A., Kondo, M. and Nishimura, M. (2011) A defect of peroxisomal membrane protein 38 causes enlargement of peroxisomes. *Plant Cell Physiol*, **52**, 2157-2172.

Nozawa, A., Nanamiya, H., Miyata, T., Linka, N., Endo, Y., Weber, A.P. and Tozawa, Y. (2007) A cell-free translation and proteoliposome reconstitution system for functional analysis of plant solute transporters. *Plant Cell Physiol*, **48**, 1815-1820.

Nury, H., Dahout-Gonzalez, C., Trezeguet, V., Lauquin, G., Brandolin, G. and Pebay-Peyroula, E. (2005) Structural basis for lipid-mediated interactions between mitochondrial ADP/ATP carrier monomers. *FEBS Lett*, **579**, 6031-6036.

Obayashi, T., Kinoshita, K., Nakai, K., Shibaoka, M., Hayashi, S., Saeki, M., Shibata, D., Saito, K. and Ohta, H. (2007) ATTED-II: a database of co-expressed genes and cis elements for identifying co-regulated gene groups in Arabidopsis. *Nucleic Acids Res*, **35**, D863-869.

Palmieri, F., Pierri, C.L., De Grassi, A., Nunes-Nesi, A. and Fernie, A.R. (2011) Evolution, structure and function of mitochondrial carriers: a review with new insights. *Plant J*, **66**, 161-181.

Pebay-Peyroula, E., Dahout-Gonzalez, C., Kahn, R., Trezeguet, V., Lauquin, G.J. and Brandolin, G. (2003) Structure of mitochondrial ADP/ATP carrier in complex with carboxyatractyloside. *Nature*, **426**, 39-44.

Rieder, B. and Neuhaus, H.E. (2011) Identification of an Arabidopsis plasma membrane-located ATP transporter important for anther development. *Plant Cell*, **23**, 1932-1944.

Robinson, A.J., Overy, C. and Kunji, E.R. (2008) The mechanism of transport by mitochondrial carriers based on analysis of symmetry. *Proc Natl Acad Sci U S A*, **105**, 17766-17771.

Sambrook, J., Fritsch, E.F. and Maniatis, T. (1989) *Molecular Cloning: A Laboratory Manual*: Cold Spring Harbor Laboratory Press.

Spyropoulos, I.C., Liakopoulos, T.D., Bagos, P.G. and Hamodrakas, S.J. (2004) TMRPres2D: high quality visual representation of transmembrane protein models. *Bioinformatics*, **20**, 3258-3260.

Sun, J., Bankston, J.R., Payandeh, J., Hinds, T.R., Zagotta, W.N. and Zheng, N. (2014) Crystal structure of the plant dual-affinity nitrate transporter NRT1.1. *Nature*, **507**, 73-77.

Thuswaldner, S., Lagerstedt, J.O., Rojas-Stutz, M., Bouhidel, K., Der, C., Leborgne-Castel, N., Mishra, A., Marty, F., Schoefs, B., Adamska, I., Persson, B.L. and Spetea, C. (2007) Identification, expression, and functional analyses of a thylakoid ATP/ADP carrier from Arabidopsis. *J Biol Chem*, **282**, 8848-8859.

Whiteman, S.A., Serazetdinova, L., Jones, A.M., Sanders, D., Rathjen, J., Peck, S.C. and Maathuis, F.J. (2008) Identification of novel proteins and phosphorylation sites in a tonoplast enriched membrane fraction of Arabidopsis thaliana. *Proteomics*, **8**, 3536-3547.

Wingenter, K., Trentmann, O., Winschuh, I., Hormiller, II, Heyer, A.G., Reinders, J., Schulz, A., Geiger, D., Hedrich, R. and Neuhaus, H.E. (2011) A member of the mitogen-activated protein 3-kinase family is involved in the regulation of plant vacuolar glucose uptake. *Plant J*, **68**, 890-900.

Zhang, Y. (2008) I-TASSER server for protein 3D structure prediction. *BMC bioinformatics*, **9**, 40.

SUPPLEMENTS

Name	RS	5'-3' sequence	purpose
KB58	NcoI	CACACCCATGGGAATGGCGGACGCTTTGATCAAT	PXN amplification
KB111	XhoI	GTGTGCTCGAGGCTAGAGGTAGCGTTTGAGAGCAACA	PXN amplification
KB49	/	CAGCGGCCCCCGAGGCTCCTTCTTCTAATGCA	PXN_S155A SDM
KB50	/	TGCATTAGAAGAAGGAGCCTCGGGGGCCGCTG	PXN_S155A SDM
KB51	/	AACAGCGGCCCCCGAGTGCCCTTCTTCTAATGC	PXN_S155C SDM
KB52	/	GCATTAGAAGAAGGGCACTCGGGGGCCGCTGTT	PXN_S155C SDM
KB53	/	CAAACAGCGGCCCCCGAGGATCCTTCTTCTAATGCAG AAG	PXN_S155D SDM
KB54	/	CTTCTGCATTAGAAGAAGGATCCTCGGGGGCCGCTGT TTG	PXN_S155D SDM

Supplementary table 1: List of used oligonucleotides. RS: restriction site (underlined in sequences); SDM: site-directed mutagenesis.

IV.3 *Manuscript 3*

Elucidating the role of peroxisomal metabolite and cofactor transport in branched-chain amino acid breakdown

Martin G. Schroers*[,1], Jan Wiese*[,1], Andreas P. M. Weber[1] and Nicole Linka[1,2]

* Co-first authors

[1] Institute for Plant Biochemistry and Cluster of Excellence on Plant Sciences (CEPLAS), Heinrich Heine University, Universitaetsstrasse 1, 40225 Duesseldorf, Germany.

[2] To whom correspondence should be addressed. E-Mail: Nicole.Linka@hhu.de.

ABSTRACT

Defects in metabolic conversion of propionic and isobutyric acid have been associated with severe human diseases. Little is known about the fate of these short monocarboxylic acids in plants. In leaf tissue these molecules are released during the degradation of branched-chain amino acids (BCAAs), phytol and odd-chain fatty acids. Here we report that *Arabidopsis thaliana* mutant plants, defective in peroxisomal metabolite or cofactor transport crucial for functional β-oxidation, suffer upon feeding of high concentrations of BCAAs or catabolic intermediates like propionate or isobutyrate. Additionally, we show this role of peroxisomal metabolism in the detoxification of amino acid catabolites to be crucial during prolonged darkness and heat stress. The peroxisomal ABC transporter, catalyzing the uptake of fatty acids, was also involved in the import of BCAA catabolites. Together with the peroxisomal carrier proteins supplying β-oxidation with ATP and NAD, it played a role in the detoxification of propionate and isobutyrate. Finally we propose an updated model for BCAA catabolism involving peroxisomal metabolism.

INTRODUCTION

Plant peroxisomes are involved in various metabolic and signaling pathways, including β-oxidation, photorespiration, auxin and jasmonic acid biosynthesis, pathogen defense, and others (Hu et al., 2012). Additionally an involvement of peroxisomal metabolism in the breakdown of branched-chain amino acid (BCAA) catabolites was postulated (Lange et al., 2004; Lucas et al., 2007; Khan and Zolman, 2010). Since peroxisomes are encircled by a single membrane, substrates and co-factors have to be imported by transporter proteins. Fatty acids are imported as acyl-CoA esters into peroxisomes via the peroxisomal ABC transporter, hereafter referred to as PXA1 (also known as AtABCD1, CTS, PED3, ACN2; (Zolman et al., 2001b). The CoA moiety is cleaved off during transport and the fatty acids are re-esterified with coenzyme A (CoA) in an ATP-dependent manner (De Marcos Lousa et al., 2013). The ATP required for peroxisomal metabolism is provided by two carrier proteins, called PNC1 and PNC2 (Arai et al., 2008; Linka et al., 2008). The peroxisomal NAD transporter PXN was implicated in supplying β-oxidation with NAD in parallel to the malate/oxaloacetate shuttle (Pracharoenwattana et al., 2007; Agrimi et al., 2012; Bernhardt et al., 2012; *Manuscript 1*). Mutations in these peroxisomal transport proteins cause an inhibition in β-oxidation, resulting in *A. thaliana* plants restricted in seedling development. Besides seedling establishment, respiration of fatty acids is required for survival in extended darkness to overcome the low carbon and energy status (Kunz et al., 2009; Slocombe et al., 2009). In senescing leaves β-oxidation is important for the mobilization of membrane lipids, which are thereby converted for relocation of carbon units to sink tissues (Yang and Ohlrogge, 2009; Troncoso-Ponce et al., 2013).

Carbohydrate oxidation primarily supports plant respiration in heterotrophic tissue, while enhanced protein degradation occurs at times when plant cells are carbon limited, for example during extended periods of darkness, leaf senescence, and under conditions of environmental and developmental stress (Araujo et al., 2011). In stressed rosette leaves of *A. thaliana* proteolysis releases amino acids that can be mobilized for use in other parts of the plant, but also provide alternative substrates for the mitochondrial electron transport chain. The BCAAs (valine, leucine, and isoleucine), aromatic amino acids and lysine can provide electrons both directly to electron transfer flavoprotein (ETF) complex as well as indirectly via their catabolic products being fed into the tricarboxylic acid (TCA) cycle (Engqvist et al., 2009;

Araujo et al., 2010; Engqvist et al., 2011). In case of BCAA breakdown, isovaleryl-CoA dehydrogenase provides electrons to the ubiquinol pool via the ETF/ETFQO complex (Araujo et al., 2010). During degradation of valine and isoleucine isobutyryl-CoA and propionyl-CoA are released in mitochondria. It was assumed that these short-chain fatty acids are further converted to 3-hydroxy-acids involving enzymes of the peroxisomal β-oxidation machinery (Zolman et al., 2001a; Lange et al., 2004; Lucas et al., 2007; Zolman et al., 2008; Khan and Zolman, 2010).

Other insides in the link between peroxisomal β-oxidation and amino acid catabolism were gained by analysis of the 3-hydroxyacyl-CoA hydrolase mutant *chy1*. This mutant is involved in valine breakdown and displays impaired β-oxidation probably due to accumulation of the toxic valine catabolite methylacrylyl-CoA (Zolman et al., 2001a; Lange et al., 2004). Since the BCAA degradation is initiated in mitochondria, the intermediates, such as propionic acid and isobutyric acid, have to be shuttled to peroxisomes for further conversion via β-oxidation. Here, we address the role of transport proteins known to be associated with peroxisomal fatty acid oxidation for a requirement in BCAA degradation and postulate enzymes which might catalyze the individual steps (see Fig. 8 and Tab. 1).

In this work we show that the peroxisomal ABC transporter PXA1, catalyzing the uptake of fatty acids, was involved in the import of short monocarboxylic acids. Together with the peroxisomal ATP carriers PNC1 and PNC2, PXA1 plays a role in detoxification of propionic acid and isobutyric acid under stress conditions such as extended darkness. Furthermore, we identified PNC, PXN, and PXA1 as negative regulators of developmental senescence. The loss of these transport proteins resulted in less seed biomass, implicating a defect in the relocation of C and N from leave sources to seed sinks.

RESULTS

Feeding of propionic acid and isobutyric acid inhibits growth of β-oxidation transport mutants

Defects in metabolic conversion of short-chain fatty acids (SCFA), including propionic acid and isobutyric acid, which are metabolic by-products, have been associated with severe diseases in humans (Childs et al., 1961; Kurita-Ochiai et al., 1995; Abe, 2012). In plants, these metabolites are released during the degradation of branched-chain amino acids (BCAAs). However, little is known about the fate of propionic acid and isobutyric acid in plants. Here, we performed feeding experiments to provide evidence for these molecules to be metabolized via peroxisomal β-oxidation. To this end, we used Arabidopsis mutants lacking peroxisomal transport proteins which are known to be required for functional β-oxidation, such as the fatty acid transporter PXA1 (*pxa1-2;* SALK_019334; Kunz et al., 2009) and NAD carrier PXN (*pxn-1*; GABI-046D01; Bernhardt et al., 2012). We generated a double mutant of the two peroxisomal ATP carriers PNC1 and PNC2 (*pnc1/2*; *pnc1-1*: SAIL_303H02; *pnc2-1*: SALK014579; Linka et al., 2008) to elucidate the role of supplying peroxisomes with ATP in propionic acid and isobutyric acid detoxification.

We assessed growth performance of these mutant lines upon provision of high levels of propionic or isobutyric acid to nine-day-old seedlings. Growth assays were performed on vertically placed half strength MS-plates containing sucrose (Fig. 1A). On propionate-containing plates *Col-0* and *pxn-1* were slightly impaired in rosette growth compared to the control plate, but performed better than *pnc1/2* and *pxa1-2,* which showed strongly reduced rosette growth. In the presence of isobutyric acid growth of *pxa1-2* and *pnc1/2* was impaired, while wild type and *pxn-1* grew almost normally (Fig. 1A). As a quantitative read-out for growth performance, we measured the length of the primary roots before and after treatment (Fig. 1B). *pnc1/2* and *pxa1-2* mutants transferred to propionic acid medium did not show root elongation, indicating a growth inhibition by this molecule at the given concentration. Roots of *Col-0* and *pxn-1* grew after transfer to this medium. Addition of isobutyric acid to the medium significantly inhibited root growth in *pxa1-2* plants within the 11-day growth period.

Previously, it was postulated that exogenously supplied propionic and isobutyric acid are metabolized inside the peroxisomes via β-oxidation (Lucas et al., 2007; Khan and Zolman, 2010). The first step of the peroxisomal propionic acid

degradation is its conversion to acrylic acid (Lucas et al., 2007). We therefore performed feeding of acrylic acid to gain further evidence, if this by-product is detoxified by peroxisomal β-oxidation (Fig. 1A). Feeding of acrylic acid led to a root growth arrest in the wild type and mutants (Fig. 1B). Regarding rosette growth we observed the same pattern as for propionic and isobutyric acid feeding, meaning impairment in all plants tested, but stronger impairment of *pnc1/2* and *pxa1-2*. This observation indicates that acrylic acid cannot as effectively be detoxified in the *pnc1/2* and *pxa-1* mutants compared to *Col-0* and *pxn-1*.

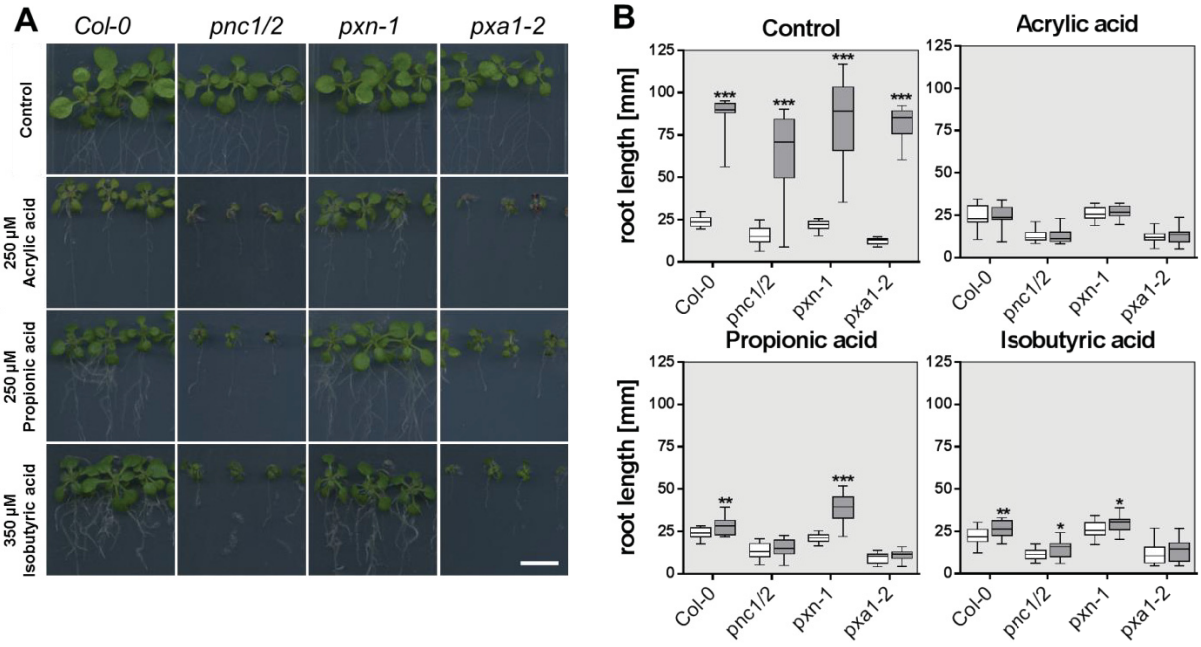

Figure 1: Exogenous supply of small carboxylic acids negatively affects growth in peroxisomal transporter mutants.

Images were taken and analyzed 1 day and 11 days after transfer to feeding plates. Primary root length between 1 day and 11 days was statistically compared for each line and condition. Plants were germinated on plates containing 0.5x MS medium supplied with 1% (w/v) sucrose and transferred to the supplemented or control plates after nine days.

(A) Photographs of *Col-0, pnc1/2, pxn-1, and pxa1-2* moved to plates containing half strength MS medium and an addition of either 0.25 mM acrylic or propionic acid or 0.35 mM isobutyric acid after 11 days.

(B) Primary root length measured 1 day (white boxes) and 11 days (grey boxes) after transfer to the feeding plates. Data represents the primary root length in mm, visualized is the mean of seven to 22 replicates ±SE. Asterisks indicate statistical differences in root length between the 1 day and the 11 days measurement (* P <0.05, ** P <0.01, *** P <0.001; Student's t-test). No significant difference means none additional root growth after transfer to feeding plates. Scale bar: 10 mm.

External supplementation of branched-chain amino acids impairs growth of β-oxidation transport mutants

Propionic acid is generated during catabolism of the BCAAs valine and isoleucine. Valine catabolism additionally generates isobutyric acid as an intermediate (Lucas et al., 2007). We analyzed growth performance in the presence of exogenous supply of BCAAs to elucidate whether peroxisomal β-oxidation related transporters are involved in BCAA catabolism. The presence of high concentrations of BCAAs negatively affected growth of the peroxisomal transporter mutants (Fig. 2). Supply of valine, leucine or isoleucine enabled growth of wild type and *pxn-1,* whereas *pnc1/2* and *pxa1-2* showed impaired rosette growth (Fig. 2A). Root elongation was not completely blocked at these conditions, which indicates an attenuated effect of BCAAs on the mutants compared to propionic acid and isobutyric acid (Fig. 2B). Taken together, PNC and PXA1 activity were required for normal growth in the presence of high levels of BCAAs. These findings provide evidences that peroxisomal β-oxidation is involved in BCAA catabolism.

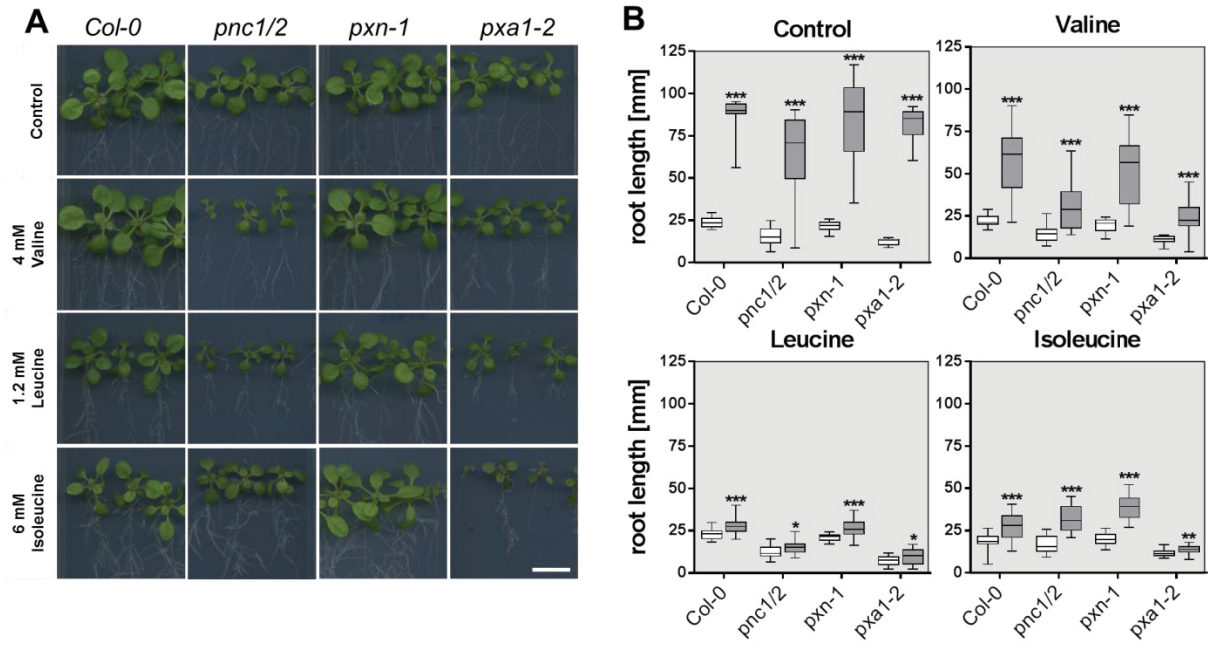

Figure 2: Exogenous supply of branched-chain amino acids negatively affects growth of peroxisomal transporter mutants.

(A) Photographs of Col-0, pnc1/2, pxn-1, and pxa1-2 moved to plates containing half strength MS medium and an addition of 4 mM valine, 1.2 mM leucine or 6 mM isoleucine after 11 days.

(B) Primary root length measured 1 day (white boxes) and 11 days (grey boxes) after transfer to the feeding plates. Data represents the primary root length in mm, visualized is the mean of seven to 22 replicates ±SE. Asterisks indicate statistical differences in root length between the 1 day and the 11 days measurement (* P <0.05, ** P <0.01, *** P <0.001; Student's t-test). No significant difference means none additional root growth after transfer to feeding plates. Scale bar: 10 mm.

Peroxisomal transport mutants are stressed in extended darkness.

Amino acids can serve as respiratory substrates when the plant is carbon starved. For example BCAAs are degraded during periods of elongated darkness to fuel the TCA cycle (Brouquisse et al., 1998; Araujo et al., 2011). We analyzed the response of β-oxidation transport mutants to prolonged darkness conditions to further elucidate an involvement of β-oxidation in BCAA breakdown.

Therefore 4-week-old *Col-0*, *pnc1/2*, *pxa1-2,* and *pxn-1* plants were transferred to the dark for periods of up to 50 h (extended darkness) and then reilluminated for 24 h (reilluminated) or kept in the dark for nine days (carbon starvation). Nine days of continuous darkness deplete plant cells of carbon and require mobilization of stored carbon in lipids and proteins (Araujo et al., 2010). Extended darkness of 50 h led to a slight degreening in all plants tested (Fig. 3A). Reillumination of darkness treated plants led to regreening of wild type and *pxn-1*, while *pxa1-2* and *pnc1/2* plants bleached to a light bluish to brown color and quickly dehydrated upon reillumination after at least 32 h of darkness within a few hours of light (Fig. 3A). Wild-type plants completely recovered, when transferred back into light, *pxn-1* displayed only some small lesions on rosette leaves (see detail in Fig. 3A) and *pxa1-2* as well as *pnc1/2* where completely unable to recover and resume growth.

To further investigate this apparent accelerated senescence, we measured chlorophyll fluorescence parameters and evaluated the flow of electrons through photosystem II (PSII), which expresses overall photosynthetic capacity as diagnostics of leaf senescence. Damage to PSII is considered as one of the first indicators of stress in a leaf. Hence, maximum quantum yield (*QYmax*) represents to which extent PSII is damaged by applied environmental changes and consequently, whether a plant can tolerate that stress (Maxwell and Johnson, 2000). *pxa1-2* displayed a mild reduction in PSII activity after one hour darkness incubation (Fig. 3B). *pnc1/2* and *pxn-1* displayed reduced *QYmax* compared to the wild type after extended darkness, while *pxn-1* showed wild-type level (Fig. 3B). Reillumination led to recovery of *QYmax* in *Col-0* and *pxn-1* to about 0.8, which is normal for healthy Arabidopsis leaves. In *pnc1/2* and *pxn-1* reillumination led to a severe drop in PSII activity, as was expected from the strongly bleached phenotypes (Fig. 3B). Keeping the plants in darkness for nine days resulted in increased PSII damage in all three mutants compared to the wild type. The observed darkness-induced damage also depended

on leaf age, with older leaves appearing to be more susceptible upon reillumination than younger leaves. Lethality upon reillumination was not observed for *Col-0* or *pxn-1*. *pxn-1* displayed significantly reduced PSII electron flow only after nine days of incubation in the dark. This observed PSII damage was further supported by reduced chlorophyll content of *pnc1/2*, *pxa1-2,* and *pxn-1* after nine days of darkness (Fig. S1), indicating that the process of senescence is more rapid in β-oxidation mutants than wild-type plants during extended darkness conditions.

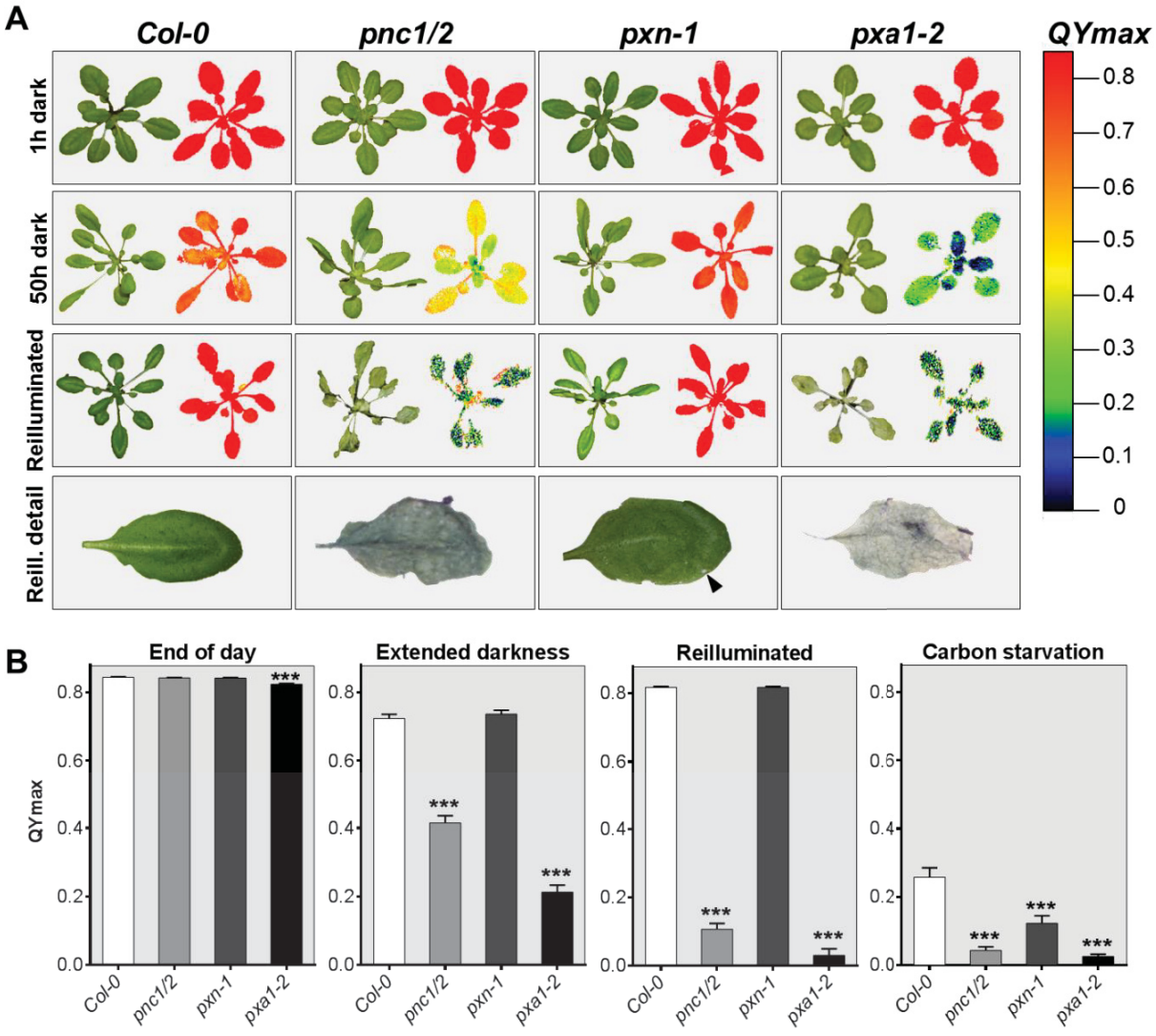

Figure 3: Response of 4-week-old *Col-0*, *pnc1/2*, *pxn-1* and *pxa1-2* plants to extended darkness.
(A) Photographs and false-color images representing *QYmax* (as indicated in the given color scale) of 4-week-old *Col-0, pnc1/2, pxn-1, and pxa1-2* at the end of day, extended darkness (50 h), and reillumination for 24 h after 50 h darkness. Mature leaves of reilluminated plants are shown in detail with an arrowhead marking a necrotic lesion.
(B) Mean (±SE) of maximum quantum yield (*QYmax*) of rosette leaves of 4-week-old *Col-0, pnc1/2, pxn-1, and pxa1-2* at the end of day, extended darkness (50 h), reillumination for 24 h after 50 h darkness and incubation in the dark for nine days (carbon starvation). Results are representative for eight independent experiments, performed with at least three biological replicates each. Differences to the *Col-0* control of each treatment were marked as statistically significant (t-test) by *** at significance level of $P < 0.001$.

Extended darkness leads to changes in metabolite content of peroxisomal transporter mutants

To further clarify the link between the accelerated leaf senescence phenotype with a defect in BCAA turnover, we analyzed the effect of prolonged darkness on peroxisomal transport mutants on metabolite level. Therefore the levels of selected sugars, hydrophilic carboxylic acids and amino acids were examined by GC-MS and HPLC-DAD.

The extended darkness treatment led to low glucose and sucrose levels in wild-type and mutant plants, suggesting that these plants were carbon starved under these conditions (Fig. 4A+B). *pnc1/2* and *pxa1-2* showed lowest glucose and sucrose content after 50 h and 9 d of darkness (Fig. 4A+B). In reilluminated leaves glucose and sucrose levels were increased, except for *pxa1-2*, indicating restoration of photoautotrophic metabolism and synthesis of glucose and sucrose from photosynthetic CO_2 fixation.

Analysis of TCA cycle intermediates showed a significant decrease in glutamate in *pnc1/2* and *pxa1-2* during the course of the extended darkness (Fig. 4C). An accumulation of 2-oxoglutarate was observed for *pnc1/2* and *pxa1-2* at 50 h dark treatment, whereas after reillumination the levels of this TCA cycle intermediate were drastically reduced in *pnc1/2* and *pxa1-2* compared to wild type and *pxn-1* (Fig. 4D). The levels of (iso)citric acid did not alter significantly between wild type and mutants during extended darkness and reillumination, but where reduced in *pnc1/2* and *pxa1-2* during carbon starvation (Fig. 4E).

Since amino acids can serve as alternative respiratory substrates during carbon starvation, free amino acid levels increase under these conditions due to elevated protein turnover (Araujo et al., 2011). Thus, we measured the amino acid profiles of wild type and mutants, who were then subjected to principal component analysis (PCA) to abstract the amino acid status for each plant extract (Fig. 5). In non-stress conditions (end of regular night) PCA variations were largely identical and actual levels confirmed the amino acid metabolism not to be significantly altered (Fig. 5A). In response to darkness *pnc1/2* and *pxa1-2* amino acid variations contrasted to *Col-0* and *pxn-1* (Fig. 5B). Both pairs showed partially overlapping variation patterns, but grouped particularly in the 2D plot. This amino acid analysis indicates that PXA1 and PNC activity is required for maintenance of amino acid homoeostasis in extended darkness.

In extended darkness most of the free BCAAs did not accumulate in the mutant lines compared to wild type (Fig. 6). Merely leucine levels were significantly but not drastically higher in *pnc1/2* (Fig. 6A). *pxa1-2* exhibited a large variation among samples for all three BCAAs under these conditions. Reillumination led to strong decrease of free BCAA levels in wild type and *pxn-1* compared to extended darkness values. In contrast, the levels of valine, isoleucine and leucine in the dark-treated *pnc1/2* and *pxa1-2* plants did not change upon reillumination. Extending the darkness treatment to nine days resulted in accumulation of BCAAs in wild-type and *pxn-1* plants, whereas the levels in *pnc1/2* and *pxa1-2* slightly declined compared to the values after 50 h of darkness. The aromatic amino acid phenylalanine also showed the pattern of BCAAs, meaning higher values in *pnc1/2* and *pxa1-2* after reillumination in comparison to *Col-0* and *pxn-1* and this pattern inversed after nine days of darkness (Fig. 6D).

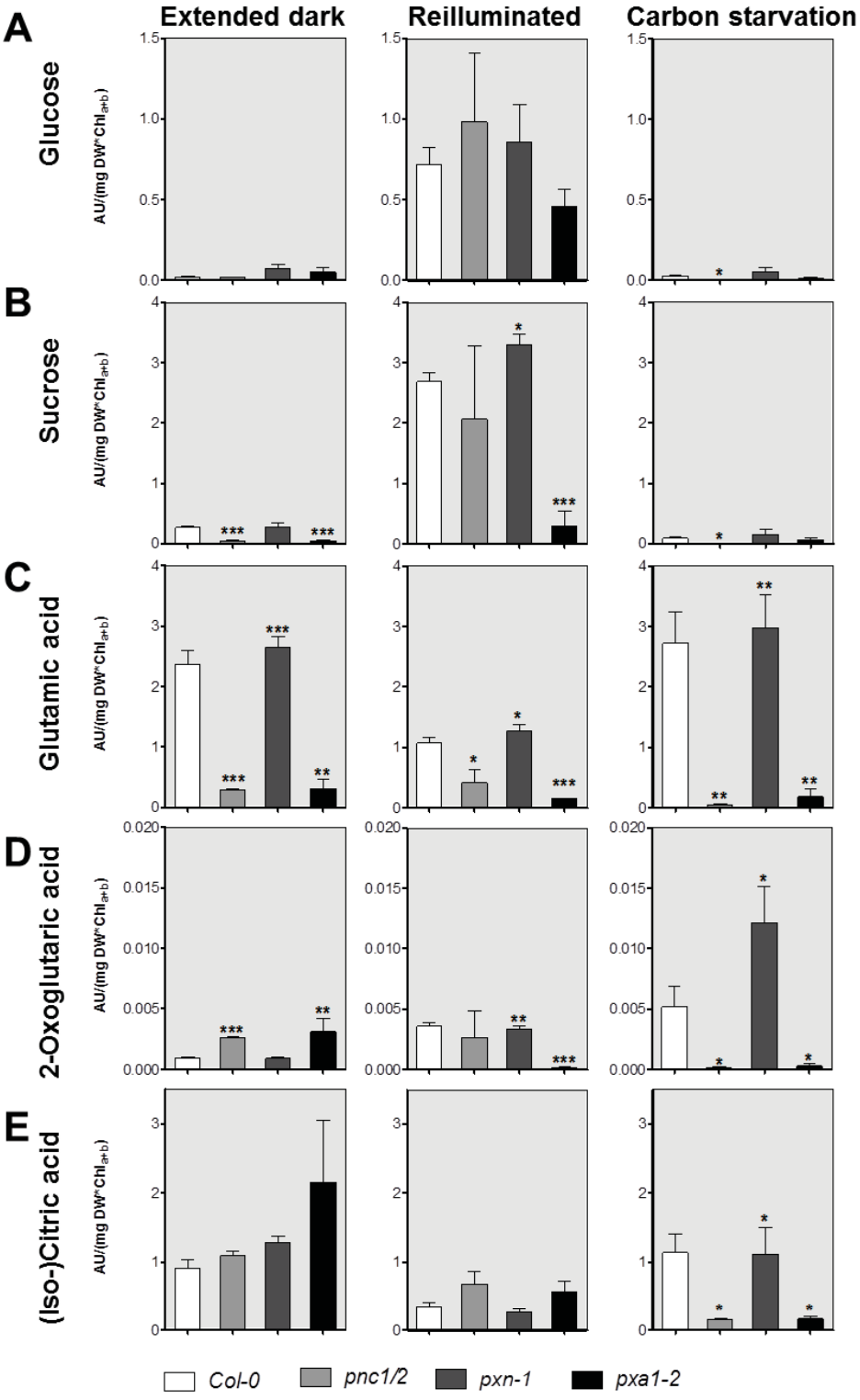

Figure 4: Extended darkness influences carbohydrates as well as respiratory metabolites in peroxisomal β-oxidation transport mutants.

(A)-(E) Levels of indicated metabolite contents of 4-week-old *Col-0, pnc1/2, pxn-1,* and *pxa1-2* in response to extended darkness (50 h darkness), reillumination (50 h darkness + 24 h light) and carbon starvation (nine days darkness). Leaf extracts were subjected to GC-MS analysis for metabolite quantification. Data represent the mean of three biological replicates (±SE). Asterisks indicate statistical significance versus the *Col-0* control in each diagram (* P<0.05, ** P<0.01, *** P<0.001; Student's t-test). The data is shown in an arbitrary unit normalized to mg dry weight. Chlorophyll$_{a/b}$ contents were used for normalization of biological replicates.

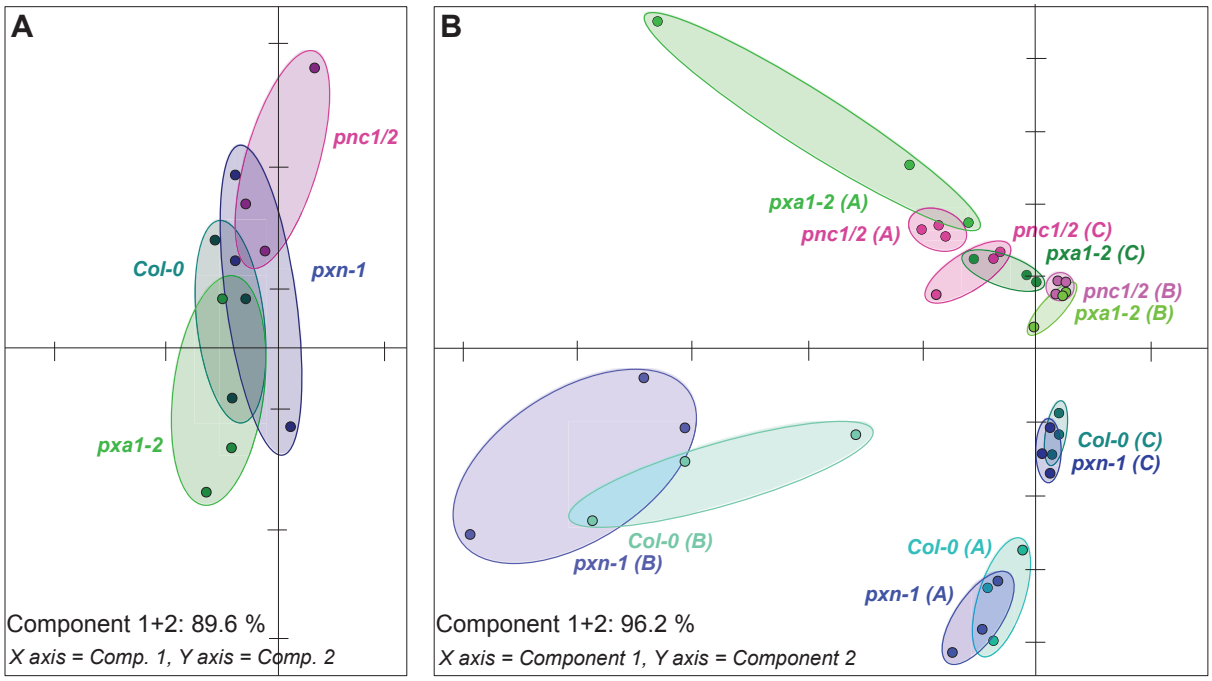

Figure 5: Principal Component Analysis (PCA) of amino acid data of *4-week-old Col-0, pnc1/2, pxn-1 and pxa1-2* exposed to extended darkness.

(A) PCA score plot of proteinogenic amino acids in non-stressed plants (end of night).

(B) PCA score plot of amino acids extract from wild type (*Col-0*) plants and the peroxisomal transporter mutants *pnc1/2*, *pxn-1*, and *pxa1-2* either exposed to 50 h of darkness *(A),* nine days of darkness *(B)* or 50 h of darkness followed by 24 h illumination *(C)* subjected to GC-MS analysis. PCA conducted with the MultiExperiment Viewer (Saeed et al., 2003). Biological replicates are encircled.

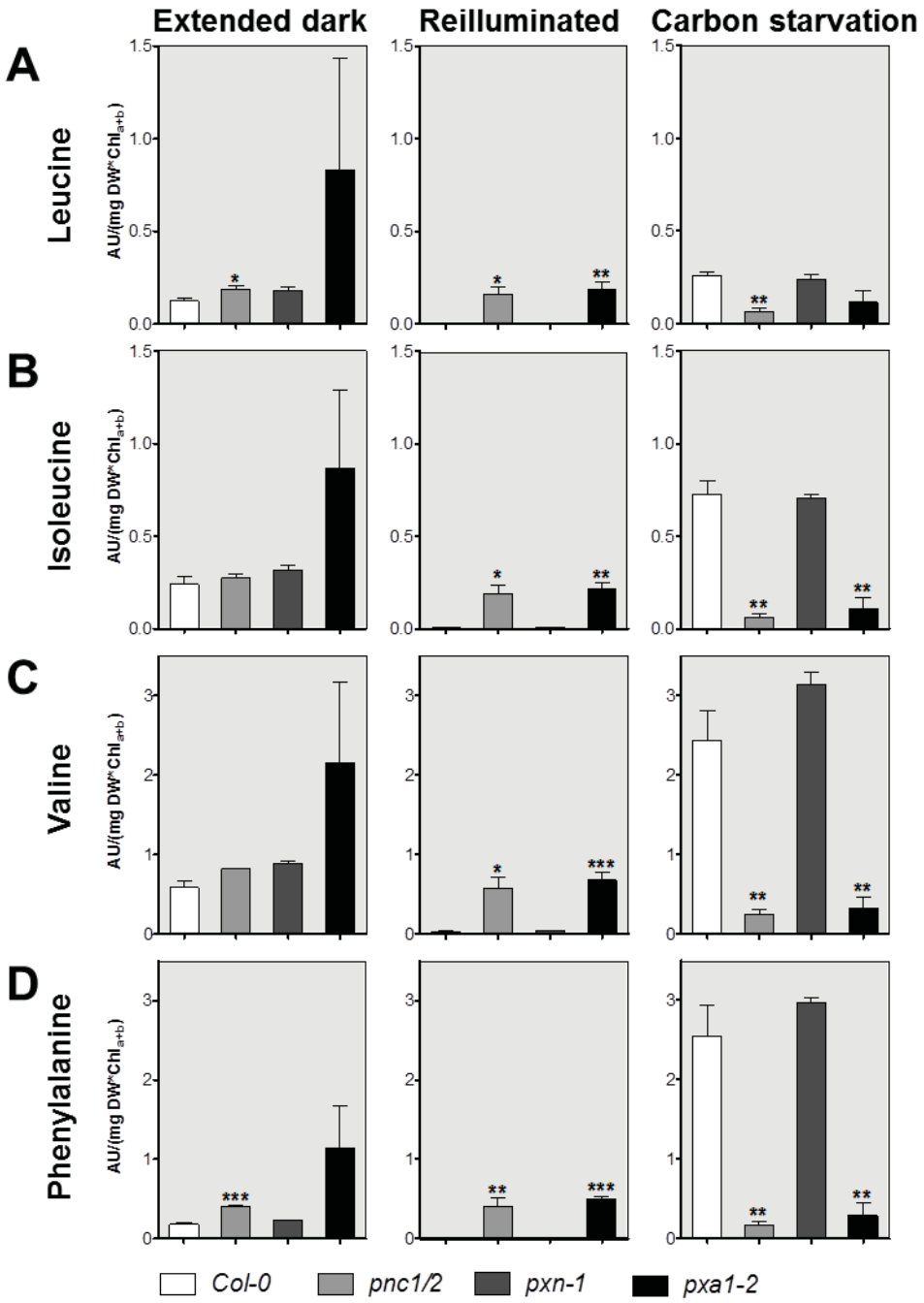

Figure 6: Extended darkness influences branched-chain and aromatic amino acids in peroxisomal β-oxidation transport mutants.

(A)-(D) Mean levels of indicated metabolite content (±SE) of 4-week-old *Col-0, pnc1/2, pxn-1* and *pxa1-2* in response to extended darkness (50 h darkness), reillumination (50 h darkness + 24 h light) and carbon starvation (9 days darkness). Leaf extracts were subjected to GC-MS analysis for metabolite quantification. Data represent the mean of three biological replicates. Asterisks indicate statistical significance versus the *Col-0* control in each diagram (* P<0.05, ** P<0.01, *** P<0.001; Student's t-test). The data is shown in an arbitrary unit normalized to mg dry weight. Chlorophyll$_{a/b}$ contents were used for normalization of biological replicates.

Reduced β-oxidation function leads to altered nutrient relocation in the final stage of leaf development

The altered mobilization of amino acids and carboxylic acids as respiratory substrates in carbon starved β-oxidation transport mutants raised the question, whether this affects nutrient remobilization and relocation in developmental senescence. We grew plants in a chamber with 50-60% relative humidity and plants were watered regularly. In these growth conditions premature leaf ageing was observed for *pnc1/2* and *pxn-1* by degreening of oldest leaves (Figure S3A). This was also reflected in chlorophyll contents measured for mature green leaves (Figure S3B). In comparison to the wild type, profiling of late senescence marker SAG12 (Balazadeh et al., 2008) revealed higher variation in the β-oxidation transporter mutants in quantitative RT-PCR analyses (Fig. 7A). *Col-0* showed SAG12 expression below that of the normalization control (0.0055 ±0.0018), in contrast to *pnc1/2* (28.98 ±27.15), *pxn-1* (8.791 ±7.527) and *pxa1-2* (6.135 ±3.471). This accelerated leaf senescence indicated that peroxisomal β-oxidation transporters negatively regulate senescence, probably by preventing the induction by metabolic stress (Wingler and Roitsch, 2008; Abbasi et al., 2009).

This finding led to the hypothesis that a β-oxidation defect befalls the next generation, because altered energy availability might lead to reduced nutrient relocation and reduced seed quality. We observed a reduced silique size of 12-week-old plants (Fig. 7B), which had already been reported for the β-oxidation core-component 3-ketoacyl-CoA thiolase (*kat2-1;* Footitt et al., 2007a; Footitt et al., 2007b). Authors suspected compromised β-oxidation to cause the defect through impaired pollen tube elongation, leading to a reduced seed number per plant. In contrast our analyses did not show changes in total seed numbers per plant, but a reduced total seed weight (Fig. 7C), resulting from reduced seed size in mutants (Fig. 7E). Seed weight was reduced significantly for *pnc1/2* and *pxn-1*, whereas no significant change was determined for *pxa1-2* (Fig. 7D). We quantified seed protein content to test for the hypothesized inability of C and N mobilization and relocation to seeds sinks. The analysis revealed that the seeds are equipped with significantly less protein, which might mirror incompetence in BCAA metabolism next to a defect in fatty acid breakdown (Fig. 7F).

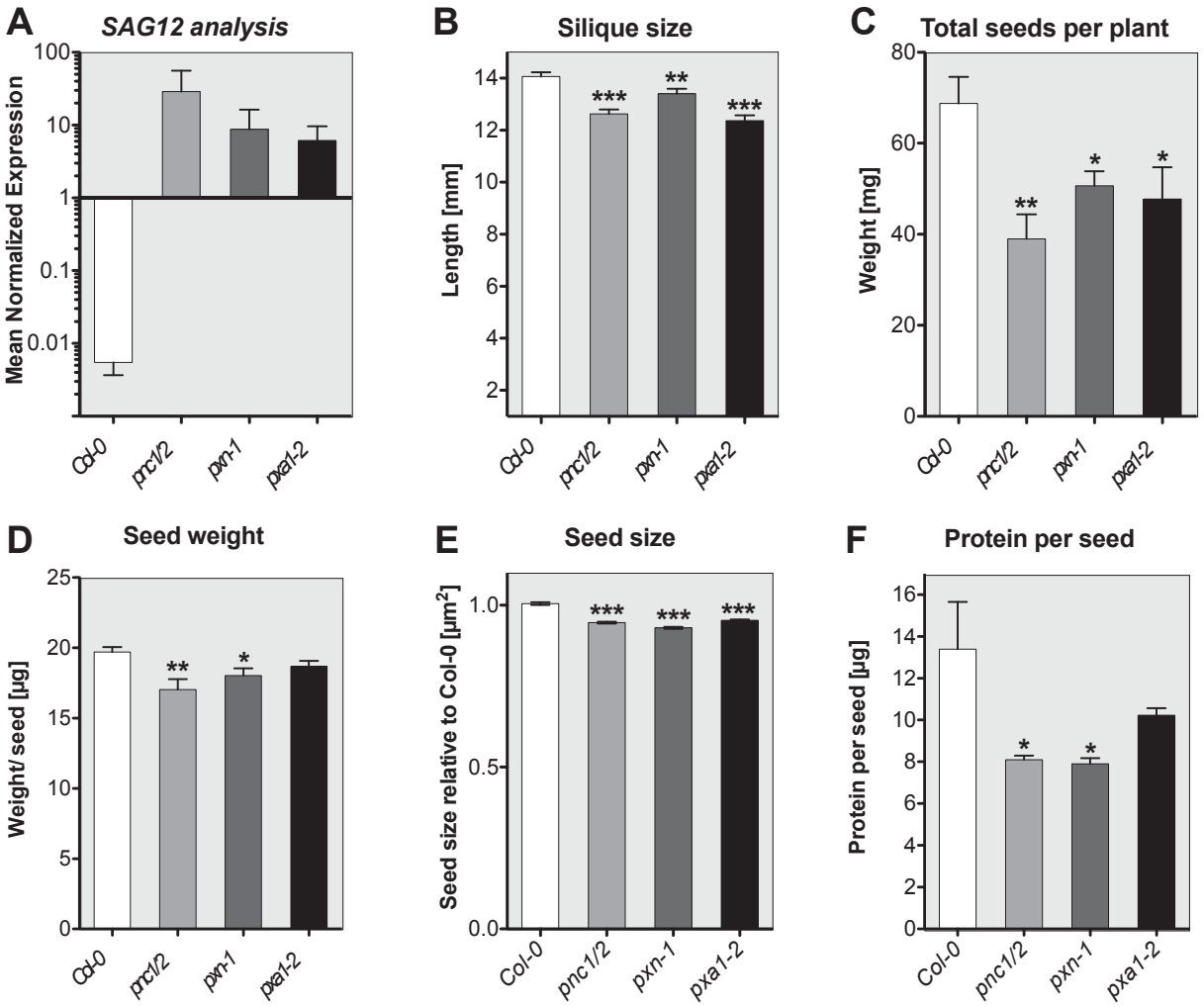

Figure 7: **Senescence and reproductive fitness features of *Col-0, pnc1/2, pxn-1 and pxa1-2*.**
(**A)** Mean normalized expression (±SE) of the senescence marker gene *SAG12* analyzed by qRT-PCR. Plant material was taken from 10-week-old rosette leaves.
(**B)** Mean silique size (±SE; n >40) in mm measured for 12 week old plants.
(C) Mean of seed yield (±SE; n= 12) per plant in mg.
(**D)** Mean of seed weight in µg (±SE; n = 6). >500 Seeds were counted automatically using the ImageJ distribution Fiji (Schindelin et al., 2012) and weighed.
(E) Mean seed size in μm^2 (±SE) relative to Col-0. 2500-6500 seeds were measured with ImageJ.
(F) Mean protein content (±SE; n = 4) per seed. Proteins were isolated from 4 samples per line containing 500-1300 seeds. The protein amount was determined using a bicinchoninic acid (BCA) assay. Data shows the protein amount per seed in µg as mean ±SE.
Differences between the mean of each mutant versus the wild type in each diagram are marked as statistically significant (t-test) by (*), (**) or (***) at respective significance levels of ($P < 0.05$), ($P < 0.01$) or ($P < 0.001$).

DISCUSSION

Our work addressed the importance of transport proteins related to peroxisomal β-oxidation beyond fatty acid catabolism. We described the role of peroxisomal transport in carbon starvation with respect to BCAA turnover, as well as propionic and isobutyric acid metabolism. We demonstrated that an impaired substrate and cofactor supply of peroxisomal β-oxidation disturbed the intracellular carbon mobilization, resulting in cellular stress. As a consequence developmental senescence and nutrient relocation was disrupted on an organism level and passed on to the next generation by reduced seed quality (Fig. 7).

Our findings enabled us to integrate PXA1, PNC and PXN in the pathway of BCAA degradation. Based on our results plant peroxisomes are involved in the detoxification of propionic acid and isobutyric acid by a modified peroxisomal β-oxidation (Fig. 8). *Arabidopsis* candidate genes encoding for enzymes necessary for this pathway are listed in Table 1. In the following discussion we will refer to the numbered enzymatic *Functions* presented in Figure 8 and Table 1.

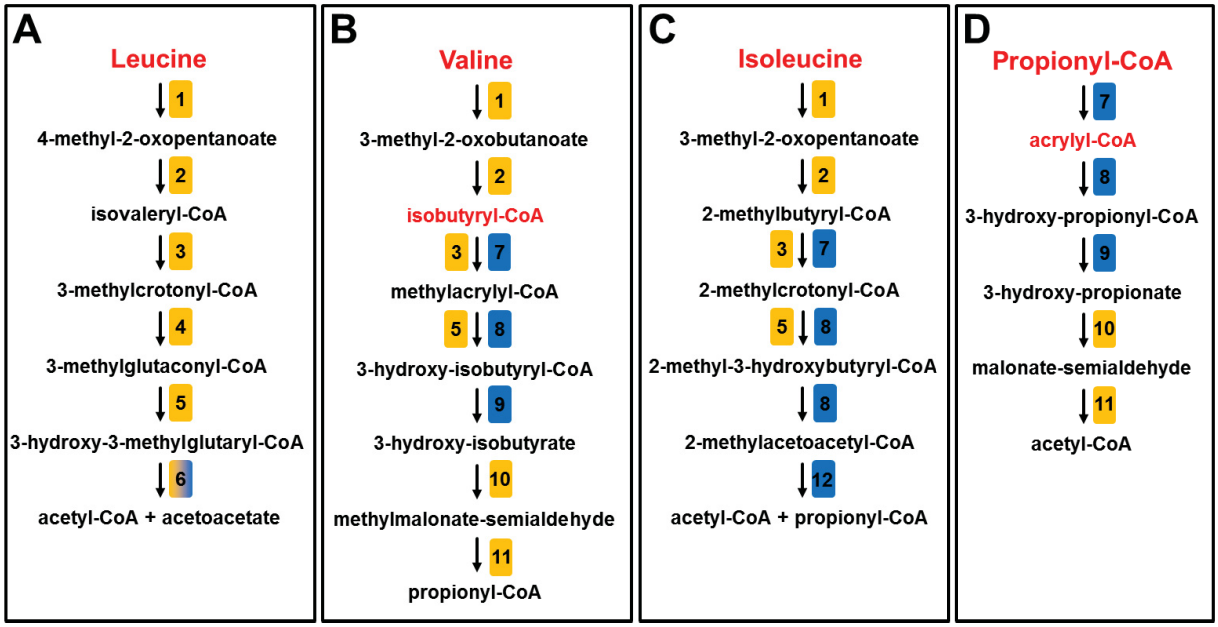

Figure 8: **Scheme of branched-chain amino acid (BCAA) degradation in Arabidopsis.** Compounds written in red have been used in feeding experiments during this study. Candidate enzymes catalyzing the reactions 1 to 12 are listed in Table 1. Orange labeled steps take place in mitochondria, the ones marked in blue supposedly in peroxisomes. The enzyme catalyzing reaction 6 is dual-targeted. Some reactions might be catalyzed either by a mitochondrial or a peroxisomal enzyme. **A:** Scheme of leucine degradation. **B:** Scheme of valine degradation, which continues with the degradation of propionyl-CoA in **D.** The scheme also shows the detoxification pathway for exogenously supplied isobutyrate, which is likely imported into peroxisomes as isobutyryl-CoA via PXA1. **C:** Scheme of isoleucine degradation, which continues with the degradation of propionyl-CoA in **D. D:** Scheme of propionyl-CoA degradation. Exogenously supplied propionate is likely to be imported into peroxisomes by PXA1 upon cytosolic conversion to propionyl-CoA

Nr.	Enzyme	Abbreviation	Locus	Localization	Reference
1	branched-chain amino acid transferase	BCAT1	At1g10060	M	1
2	branched-chain α-ketoacid dehydrogenase complex	BCKDC E1 α	At5g09300	M	2, 3, 4
		BCKDC E1 β	At3g13450	M	
		BCKDC E2 / BCE2	At3g06850	M	
		BCKDC E3 / LPD2	At3g17240	M	
3	isovaleryl-CoA dehydrogenase	IVD / IVDH	At3g45300	M	5
4	3-methylcrotonoyl-CoA carboxylase	MCCA	At1g03090	M	6
		MCCB	At4g34030	M	
5	enoyl-CoA hydratase	ECHD	At4g16800	M	
6	3-hydroxymethyl-3-methylglutaryl-CoA lyase	HMG-CoAL	At2g26800	M/**P**	4, 7
7	acyl-CoA oxidase (ACX1-ACX6)	ACX1	At4g16760	**P**	8
		ACX2	At5g65110	**P**	
		ACX3	At1g06290	**P**	
		ACX4	At3g51840	**P**	
		ACX5	At2g35690	**P**	
		ACX6	At1g06310	**P**	
8	multifunctional protein 2	MFP2	At3g06860	**P**	9, 10
9	3-hydroxyacyl-CoA hydrolase	CHY1	At5g65940	**P**	11, 12, 13
10	3-hydroxyisobutyrate dehydrogenase	HIBDH	At1g71170	M	
			At1g71180	M	
			At4g20930	M	
			At4g29120	M	
11	(Methyl) malonate semialdehyde dehydrogenase	ALDH6B2	At2g14170	M	
12	Acetyl-CoA−Acetyltransferase	AACT2	At5g48230	**P**	14, 15

Table 1: Candidates for BCAA degrading enzymes in Arabidopsis
The table lists enzymes that can catalyze the different steps during BCAA degradation. The reaction number (**Nr.**) is related to the respective numbers in Fig. 8. Localization of the enzymes is either in mitochondria (**M**) or peroxisomes (**P**). References: 1: (Schuster and Binder, 2005); 2-4: (Fujiki et al., 2000; 2002; Taylor et al., 2004); 5: (Daschner et al., 2001); 6: (Che et al., 2002); 7: (Reumann et al., 2004); 8: (Khan et al., 2012); 9+10: (Richmond and Bleecker, 1999; Rylott et al., 2006); 11-13: (Zolman et al., 2001a; Lange et al., 2004; Lucas et al., 2007); 14+15: (Reumann et al., 2007; Jin et al., 2012).

Peroxisomal β-oxidation is involved in BCAA catabolism

Exogenous supply of BCAAs or the catabolic intermediates propionic acid, acrylic acid or isobutyric acid led to severe growth inhibition in *pnc1/2* and *pxa1-2* plants (Fig. 1+2), indicating the importance of peroxisomal β-oxidation for degradation of BCAA and small carboxylic acids. Previously, an involvement of peroxisomes in the detoxification of exogenously supplied isobutyrate and propionate has been shown for a mutant of the peroxisomal 3-hydroxyacyl-CoA hydrolase CHY1 (Lucas et al., 2007; Khan and Zolman, 2010); *Function 9* in Fig. 8 and Tab. 1).

Isobutyrate and propionate are likely to be imported into peroxisomes as their respective CoA-esters via PXA1, explaining the growth defect observed during feeding experiments conducted with the respective mutant (Fig. 1). The CoA-moiety is cleaved off during PXA1 mediated transport, which determines ATP consumption for re-activation to CoA-esters for further metabolic processing (De Marcos Lousa et al., 2013). The strong defect of *pnc1/2* plants in the degradation of isobutyric and

propionic acid (Fig. 1) reflects the necessity of intraperoxisomal ATP as a co-substrate of short-chain carboxylic acid CoA-ester synthesis.

The thioesterification is followed up by an oxidation (*Function 7*). Oxidation of isobutyryl-CoA to methylacrylyl-CoA is unlikely to be catalyzed by the mitochondrial isovaleryl-CoA dehydrogenase 1 (IVD1, *Function 3*), since this enzyme only shows 20% activity towards isobutyryl-CoA, relative to the activity for the leucine catabolite isovaleryl-CoA (Daschner et al., 2001). This implies that not only propionyl-CoA but also isobutyryl-CoA needs to enter the peroxisome for β-oxidation.

The next two steps during isobutyrate and propionate detoxification, hydration (*Function 8*) and thiolysis (*Function 9*), give rise to 3-hydroxy-isobutyrate and 3-hydroxy-propionate (Fig. 8B+D). Enzymes with the ability to further metabolize these molecules to propionyl-CoA or acetyl-CoA were not identified as peroxisomal but rather assumed to reside within mitochondria. Therefore, the peroxisomal conversion ends in the production of 3-hydroxy acids, which was already confirmed by analysis of *chy1* (Lucas et al., 2007). The last two steps of isobutyrate and propionate catabolism are likely localized in mitochondria, the site where 3-hydroxy acids are proposed to be converted to acetyl-CoA to fuel the TCA cycle (Lucas et al., 2007).

Feeding of BCAAs led to growth inhibition in *pnc1/2* and *pxa1-2* plants (Fig. 2). Since isobutyryl-CoA and propionyl-CoA are both intermediates of valine catabolism, a similar effect of these three compounds was expected and observed. Isoleucine feeding led to similar results, indicating a peroxisomal role in isoleucine degradation. Peroxisomal acyl-CoA oxidases (ACX) and the multifunctional protein 2 (MFP2, *Functions 7 and 8*) are candidates likely functioning during peroxisomal detoxification of exogenous isobutyrate and propionate (Lucas et al., 2007). Therefore we propose these enzymes to also catalyze reactions of valine and isoleucine catabolism (Fig. 8B+C). Since growth of the ABC-transporter mutant *pxa1-2* is compromised by exogenous isoleucine, an intermediate of isoleucine degradation is likely to be imported into peroxisomes via PXA1. Up to now no mitochondrial enzyme has been identified to catalyze the oxidation of 2-methylbutyryl-CoA to 2-methylcrotonyl during isoleucine catabolism. This reaction could possibly be catalyzed by a peroxisomal ACX (*Function 7*), making 2-methylbutyryl-CoA a candidate for a novel PXA1 substrate. Propionyl-CoA arising from isoleucine degradation through thiolysis of 2-methylacetoacetyl-CoA (*Function 12*) is likely generated directly inside the peroxisome and therefore does not require PXA1-mediated import. This thiolysis is

catalyzed by acetyl-CoA acetyltransferase 1 in human (Middleton and Bartlett, 1983), whose closest Arabidopsis homologue (AACT2) is localized to peroxisomes (Reumann et al., 2007).

Growth of *pnc1/2* and *pxa1-2* seedlings was affected by the presence of exogenous leucine, although leucine catabolism was proposed to be restricted to mitochondria, where leucine is metabolized to acetyl-CoA and acetoacetate (Fig. 8A; Daschner et al., 2001). The last step of leucine degradation is catalyzed by a hydroxymethylglutaryl-CoA lyase, which was reported to be dual-localized to mitochondria and peroxisomes and thereby might represent a link between leucine degradation and peroxisomal metabolism (Reumann et al., 2004). Peroxisomes could also play a role in the conversion of acetoacetate. Bacteria and mammals were shown to convert acetoacetate to acetyl-CoA in a two-step pathway where acetoacetate is activated to acetoacetyl-CoA and finally thiolysed to two molecules of acetyl-CoA (Pauli and Overath, 1972; Fukao et al., 1997). No homologues of the corresponding activating enzymes could be detected in plants, but it is reasonable to assume, that one of the 64 acyl activating enzymes encoded in the *Arabidopsis* genome accepts acetoacetate as a substrate (Shockey and Browse, 2011). The thiolysis could be catalyzed by acetyl-CoA-acetyltransferase 2 (AACT2), which is peroxisomal localized (Reumann et al., 2007) and possibly also functions during isoleucine degradation (*Function 12*).

Secondary effects could also partly cause the reduced seedling growth of *pnc1/2* and *pxa1-2* in the presence of exogenous leucine. Leucine has been shown to be a regulator of gene expression: clusters of genes involved in protein or lipid degradation have been identified to be upregulated under high levels of leucine, which could interfere with peroxisome function (Hannah et al., 2010).

Since NAD is only indirectly required in the form of NADH for H_2O_2 detoxification via the peroxisomal glutathione-ascorbate cycle, no effects of BCAA or intermediate catabolite feeding where expected and observed regarding the PXN mutant (Fig. 1+2).

Our data strongly suggests a peroxisomal role in the degradation of all three BCAAs. In contrary, experiments measuring the O_2 consumption of isolated Arabidopsis mitochondria supplied with exogenous BCAA demonstrated the ability of mitochondria to degrade BCAAs completely and thereby supplying the TCA-cycle with acetyl-CoA (Taylor et al., 2004). Two parallel degradation pathways, one sole

mitochondrial and one involving peroxisomes, would explain these contrarious findings. Further feeding experiments with additional compounds like 2-methylbutyryl-CoA and more peroxisomal mutants like *acx* and *mfp2* will help to extend our knowledge of the peroxisomal role during BCAA catabolism.

β-oxidation is needed to survive extended darkness

In extended darkness energy equivalents have to be generated independently of photosynthesis. Darkness starved plants are bound to grow or sustain metabolic processes heterotrophically and trigger the degradation of cellular macromolecules, such as membrane lipids and proteins. This process releases free fatty acids and amino acids, which can both be used as respiratory substrates to generate energy in the form of ATP (Araujo et al., 2011). *pxa1-2* mutants were depicted as incapable to degrade membrane lipids and displayed a lowered ATP/ADP ratio after >24 hours of darkness (Kunz et al., 2009). The importance of β-oxidation related proteins, e.g., KAT2, CHY1, but also the peroxisomal citrate synthase in mature plants subjected to darkness has been previously addressed (Castillo and Leon, 2008; Dong et al., 2009; Kunz et al., 2009). Our study expands this knowledge and presents the impact of the three remaining peroxisomal transport proteins on tolerance to extended darkness: the ATP transporters PNC1, and PNC2 (Arai et al., 2008; Linka et al., 2008) and the NAD carrier PXN (Agrimi et al., 2012; Bernhardt et al., 2012; *Manuscript 1*).

Exposure of the transport mutants to prolonged darkness led to decreased *QYmax* of PSII (Fig. 3). While *pnc1/2* and *pxa1-2* showed a strong reduction already after 50 hours of darkness, *pxn-1* was distinguishable from wild types only after nine days of darkness. This reflected findings of the rather mild effect of *pxn-1* during seedling establishment. *pxn-1* mutants displayed a delay rather than a block in storage oil mobilization and are able to grow wild-type-like without supplementation of exogenous sucrose (Bernhardt et al., 2012). In contrast seedling establishment of *pxa1-2* and *pnc1/2* is strictly “sucrose-dependent” (Zolman et al., 2001b; Linka et al., 2008; Kessel-Vigelius et al., unpublished). *pxn-1* also only showed a mild resistance to root growth inhibition by 2,4-DB compared to *pxa1-2* or *pnc1/2* (Zolman et al., 2001b; Linka et al., 2008; Bernhardt et al., 2012).

The importance of BCAA breakdown during extended darkness is demonstrated by the darkness sensitivity of mitochondrial leucine catabolic enzyme IVD1 mutants (Araujo et al., 2010). Plants impaired in GDH function (glutamate

dehydrogenase) also suffer from extended darkness due to restrictions in amino acid catabolism (Miyashita and Good, 2008a; 2008b). The conversion of glutamate to 2-oxoglutarate catalyzed by GDH fuels the TCA cycle in stress conditions and is a key reaction in plant C and N metabolism. 2-oxoglutarate is needed as acceptor for the amino group transferred by aminotransferases as first step of amino acid catabolism (Fig. 8, *Function 1*). A closer look at metabolite levels in extended darkness (50 h) revealed a change in glutamate and 2-oxoglutarate pools in peroxisomal transporter mutants. *pnc1/2* and *pxa1-2* exhibited decreased glutamate pools compared to the wild type in extended darkness, while the same extracts displayed increased 2-oxoglutarate levels (Fig. 4C+D). In contrast to *pnc1/2* and *pxa1-2, Col-0* appears to produce glutamate by amination of 2-oxoglutarate, indicating fully functional amino acid catabolism in wild-type plants, while *pnc1/2* and *pxa1-2* are impaired. 2-oxoglutarate and glutamate amounts declined after 9 days of darkness in *pnc1/2* and *pxa1-2* and are likely to be respired in the TCA cycle. During carbon starvation we also noted less (iso-)citric acid in these mutants (Fig. 4E). It may be reasonable to assume that carbon starved *Col-0* and *pxn-1* plants disposed of a C-source that was not available to *pnc1/2* and *pxa1-2*. Amino acids can be used as respiratory substrates and this process was negatively affected in *pnc1/2* and *pxa1-2* plants during dark-induced carbon starvation: cells could not efficiently use amino acids, as well as membrane lipids, as energy source and thus the pools of TCA cycle intermediates, like isocitrate and 2-oxoglutarate, were depleted.

Additionally to the changes regarding TCA cycle intermediates, *pnc1/2* and *pxa1-2* showed differences in BCAA contents (Fig. 6), which have been suggested to be preferably consumed to support respiratory growth in carbon starvation (Araujo et al., 2010). In *Col-0* and *pxn-1* plants free BCAAs accumulated in the leaves from 50 h darkness to nine days darkness, indicating that proteolysis was elevated under these conditions (Araujo et al., 2011). *pnc1/2* and *pxa1-2* did unexpectedly not show BCAA accumulation from 50 h darkness to nine days darkness, indicating that proteolysis was impaired in these mutants. Future research will need to address if there is a feedback inhibition in BCAA degradation possibly to a buildup of propionyl-CoA or isobutyryl-CoA and if this influences proteolysis as the source of free amino acids.

BCAA pools even declined in *pnc1/2* and *pxa1-2* plants during the nine days darkness period, hinting on a peroxisome-independent BCAA catabolism pathway, since it is unreasonable to assume that the free BCAAs have been used for protein

biosynthesis. However, if such a parallel catabolism pathway for BCAAs exists, its capacity is insufficient to degrade large amounts. Otherwise feeding of BCAAs would have shown a less severe effect on *pnc1/2* and *pxa1-2* plants (Fig. 2).

Channeling of free amino acids into synthesis of new proteins is likely the cause for declined BCAA levels in wild type and *pxn-1* upon reillumination (Fig. 6). In contrast, reilluminated *pnc1/2* and *pxa1-2* plants were heavily impaired and did not mobilize amino acids into protein synthesis (Fig. 6).

Malfunctional β-oxidation entails the risk of an increase in free fatty acid and pheophorbide a levels

The effect of extended darkness was described for *pxa1-2* regarding the accumulation of pheophorbide a (PhA) and free fatty acids (FFA; Kunz et al., 2009). In *pxa1-2* plants the impaired peroxisomal β-oxidation leads to damaging of the chloroplast membranes by high levels of FFA. This results in accumulation of the chlorophyll catabolite PhA (Kunz et al., 2009). PhA is phototoxic, which explains the rapid bleaching of *pxa1-2* leaves upon reillumination, which we also observed for *pnc1/2* (Pruzinska et al., 2003; Tanaka et al., 2003; Fig. 3A). PhA oxygenase (PaO) catalyzes the oxidation of PhA. Plants lacking PaO show the same rapid bleaching of leaves, when transferred to light after darkness-induced chlorophyll degradation (Tanaka et al., 2003).

FFA increase was thought to lead to membrane damage due to membrane permeabilization (Schonfeld and Wojtczak, 2008). This could be the cause of PSII electron transport reduction observed in *pxa1-2* and *pnc1/2* (Fig. 3B). Peroxisomal β-oxidation in *pxn-1* is not completely blocked; therefore the plants likely do not accumulate fatty acids and did not show the drastic photobleaching phenotype. The same effect of FFA accumulation seems to appear during stress, where adjustments of membrane lipid composition necessitates increased fatty acid turnover (Falcone et al., 2004; Larkindale et al., 2005). Heat stress led to increased damage in membrane-bound photosystems in *pnc1/2, pxa1-2,* and *pxn-1* probably due to ROS formation (Fig. S2A; Kipp and Boyle, 2013); enhanced ROS production might also explain the necrotic lesions observed for *pnc1/2, pxa1-2,* and *pxn-1* plants after exposure to high temperatures (Fig. S2B). In conditions of high ROS peroxisomal catalase is inactivated (Williams, 1928; Kono and Fridovich, 1982) and a membrane bound complex of ascorbate peroxidase (APX) and monodehydroascorbate

reductase accounts for prevention of peroxisomal ROS leakage: APX reduces H_2O_2 to water using ascorbate as electron donor, oxidizing it to monodehydroascorbate (MDA). MDA regeneration comes along with NADH oxidation in the process (del Rio et al., 2006). This ROS detoxification pathway might explain the observed reduced quantum yield obtained for the NAD transporter mutant *pxn-1* in the basal heat stress assay, where *pnc1/2* plants demonstrate wild-type behavior (Fig. S2A). Furthermore, heat denatured proteins need to be degraded, leading to enhanced amino acid concentrations (Araujo et al., 2011). BCAA degradation gives rise to propionyl-CoA and isobutyryl-CoA, which require conversion to prevent toxic effects. Propionyl-CoA has been described as a potent inhibitor of many CoA dependent enzymes (Schwab et al., 2006).

CONCLUSION

Peroxisomal β-oxidation is more deeply integrated in plant primary metabolism in vegetative and reproductive tissue than previously anticipated. We could show that especially in stress-conditions β-oxidation seems to contribute not only to fatty acid degradation but also to detoxification of amino acid catabolites. The data presented strongly suggests a direct involvement of peroxisomal β-oxidation in BCAA catabolism pathways, but also hints on alternative pathways of limited efficiency, which are peroxisome-independent. Additionally there is strong evidence for propionyl-CoA, isobutyryl-CoA, and possibly 2-methylbutyryl-CoA for being newly identified substrates of the peroxisomal ABC-transporter PXA1.

MATERIALS AND METHODS

Materials

Chemicals were purchased from Sigma-Aldrich. Reagents and enzymes for recombinant DNA techniques were obtained from New England Biolabs and Promega.

Isolation of T-DNA Insertion lines

pnc1-1 (SAIL_303H02), *pnc2-1* (SALK014579) and *pxa1-2* (SALK_019334) *Arabidopsis thaliana* mutants were obtained from the Nottingham Arabidopsis Stock Centre. We constructed the *pnc1/2* mutant by crossing of *pnc1-1* and *pnc2-1* (Kessel-Vigelius et al., unpublished). *pxn-1* was obtained from the GABI-Kat project of the Bielefeld University (GABI-046D01; Bernhardt et al., 2012).

Plant cultivation

Seeds were surface sterilized, stratified for 4-7 days at 4°C and germinated on 0.8% (w/v) agar-solidified half-strength MS medium (Duchefa; with 1% (w/v) sucrose, if indicated). Plants were incubated in a 16 h light/8 h dark cycle (22/18°C) in growth chambers (100 µmol m^{-2} s^{-1} light intensity).

For the analysis of seedling growth, plants were grown on half-strength MS agar plates supplemented with or without sucrose in constant darkness or in short-day conditions (8 h light/16 h dark cycles). After the indicated period, seedlings were photographed or scanned and roots or hypocotyls were measured using Fiji (ImageJ; Schindelin et al., 2012). Plate additives were added from solutions adjusted to pH 5.6. For extended darkness treatments, 25-30 day old plants were subjected to prolonged night conditions at the start of the regular night for the time indicated. To determine seed parameters plants were grown randomized and the position of plant trays was systematically rotated to minimize light effects.

PAM fluometry

In vivo chlorophyll a fluorescence assays were performed using the FluorCam FC 800-C (Photon Systems Instruments). 25-30 day-old dark-treated plants were taken directly out of the growth cabinet and used for fluorescence measurements. To investigate defects in the photosynthetic apparatus standard settings of the

manufacturer's software were used.

Leaf metabolite analysis

Preparation of samples for metabolic analysis was performed as described by Fiehn (2006). Samples were harvested by shock freezing rosette leaves in liquid nitrogen. Leaves were ground in liquid nitrogen, freeze dried and 5 mg of leaf powder was used for extraction with 1.5 ml of pre-chilled (–20°C) mixture of H_2O/methanol/$CHCl_3$ (1:2.5:1) containing 50 µM ribitol. Following incubation under gentle agitation for 6 min at 4°C on a rotating device, samples were centrifuged for 2 min at 20,000 g.
50 µL of the supernatant were dried and used for further analysis by gas chromatography/electron-impact time-of-flight mass spectrometry, as previously described (Lee and Fiehn, 2008). Metabolite content is expressed relative to the internal standard ribitol. Extracts were additionally subjected to amino acid analysis by high-performance liquid chromatography (ZORBAX Rapid Resolution HT Eclipse Plus C18, 2.1 x 50 mm, 1.8 µm column) coupled to a diode array detector (DAD). Chlorophyll was quantified from methanol extract according to Lichtenthaler and Wellburn (1983) and used for normalization of the three independent biological replicates.

Total seed protein quantification

Total protein content of *Col-0*, *pnc1/2*, *pxn-1,* and *pxa1-2* seeds was measured in six replicates. 10 – 25 mg (500 – 1300) seeds were homogenized with 1 ml extraction buffer (10% w/v Glycerol, 0.8 mM DTT, 1 mM PMSF 0.5% w/v, 100 mM Tris; pH: 8) using steel beads and a bead mill. The aqueous phase was purified 3 times by centrifugation (table centrifuge, 20,000 g). Protein concentrations were measured in 4 technical replicates using Pierce BCA Protein Assay Kit (Thermo Scientific).

Quantitative reverse transcriptase-polymerase chain reaction (qRT-PCR)

RNA was isolated from 10-week-old *A. thaliana* rosette leaves after a protocol developed by Chomczynski and Sacchi (1987). RNA integrity was determined on a 1% Agarose gel. Prior to cDNA synthesis, RNA was treated with RNase-free RQ1-DNase (Promega) as recommended by the manufacturer. The Arabidopsis thaliana senescence associated gene 12 (SAG12; At5g45890) transcript was examined via quantitative reverse transcription PCR (qRT-PCR). For this analysis the messenger

RNAs (mRNAs) of the total RNA were transcribed into complementary DNAs (cDNAs) using the Superscript III RNase H-Reverse Transcriptase (Invitrogen, Life Technologies). The cDNA synthesis was performed according to the manufacturers' instructions. The resulted cDNA pools were used as template for Real-time PCR with *A. thaliana* SAG12 specific oligonucleotides JW149 (TGCGGTAAATCAGTTTGCTG) and JW150 (ACGGCGACATTTTAGTTTGG). Transcript levels in *A. thaliana* were determined by quantitative RT-PCR with the MESA-SYBR-Green II Kit without ROX (Eurogentec Germany GmbH) according to the manuals instructions, run with the Standard SYBR-Green protocol of the StepOnePlus™ Real-Time PCR System (Applied Biosystems). Tip41-like specific oligonucleotides published by Czechowski et al. (2005) were used as reference primer pair.

Bioinformatic and statistical analysis

Pearson correlation analysis and PCA score plots were performed with the Multiple Experiment Viewer (Saeed et al., 2003). Statistical analyses were performed with GraphPad Prism 5.0. Quantitative analysis results are presented as means ±SE from repeated experiments as indicated in the figure legends. Pairwise Student's t-test was used to analyze statistical significance.

List of supplemented data

Fig. S1 Mean of chlorophyll concentration of 4-week-old *Col-0*, *pnc1/2, pxn-1,* and *pxa1-2* at the end of day, extended darkness (50 h), reillumination for 24 h after 50 h darkness and incubation in the dark for nine days (carbon starvation).

Fig. S2 Heat stress treatment of 4-week-old *Col-0*, *pnc1/2*, *pxn-1,* and *pxa1-2*

Fig. S3 *pnc1/2* and *pxn-1* display accelerated leaf senescence

ACKNOWLEDGEMENTS

We thank Sarah Keßel-Vigelius for providing us with *pnc1/2* seeds. Elisabeth Klemp and Katrin Weber are acknowledged for help with GC-MS and HPLC-DAD analysis of plant extracts.

AUTHOR CONTRIBUTIONS

Martin Schroers and Jan Wiese performed the experiments and wrote the manuscript. Andreas Weber and Nicole Linka provided lab space and helpful discussions. Martin Schroers, Jan Wiese, and Nicole Linka designed the experiments.

REFERENCES

Abbasi, A.-R., Saur, A., Hennig, P., Tschiersch, H., Hajirezaei, M., Hofius, D., Sonnewald, U. and Voll, L.M. (2009) Tocopherol deficiency in transgenic tobacco (Nicotiana tabacum L.) plants leads to accelerated senescence. *Plant Cell Environ*, **32**, 144-157.

Abe, K. (2012) Butyric acid induces apoptosis in both human monocytes and lymphocytes equivalently. *Journal of oral science*, **54**, 7-14.

Agrimi, G., Russo, A., Pierri, C.L. and Palmieri, F. (2012) The peroxisomal NAD+ carrier of Arabidopsis thaliana transports coenzyme A and its derivatives. *J Bioenerg Biomembr*, **44**, 333-340.

Arai, Y., Hayashi, M. and Nishimura, M. (2008) Proteomic identification and characterization of a novel peroxisomal adenine nucleotide transporter supplying ATP for fatty acid beta-oxidation in soybean and Arabidopsis. *Plant Cell*, **20**, 3227-3240.

Araujo, W.L., Ishizaki, K., Nunes-Nesi, A., Larson, T.R., Tohge, T., Krahnert, I., Witt, S., Obata, T., Schauer, N., Graham, I.A., Leaver, C.J. and Fernie, A.R. (2010) Identification of the 2-hydroxyglutarate and isovaleryl-CoA dehydrogenases as alternative electron donors linking lysine catabolism to the electron transport chain of Arabidopsis mitochondria. *Plant Cell*, **22**, 1549-1563.

Araujo, W.L., Tohge, T., Ishizaki, K., Leaver, C.J. and Fernie, A.R. (2011) Protein degradation - an alternative respiratory substrate for stressed plants. *Trends Plant Sci*, **16**, 489-498.

Balazadeh, S., Parlitz, S., Mueller-Roeber, B. and Meyer, R.C. (2008) Natural developmental variations in leaf and plant senescence in Arabidopsis thaliana. *Plant Biol (Stuttg)*, **10 Suppl 1**, 136-147.

Bernhardt, K., Wilkinson, S., Weber, A.P. and Linka, N. (2012) A peroxisomal carrier delivers NAD(+) and contributes to optimal fatty acid degradation during storage oil mobilization. *Plant J*, **69**, 1-13.

Brouquisse, R., Gaudillere, J.P. and Raymond, P. (1998) Induction of a carbon-starvation-related proteolysis in whole maize plants submitted to Light/Dark cycles and to extended darkness. *Plant Physiol*, **117**, 1281-1291.

Castillo, M.C. and Leon, J. (2008) Expression of the beta-oxidation gene 3-ketoacyl-CoA thiolase 2 (KAT2) is required for the timely onset of natural and dark-induced leaf senescence in Arabidopsis. *J Exp Bot*, **59**, 2171-2179.

Che, P., Wurtele, E.S. and Nikolau, B.J. (2002) Metabolic and environmental regulation of 3-methylcrotonyl-coenzyme A carboxylase expression in Arabidopsis. *Plant Physiol*, **129**, 625-637.

Childs, B., Nyhan, W.L., Borden, M., Bard, L. and Cooke, R.E. (1961) Idiopathic hyperglycinemia and hyperglycinuria: a new disorder of amino acid metabolism. I. *Pediatrics*, **27**, 522-538.

Chomczynski, P. and Sacchi, N. (1987) Single-step method of RNA isolation by acid guanidinium thiocyanate-phenol-chloroform extraction. *Analytical biochemistry*, **162**, 156-159.

Czechowski, T., Stitt, M., Altmann, T., Udvardi, M.K. and Scheible, W.R. (2005) Genome-wide identification and testing of superior reference genes for transcript normalization in Arabidopsis. *Plant Physiol*, **139**, 5-17.

Daschner, K., Couee, I. and Binder, S. (2001) The mitochondrial isovaleryl-coenzyme a dehydrogenase of arabidopsis oxidizes intermediates of leucine and valine catabolism. *Plant Physiol*, **126**, 601-612.

De Marcos Lousa, C., van Roermund, C.W., Postis, V.L., Dietrich, D., Kerr, I.D., Wanders, R.J., Baldwin, S.A., Baker, A. and Theodoulou, F.L. (2013) Intrinsic acyl-CoA thioesterase activity of a peroxisomal ATP binding cassette transporter is required for transport and metabolism of fatty acids. *Proc Natl Acad Sci U S A*.

del Rio, L.A., Sandalio, L.M., Corpas, F.J., Palma, J.M. and Barroso, J.B. (2006) Reactive oxygen species and reactive nitrogen species in peroxisomes. Production, scavenging, and role in cell signaling. *Plant Physiol*, **141**, 330-335.

Dong, C.H., Zolman, B.K., Bartel, B., Lee, B.H., Stevenson, B., Agarwal, M. and Zhu, J.K. (2009) Disruption of Arabidopsis CHY1 reveals an important role of metabolic status in plant cold stress signaling. *Mol Plant*, **2**, 59-72.

Engqvist, M., Drincovich, M.F., Flugge, U.I. and Maurino, V.G. (2009) Two D-2-hydroxy-acid dehydrogenases in Arabidopsis thaliana with catalytic capacities to participate in the last reactions of the methylglyoxal and beta-oxidation pathways. *J Biol Chem*, **284**, 25026-25037.

Engqvist, M.K.M., Kuhn, A., Wienstroer, J., Weber, K., Jansen, E.E.W., Jakobs, C., Weber, A.P.M. and Maurino, V.G. (2011) Plant D-2-hydroxyglutarate dehydrogenase participates in the catabolism of lysine especially during senescence. *J Biol Chem*, **286**, 11382-11390.

Falcone, D.L., Ogas, J.P. and Somerville, C.R. (2004) Regulation of membrane fatty acid composition by temperature in mutants of Arabidopsis with alterations in membrane lipid composition. *BMC Plant Biol*, **4**, 17.

Fiehn, O. (2006) Metabolite profiling in Arabidopsis. *Methods Mol Biol*, **323**, 439-447.

Footitt, S., Cornah, J.E., Pracharoenwattana, I., Bryce, J.H. and Smith, S.M. (2007a) The Arabidopsis 3-ketoacyl-CoA thiolase-2 (kat2-1) mutant exhibits increased flowering but reduced reproductive success. *J Exp Bot*, **58**, 2959-2968.

Footitt, S., Dietrich, D., Fait, A., Fernie, A.R., Holdsworth, M.J., Baker, A. and Theodoulou, F.L. (2007b) The COMATOSE ATP-binding cassette transporter is required for full fertility in Arabidopsis. *Plant Physiol*, **144**, 1467-1480.

Fujiki, Y., Ito, M., Itoh, T., Nishida, I. and Watanabe, A. (2002) Activation of the promoters of Arabidopsis genes for the branched-chain alpha-keto acid dehydrogenase complex in transgenic tobacco BY-2 cells under sugar starvation. *Plant Cell Physiol*, **43**, 275-280.

Fujiki, Y., Sato, T., Ito, M. and Watanabe, A. (2000) Isolation and characterization of cDNA clones for the e1beta and E2 subunits of the branched-chain alpha-ketoacid dehydrogenase complex in Arabidopsis. *J Biol Chem*, **275**, 6007-6013.

Fukao, T., Song, X.Q., Mitchell, G.A., Yamaguchi, S., Sukegawa, K., Orii, T. and Kondo, N. (1997) Enzymes of ketone body utilization in human tissues: protein and messenger RNA levels of succinyl-coenzyme A (CoA):3-ketoacid CoA transferase and mitochondrial and cytosolic acetoacetyl-CoA thiolases. *Pediatric research*, **42**, 498-502.

Hannah, M.A., Caldana, C., Steinhauser, D., Balbo, I., Fernie, A.R. and Willmitzer, L. (2010) Combined transcript and metabolite profiling of Arabidopsis grown under widely variant growth conditions facilitates the identification of novel metabolite-mediated regulation of gene expression. *Plant Physiol*, **152**, 2120-2129.

Hu, J., Baker, A., Bartel, B., Linka, N., Mullen, R.T., Reumann, S. and Zolman, B.K. (2012) Plant peroxisomes: biogenesis and function. *Plant Cell*, **24**, 2279-2303.

Jin, H., Song, Z. and Nikolau, B.J. (2012) Reverse genetic characterization of two paralogous acetoacetyl CoA thiolase genes in Arabidopsis reveals their importance in plant growth and development. *Plant J*, **70**, 1015-1032.

Khan, B.R., Adham, A.R. and Zolman, B.K. (2012) Peroxisomal Acyl-CoA oxidase 4 activity differs between Arabidopsis accessions. *Plant Mol Biol*, **78**, 45-58.

Khan, B.R. and Zolman, B.K. (2010) pex5 Mutants that differentially disrupt PTS1 and PTS2 peroxisomal matrix protein import in Arabidopsis. *Plant Physiol*, **154**, 1602-1615.

Kipp, E. and Boyle, M. (2013) The Effects of Heat Stress on Reactive Oxygen Species Production and Chlorophyll Concentration in Arabidopsis Thaliana. *Research in Plant Sciences*, **1**, 20-23.

Kono, Y. and Fridovich, I. (1982) Superoxide radical inhibits catalase. *J Biol Chem*, **257**, 5751-5754.

Kunz, H.H., Scharnewski, M., Feussner, K., Feussner, I., Flugge, U.I., Fulda, M. and Gierth, M. (2009) The ABC transporter PXA1 and peroxisomal beta-oxidation are vital for metabolism in mature leaves of Arabidopsis during extended darkness. *Plant Cell*, **21**, 2733-2749.

Kurita-Ochiai, T., Fukushima, K. and Ochiai, K. (1995) Volatile fatty acids, metabolic by-products of periodontopathic bacteria, inhibit lymphocyte proliferation and cytokine production. *Journal of dental research*, **74**, 1367-1373.

Lange, P.R., Eastmond, P.J., Madagan, K. and Graham, I.A. (2004) An Arabidopsis mutant disrupted in valine catabolism is also compromised in peroxisomal fatty acid beta-oxidation. *FEBS Lett*, **571**, 147-153.

Larkindale, J., Hall, J.D., Knight, M.R. and Vierling, E. (2005) Heat stress phenotypes of Arabidopsis mutants implicate multiple signaling pathways in the acquisition of thermotolerance. *Plant Physiol*, **138**, 882-897.

Lee, D.Y. and Fiehn, O. (2008) High quality metabolomic data for Chlamydomonas reinhardtii. *Plant Methods*, **4**, 7-7.

Lichtenthaler, H.K. and Wellburn, A.R. (1983) Determinations of total carotenoids and chlorophylls a and b of leaf extracts in different solvents. *Biochem. Soc. Trans.*

Linka, N., Theodoulou, F.L., Haslam, R.P., Linka, M., Napier, J.A., Neuhaus, H.E. and Weber, A.P. (2008) Peroxisomal ATP import is essential for seedling development in Arabidopsis thaliana. *Plant Cell*, **20**, 3241-3257.

Lucas, K.A., Filley, J.R., Erb, J.M., Graybill, E.R. and Hawes, J.W. (2007) Peroxisomal metabolism of propionic acid and isobutyric acid in plants. *J Biol Chem*, **282**, 24980-24989.

Maxwell, K. and Johnson, G.N. (2000) Chlorophyll fluorescence--a practical guide. *J Exp Bot*, **51**, 659-668.

Middleton, B. and Bartlett, K. (1983) The synthesis and characterisation of 2-methylacetoacetyl coenzyme A and its use in the identification of the site of the defect in 2-methylacetoacetic and 2-methyl-3-hydroxybutyric aciduria. *Clinica chimica acta; international journal of clinical chemistry*, **128**, 291-305.

Miyashita, Y. and Good, A.G. (2008a) Glutamate deamination by glutamate dehydrogenase plays a central role in amino acid catabolism in plants. *Plant Signal Behav*, **3**, 842-843.

Miyashita, Y. and Good, A.G. (2008b) NAD(H)-dependent glutamate dehydrogenase is essential for the survival of Arabidopsis thaliana during dark-induced carbon starvation. *J Exp Bot*, **59**, 667-680.

Pauli, G. and Overath, P. (1972) ato Operon: a highly inducible system for acetoacetate and butyrate degradation in Escherichia coli. *Eur J Biochem*, **29**, 553-562.

Pracharoenwattana, I., Cornah, J.E. and Smith, S.M. (2007) Arabidopsis peroxisomal malate dehydrogenase functions in beta-oxidation but not in the glyoxylate cycle. *Plant J*, **50**, 381-390.

Pruzinska, A., Tanner, G., Anders, I., Roca, M. and Hortensteiner, S. (2003) Chlorophyll breakdown: pheophorbide a oxygenase is a Rieske-type iron-sulfur protein, encoded by the accelerated cell death 1 gene. *Proc Natl Acad Sci U S A*, **100**, 15259-15264.

Reumann, S., Babujee, L., Ma, C., Wienkoop, S., Siemsen, T., Antonicelli, G.E., Rasche, N., Luder, F., Weckwerth, W. and Jahn, O. (2007) Proteome analysis of Arabidopsis leaf peroxisomes reveals novel targeting peptides, metabolic pathways, and defense mechanisms. *Plant Cell*, **19**, 3170-3193.

Reumann, S., Ma, C., Lemke, S. and Babujee, L. (2004) AraPerox. A database of putative Arabidopsis proteins from plant peroxisomes. *Plant Physiol*, **136**, 2587-2608.

Richmond, T.A. and Bleecker, A.B. (1999) A defect in beta-oxidation causes abnormal inflorescence development in Arabidopsis. *Plant Cell*, **11**, 1911-1924.

Rylott, E.L., Eastmond, P.J., Gilday, A.D., Slocombe, S.P., Larson, T.R., Baker, A. and Graham, I.A. (2006) The Arabidopsis thaliana multifunctional protein gene (MFP2) of peroxisomal beta-oxidation is essential for seedling establishment. *Plant J*, **45**, 930-941.

Saeed, A.I., Sharov, V., White, J., Li, J., Liang, W., Bhagabati, N., Braisted, J., Klapa, M., Currier, T., Thiagarajan, M., Sturn, A., Snuffin, M., Rezantsev, A., Popov, D., Ryltsov, A., Kostukovich, E., Borisovsky, I., Liu, Z., Vinsavich, A., Trush, V. and Quackenbush, J. (2003) TM4: a free, open-source system for microarray data management and analysis. *BioTechniques*, **34**, 374-378.

Schindelin, J., Arganda-Carreras, I., Frise, E., Kaynig, V., Longair, M., Pietzsch, T., Preibisch, S., Rueden, C., Saalfeld, S., Schmid, B., Tinevez, J.Y., White, D.J., Hartenstein, V., Eliceiri, K., Tomancak, P. and Cardona, A. (2012) Fiji: an open-source platform for biological-image analysis. *Nature methods*, **9**, 676-682.

Schonfeld, P. and Wojtczak, L. (2008) Fatty acids as modulators of the cellular production of reactive oxygen species. *Free Radic Biol Med*, **45**, 231-241.

Schuster, J. and Binder, S. (2005) The mitochondrial branched-chain aminotransferase (AtBCAT-1) is capable to initiate degradation of leucine, isoleucine and valine in almost all tissues in Arabidopsis thaliana. *Plant Mol Biol*, **57**, 241-254.

Schwab, M.A., Sauer, S.W., Okun, J.G., Nijtmans, L.G.J., Rodenburg, R.J.T., van den Heuvel, L.P., Drose, S., Brandt, U., Hoffmann, G.F., Ter Laak, H., Kolker, S. and Smeitink, J.A.M. (2006) Secondary mitochondrial dysfunction in propionic aciduria: a pathogenic role for endogenous mitochondrial toxins. *Biochem J*, **398**, 107-112.

Shockey, J. and Browse, J. (2011) Genome-level and biochemical diversity of the acyl-activating enzyme superfamily in plants. *Plant J*, **66**, 143-160.

Slocombe, S.P., Cornah, J., Pinfield-Wells, H., Soady, K., Zhang, Q., Gilday, A., Dyer, J.M. and Graham, I.A. (2009) Oil accumulation in leaves directed by modification of fatty acid breakdown and lipid synthesis pathways. *Plant Biotechnol J*, **7**, 694-703.

Tanaka, R., Hirashima, M., Satoh, S. and Tanaka, A. (2003) The Arabidopsis-accelerated cell death gene ACD1 is involved in oxygenation of pheophorbide a: inhibition of the pheophorbide a oxygenase activity does not lead to the "stay-green" phenotype in Arabidopsis. *Plant Cell Physiol*, **44**, 1266-1274.

Taylor, N.L., Heazlewood, J.L., Day, D.A. and Millar, A.H. (2004) Lipoic acid-dependent oxidative catabolism of alpha-keto acids in mitochondria provides evidence for branched-chain amino acid catabolism in Arabidopsis. *Plant Physiol*, **134**, 838-848.

Troncoso-Ponce, M.A., Cao, X., Yang, Z. and Ohlrogge, J.B. (2013) Lipid turnover during senescence. *Plant science : an international journal of experimental plant biology*, **205-206**, 13-19.

Williams, J. (1928) The Decomposition of Hydrogen Peroxide by Liver Catalase. *J Gen Physiol*, **11**, 309-337.

Wingler, A. and Roitsch, T. (2008) Metabolic regulation of leaf senescence: interactions of sugar signalling with biotic and abiotic stress responses. *Plant Biol (Stuttg)*, **10 Suppl 1**, 50-62.

Yang, Z. and Ohlrogge, J.B. (2009) Turnover of fatty acids during natural senescence of Arabidopsis, Brachypodium, and switchgrass and in Arabidopsis beta-oxidation mutants. *Plant Physiol*, **150**, 1981-1989.

Zolman, B.K., Martinez, N., Millius, A., Adham, A.R. and Bartel, B. (2008) Identification and characterization of Arabidopsis indole-3-butyric acid response mutants defective in novel peroxisomal enzymes. *Genetics*, **180**, 237-251.

Zolman, B.K., Monroe-Augustus, M., Thompson, B., Hawes, J.W., Krukenberg, K.A., Matsuda, S.P. and Bartel, B. (2001a) chy1, an Arabidopsis mutant with impaired beta-oxidation, is defective in a peroxisomal beta-hydroxyisobutyryl-CoA hydrolase. *J Biol Chem*, **276**, 31037-31046.

Zolman, B.K., Silva, I.D. and Bartel, B. (2001b) The Arabidopsis pxa1 mutant is defective in an ATP-binding cassette transporter-like protein required for peroxisomal fatty acid beta-oxidation. *Plant Physiol*, **127**, 1266-1278.

SUPPLEMENTS

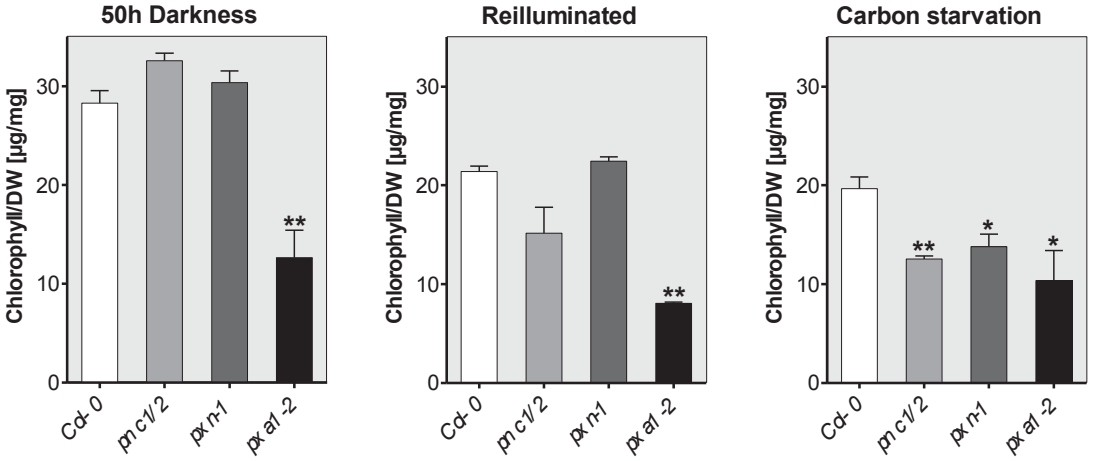

Figure S1: Chlorophyll concentrations are altered in peroxisomal transporter mutants during elongated darkness.

Mean of chlorophyll concentration (+SE; n=3) of 4-week-old *old Col-0, pnc1/2, pxn-1 and pxa1-2* at the end of day, extended darkness (50 h), reillumination for 24 h after 50 h darkness and incubation in the dark for nine days (Carbon starvation). Differences between the mean of biological replicates of each measurement were marked as statistically significant (t-test) with the Col-0 control by (*) or (**) at respective significance levels of ($P < 0.05$) or ($P < 0.01$).

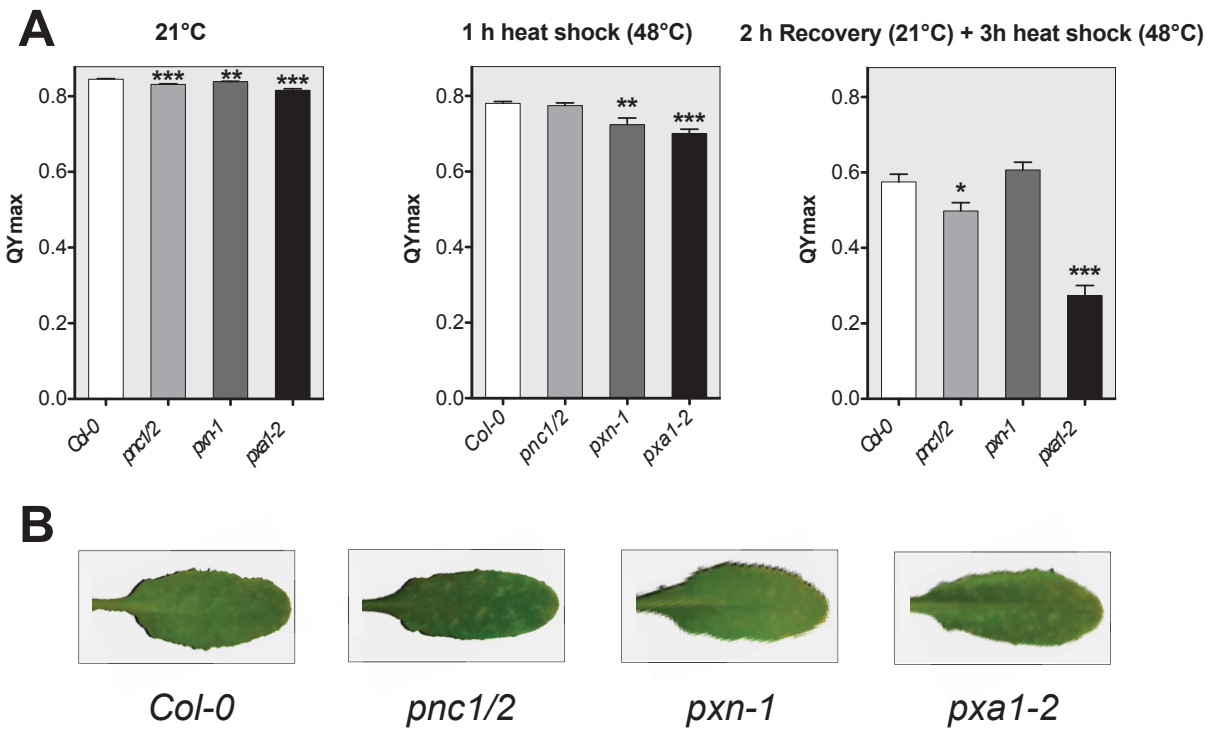

Figure S2: **Heat stress treatment of 4-week-old *Col-0*, *pnc1/2*, *pxn-1* and *pxa1-2*.**
(A) Mean of maximum quantum yield (+SE; n=3) of 4-week-old *Col-0*, *pnc1/2*, *pxn-1* and *pxa1-2* after exposure to at least 1 hour darkness in different temperatures. Heat treatments were: 21°C (control), 1 h heat shock (48°C) and 1 h heat shock (48°C) followed by 2 h recovery at 21°C and an additional 3 h heat shock (48°C). Differences between the mean (+SE) of each treatment were marked as statistically significant (t-test) with the Col-0 control by (*), (**) or (***) at respective significance levels of ($P < 0.05$), ($P < 0.01$) or ($P < 0.001$).
(B) Photograph of heat stressed leaves 24 h after the treatment. Necrotic lesions are more abundant for *pxa1-2*, *pnc1/2* and *pxn-1*.

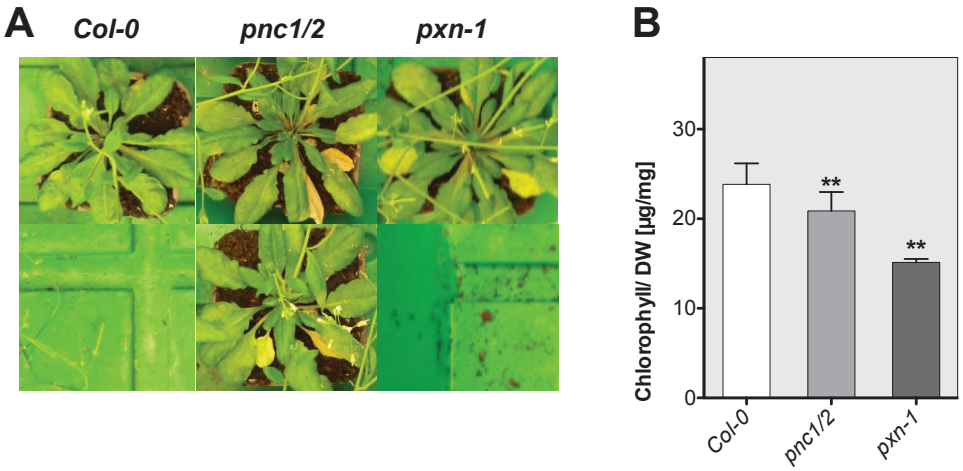

Figure S3: *pnc1/2* and *pxn-1* display accelerated leaf senescence.
(A) Photographs of *Col-0*, *pnc1/2* and *pxn-1* plants during natural senescence, showing the peroxisomal transporter mutants exhibiting completely yellow leaves.
(B) In still green but aged rosette leaves chlorophyll contents of *pnc1/2* and *pxn-1* are reduced in comparison to the wild type. Differences between the mean of at least three biological replicates (±SE) of each measurement were marked as statistically significant (t-test) with the *Col-0* control by ** at significance level of $P < 0.01$.

Concluding remarks

Our knowledge about the involvement of peroxisomes in different metabolic pathways keeps expanding. Here e.g., we were able to confirm the postulated role of peroxisomes during BCAA breakdown (*Manuscript 3*). Some of these metabolic pathways require the function of yet unidentified peroxisomal transport proteins for shuttling metabolites or cofactors. Peroxisomal β-oxidation for example is dependent on CoA and since PXN does likely not mediate CoA import *in vivo* (*Manuscript 1*), an unidentified CoA transporter is possibly present in the peroxisomal membrane. CoA could alternatively be synthesized directly inside peroxisomes, because the dephospho-CoA kinase which catalyzes the phosphorylation of dephospho-CoA to CoA has been found in peroxisomes (Reumann et al., 2009). However, this would require a transporter for dephospho-CoA import. Other examples for unknown peroxisomal transporters are the carrier proteins (or possibly a single carrier) mediating malate and/or oxaloacetate import and export as part of the malate/oxaloacetate shuttle.

Identification and functional characterization of yet unknown peroxisomal transport proteins will be a challenging task for the coming years and will improve our overall knowledge on peroxisomal functions. Additionally, understanding how known and yet unknown peroxisomal carriers are regulated is an important question that has to be addressed by future studies.

Reumann, S., Quan, S., Aung, K., Yang, P., Manandhar-Shrestha, K., Holbrook, D., Linka, N., Switzenberg, R., Wilkerson, C.G., Weber, A.P., Olsen, L.J. and Hu, J. (2009) In-depth proteome analysis of Arabidopsis leaf peroxisomes combined with in vivo subcellular targeting verification indicates novel metabolic and regulatory functions of peroxisomes. *Plant Physiol*, **150**, 125-143.

VI. Previously published manuscript

VI.1 *Manuscript 4*

An engineered plant peroxisome and its application in biotechnology

Sarah K.-Kessel-Vigelius[*,1], Jan Wiese[*,1], Martin G. Schroers[*,1], Thomas J. Wrobel[*,1], Florian Hahn[1] and Nicole Linka[1,2]

* Co-first authors

[1] Institute for Plant Biochemistry and Cluster of Excellence on Plant Sciences (CEPLAS), Heinrich Heine University, Universitaetsstrasse 1, 40225 Duesseldorf, Germany.

[2] To whom correspondence should be addressed. E-Mail: Nicole.Linka@hhu.de.

Plant Science 210 (2013) 232–240

Contents lists available at SciVerse ScienceDirect

Plant Science

journal homepage: www.elsevier.com/locate/plantsci

Review

An engineered plant peroxisome and its application in biotechnology☆

Sarah K. Kessel-Vigelius[1], Jan Wiese[1], Martin G. Schroers[1], Thomas J. Wrobel[1], Florian Hahn, Nicole Linka*

Heinrich-Heine University, Plant Biochemistry, Universitätsstrasse 1, Building 26.03.01, D-40225 Düsseldorf, Germany

ARTICLE INFO

Article history:
Received 20 March 2013
Received in revised form 8 June 2013
Accepted 10 June 2013
Available online 17 June 2013

Keywords:
Peroxisome
Biotechnology
Genetic engineering
Metabolism
Stress tolerance

ABSTRACT

Plant metabolic engineering is a promising tool for biotechnological applications. Major goals include enhancing plant fitness for an increased product yield and improving or introducing novel pathways to synthesize industrially relevant products. Plant peroxisomes are favorable targets for metabolic engineering, because they are involved in diverse functions, including primary and secondary metabolism, development, abiotic stress response, and pathogen defense. This review discusses targets for manipulating endogenous peroxisomal pathways, such as fatty acid β-oxidation, or introducing novel pathways, such as the synthesis of biodegradable polymers. Furthermore, strategies to bypass peroxisomal pathways for improved energy efficiency and detoxification of environmental pollutants are discussed. In sum, we highlight the biotechnological potential of plant peroxisomes and indicate future perspectives to exploit peroxisomes as biofactories.

Contents

1. Introduction

Plants have evolved the ability to produce a wide range of molecules. Many of these compounds are of biotechnological importance, as they serve as food, colorants, flavors, fragrances, traditional medicines, pharmaceuticals, cosmetics, and renewable fuels [1]. Their chemical synthesis is often difficult and expensive, thus genetic engineering is an alternative approach to optimize the production of desired metabolites in plants.

In plants, biochemical pathways are compartmentalized and individual steps of a particular pathway are distributed over

Abbreviations: H_2O_2, hydrogen peroxide; JA, jasmonic acid; PHA, polyhydroxyalkanoate; ROS, reactive oxygen species.

* Corresponding author. Tel.: +49 0211 81 10412.
E-mail addresses: Sarah.Vigelius@hhu.de (S.K. Kessel-Vigelius), Jan.Wiese@hhu.de (J. Wiese), Martin.Schroers@hhu.de (M.G. Schroers), Thomas.Jan.Wrobel@hhu.de (T.J. Wrobel), Florian.Hahn@hhu.de (F. Hahn), Nicole.Linka@hhu.de (N. Linka).
[1] Co-first authors.

0168-9452/$ – see front matter © 2013 The Authors. Published by Elsevier Ireland Ltd. All rights reserved.
http://dx.doi.org/10.1016/j.plantsci.2013.06.005

different compartments. In this context, peroxisomes, which are subcellular organelles 1 μm in diameter [2], represent as organelles at a metabolic crossroads [3,4], because they participate in one or more steps in many significant metabolic reactions, including primary carbon metabolism (e.g. beta-oxidation of fatty acids and photorespiration), secondary metabolism (e.g. production of glucosinolates), development (e.g. synthesis of plant hormones), abiotic stress response, and pathogen defense [4].

Thus, peroxisomes are an attractive target for metabolic engineering, to increase yield and quality of plant products. Manipulation of peroxisomal scavenging systems for reactive oxygen species (ROS) might enhance plant fitness under environmental stress conditions [5]. Besides altering peroxisomal functions, novel pathways can be implemented in peroxisomes, enabling the synthesis of desired metabolites or degradation of toxic molecules. The following characteristics illustrate why peroxisomes are well suited for biotechnological purposes:

(i) Peroxisomes are surrounded by a single lipid bilayer membrane [4]. Novel reactions can be compartmentalized within peroxisomes. A peroxisomal compartmentation is favorable because end products or intermediates can be toxic for the cell. As peroxisomes are equipped with efficient ROS-detoxifying systems [6], ROS-producing reactions can be introduced in peroxisomes without deleterious effects.
(ii) Peroxisomes allow an efficient targeting of heterologous proteins, since protein-targeting signals for the peroxisome are well established. Soluble, nuclear-encoded proteins are targeted to peroxisomes by two different targeting signals, which direct soluble proteins to peroxisomes. Most proteins use the Type 1 Peroxisomal Targeting Signal (PTS1) to enter peroxisomes, which consists of three amino acids at the carboxyl terminus (SKL, or a conserved variant) [7,8]. The Type 2 Peroxisomal Targeting Signal (PTS2) is a conserved nonapeptide (9 amino acids), which is attached to the amino terminus of peroxisomal proteins [9]. Fusion of either signal peptide to a heterologous protein results in direct targeting to peroxisomes. Thus, the enzymatic content of peroxisomes can be easily modified. In contrast to plastids and mitochondria, the peroxisomal protein import machinery is able to import fully folded proteins and stable protein complexes in a receptor-independent fashion [4]. The import of heterologous protein complexes into peroxisomes depends on a mechanism called piggybacking, where a protein without a peroxisomal targeting signal uses a PTS-carrying protein as shuttle [10,11]. Therefore, coupling of a shuttle protein to other proteins might enable the targeting of even larger protein complexes to peroxisomes without modifying the import receptor machinery.
(iii) Peroxisomes are highly dynamic organelles, which are able to adjust size and number [12]. They multiply by fission and proliferation [4]. Latter is induced by various environmental, developmental and metabolic cues and is controlled by the PEROXIN11 protein family and several transcription factors [13,14]. A rapid increase in peroxisome number allows an accumulation of substances produced in peroxisomes [2].

In recent years, major progress has been made in genomics and proteomics, revealing the diversity of peroxisomal metabolism [4,15]. However, mechanisms to exploit plant peroxisomes for optimizing metabolism or modifying metabolic fluxes toward compounds of interest are not well studied. Here, we present recent pioneering approaches to produce plant peroxisome biofactories. Moreover, we indicate putative targets and possible strategies that in the future could be exploited to engineer peroxisomes for biotechnological purposes.

2. Improving seed oil yield and quality

One of the major goals of agricultural biotechnology is to increase the content and/or improve the value of oils in oilseed plants, including sunflower, soybean, palm, oilseed rape, and maize crops [16]. Oilseed crops are not only important for human nutrition [17], but can also be used for a variety of chemical applications.

Plants are able to produce a wide range of different fatty acids, whereas the number of fatty acids shared between plant species is relatively low. All conventional crops contain palmitic acid, stearic acid, oleic acid, linoleic acid, and linolenic acid. These are termed "usual" fatty acids. Fatty acids, which in their chemical structures differ from usual fatty acids, are referred to as "unusual" fatty acids. Unusual fatty acids, exhibiting hydroxylations or acetylations, are of major industrial interest, as they provide raw materials for the generation of biopolymers or fuels [18].

Vegetable oils, for example, serve as a sustainable replacement of petroleum-based chemicals [16]. One appealing method to produce high-value oils is the genetic engineering of plants accumulating ricinoleic acid, which serves as precursor for economically-viable products, such as ink, lubricants, varnishes, emulsifiers, nylon, or biodiesel [18,19].

The bottleneck for increased oilseed content and the production of 'designer oils' is the channeling of fatty acids into storage oil. Inefficient integration arises either by enhanced biosynthesis of native fatty acids or by the low affinity of acyltransferases to unusual fatty acids [20,21]. As a consequence, accumulated fatty acids are degraded via peroxisomal beta-oxidation, which simultaneously operates during lipid synthesis (Fig. 1).

Inactivating peroxisomal beta-oxidation enzymes by using specific promoters only active during seed filling could minimize such futile cycling. Another strategy is to produce the desired oil in a specific plant tissue with low beta-oxidation activity (e.g. leaves). Leaf-specific oil production might be favorable if the accumulation of industrial-valuable oil in seeds affected germination or seedling establishment [22].

3. Plant peroxisomes confer stress tolerance

Various abiotic and biotic stress conditions, such as salinity, heat, cold, drought, and pathogen infection induce oxidative stress in plants. This results in overproduction of ROS in chloroplasts, mitochondria, and peroxisomes, with highly oxidative metabolism [23,24]. Plants are unable to escape exposure to environmental stresses, thus they have developed a complex antioxidant defense system to control ROS levels and protect cells from oxidative injury [6]. Here, we present several strategies to improve stress tolerance in plants through modified peroxisomal metabolism circumventing oxidative stress and thereby increasing fitness [25].

3.1. Increasing the peroxisome population

Plant peroxisomes multiply under stress conditions. In plants the PEROXIN11 family, which consist of five isoforms (a–e), controls proliferation of peroxisomes. When overexpressed, the number of peroxisomes increases. Conversely, reducing the expression of PEX11 genes results in decreased peroxisome abundance [26]. The expression of PEX11b is controlled through a phytochrome A-dependent pathway, involving the far-red light photoreceptor phyA and the bZIP transcription factor HY5 homolog [13,27].

Additionally, peroxisomal proliferation is induced by environmental stimuli and various stresses, such as high light intensities, H_2O_2, ozone, xenobiotics, cadmium, salt, pathogens, and senescence. However, little is known about the principal molecular mechanisms [28–33]. Stress-induced peroxisome proliferation

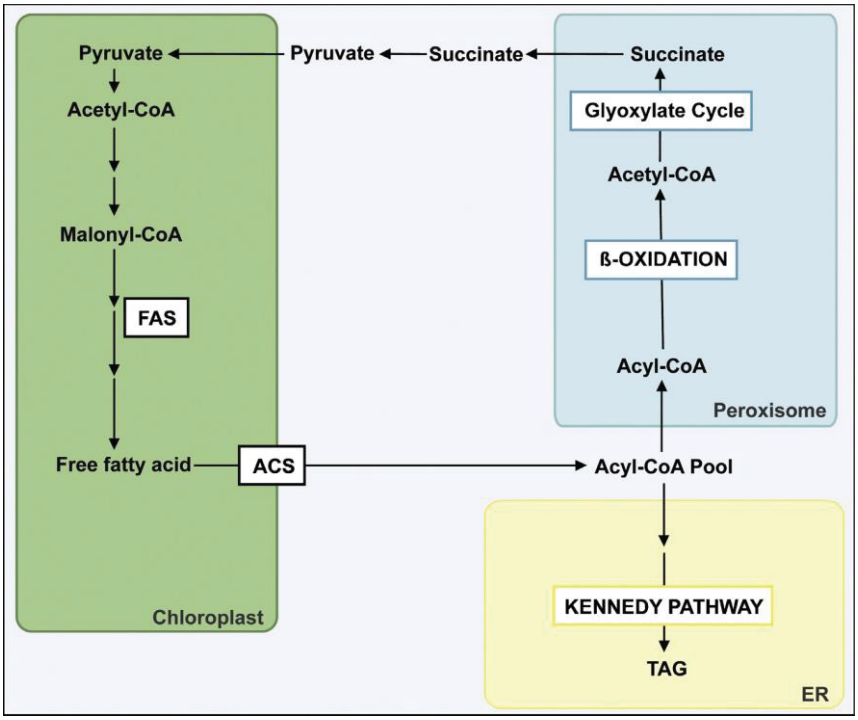

Fig. 1. Fatty acids synthesis and catabolism take place simultaneously in plant cells. In chloroplasts fatty acids (FAs) are generated from acyl-CoA and pyruvate via the fatty acid synthesis complex and are then released into the cytosol. FAs are either catabolized via peroxisomal β-oxidation or incorporated into triacylglycerols via the Kennedy pathway in the ER. CoA, coenzyme A; FAS, fatty acid synthesis complex; ACS, acyl CoA synthetase; ER, endoplasmic reticulum; TAG, triacylglycerol.

may reflect the ability to cope with oxidative damage. Consequently, controlling the peroxisomal population is a promising strategy to enhance stress tolerance in plants.

Introduction of a peroxisome proliferator-activated receptor from *Xenopus laevis* in tobacco plants leads to increased peroxisome number in transgenic tobacco plants [34]. Expression of this regulatory complex increases peroxisome number in transgenic tobacco plants, as it was previously reported for animal tissues [35]. The activity of peroxisomal enzymes involved in ROS-scavenging is increased, leading to potentially improved resistance to oxidative stress [36]. The induced peroxisome proliferation disrupts the plant's redox state, leading to modified salicylic acid levels and altered expression patterns of jasmonic acid and ethylene biosynthesis genes. These changes positively affect pathogen resistance [36].

In an independent approach, an enlarged peroxisome population was produced by up-regulation of the *Arabidopsis* peroxisome biogenesis gene PEX11, the regulator of peroxisome proliferation [13]. However, increasing the peroxisome number did not result in elevated salt tolerance in *Arabidopsis* seedlings and older plants [37]. Future studies need to elucidate if manipulating peroxisome biogenesis can be a strategy to alter stress tolerance. However, understanding regulation and all possible side-effects is crucial when increasing the peroxisomal population.

3.2. Improving peroxisomal ROS-scavenging systems

Under non-stress conditions ROS produced by peroxisomal metabolism are scavenged by the simultaneous action of the peroxisomal antioxidant systems catalase, ascorbate peroxidase and the ascorbate–glutathione cycle [38]. However, under oxidative stress conditions peroxisomal ROS generation is enhanced and ROS scavenging is insufficient [38]. The ability to cope with an increased ROS production is correlated with upregulation of peroxisomal antioxidant systems in natural stress-tolerant plant species [39,40]. One goal for engineering plants with wide-ranging stress resistance would be improving the peroxisomal ROS scavenging machinery (i.e. modulate the gene expression and enzymatic activity).

Catalase as a prominent H_2O_2 scavenger is an important target. It is highly abundant in plant peroxisomes but has a low substrate affinity [41]. Modulation of its catalytic activity might be a starting-point to overcome this drawback, leading to more efficient ROS detoxification in plant peroxisomes. Because bacterial catalases offer higher H_2O_2 affinity, several studies have ectopically expressed the *Escherichia coli* catalase in plant species such as tobacco, tomato, and rice [42–44]. The resulting transgenic plants displayed an increased protection against oxidative stress. The same outcome was achieved by overexpression of the peroxisomal ascorbate peroxidase (APX), which acts in tandem with catalase to degrade H_2O_2 [45,46]. Alternatively, an enhanced ascorbate–glutathione cycle in the peroxisomal matrix could reduce plant stress [38]. To accomplish this task various modifications are required simultaneously: (i) enlarging the peroxisomal glutathione and ascorbate pool by stimulating biosynthesis and uptake into peroxisomes, (ii) increasing the NADPH levels in peroxisomes by over-expressing the peroxisomal NAD kinase for NADPH production [47], and (iii) constitutive peroxisomal targeting of glutathione reductase, which carries a weak peroxisomal targeting signal and is located in the cytosol and peroxisomes [48]. Previous studies have successfully induced the biosynthesis of glutathione and ascorbate, resulting in higher glutathione and ascorbate levels in the cytosol [49,50]. To increase peroxisomal import of glutathione and ascorbate, specific peroxisomal transport proteins remain to be identified. To date, modifying the redox state of peroxisomal ascorbate and glutathione pools is feasible [47,48]. Enhancing glutathione and ascorbate uptake remains to be achieved in future, since corresponding peroxisomal transporters have not been identified thus far.

3.3. Improved pest and pathogen resistance

Plants suffer from infections caused by fungi, bacteria, viruses and nematodes. Peroxisomes play a substantial role in disease resistance and are targets for genetic improvement to confer pathogen tolerance in plants [4].

The phytohormone jasmonic acid (JA) is a lipid-derived signaling molecule that induces plant defense mechanisms [51]. Its production is triggered in response to tissue injury (wounding) caused by herbivore attack. The last steps of JA biosynthesis occur in peroxisomes [51]. The JA precursor 12-oxo-phytodienoic acid (OPDA) is imported into peroxisomes and is subsequently reduced to OPC8:0 (3-oxo-2-(2′[*Z*]-pentenyl)-cyclopentan-1-octanoic acid), In three rounds of peroxisomal beta-oxidation activated OPC8:0 is converted to JA [52]. Overexpression of the transcription factor WRKY30 in rice resulted in a constitutive expression of plastidic JA biosynthesis genes. This was associated with increased endogenous JA accumulation and enhanced tolerance against fungal pathogens [53]. As JA biosynthetic enzymes locate to companion cells and sieve elements of the vascular bundle [54], it might be beneficial to not only improve biosynthesis, but extend JA production to other tissues to prime plants against herbivore attack. This involves exploiting a natural peroxisomal function.

Plant peroxisomes contribute to extracellular defense mechanisms against fungi by preventing colonization. Upon fungal invasion peroxisomes migrate toward the site of invasion [55]. Under these conditions the myrosinase PEN2, which is bound to the peroxisomal membrane, hydrolyzes indolic glucosinolates to antifungal defense compounds protecting plants against fungal entry [56]. Furthermore, certain benzylglucosinolates play a role in pathogen defense and are found in developing seeds and germinating seedlings [57]. These active defense molecules are synthesized in the cytosol by transferring a benzoyl moiety from benzoyl-CoA to a hydroxylated aliphatic glucosinolate, though the precursor benzoyl-CoA is primarily produced from cinnamic acid via peroxisomal beta-oxidation [58–60].

Engineering levels of these defense compounds might enhance plant immunity against pathogens. This can be achieved by targeting either biosynthetic or regulatory genes of glucosinolate biosynthesis [58,61]. Glucosinolates are naturally found in crucifers, including oilseed rape and *Arabidopsis*, but their production could be successfully implemented in non-cruciferous plants, such as tobacco [62]. However, cruciferous crop seeds with high glucosinolate content are unwanted as primary food source for animals or humans, because these metabolites have a bitter taste [63]. An agricultural challenge for the future is to eliminate glucosinolates from edible parts of crops, but retain their synthesis in source tissues for protection against pathogen attack. Specific expression and suppression of peroxisomal modules involved in benzylglucosinolate production might be a promising approach to solve this problem.

3.4. Peroxisomal small heat shock proteins for enhanced stress tolerance

Small heat-shock proteins are induced in response to various stresses. They act as molecular chaperones preventing the aggregation of nascent and stress-accumulated misfolded proteins [64,65]. Two peroxisome-located small heat-shock proteins called AtAcd31.2 and AtHsp15.7 were identified in *Arabidopsis* [66]. AtAcd31.2 is constitutively expressed, whereas AtHsp15.7 expression is strongly induced by heat and oxidative stress [66], suggesting that peroxisomal small heat-shock proteins play a role in protecting proteins under both physiological and stress conditions [67]. The overexpression of small heat-shock proteins might be a useful strategy to produce plants with enhanced tolerance against different stresses. Previous studies have demonstrated that substantial tolerance to salt, drought and high light can be achieved by over-expressing cytosolic or plastidic heat-shock proteins [67–69].

4. Modulating auxin synthesis in peroxisomes

Peroxisomes are involved in biogenesis of the auxin indole-3-acetic acid. Indole-3-butyric acid is metabolized to the active form indole-3-acetic acid by removing two side-chain methylene units in a process similar to fatty acid beta-oxidation [70,71]. It has been shown that indole-3-butyric acid-derived auxin influences cell expansion in certain cell types, resulting in elongated root hairs and enlarged cotyledons [72]. Elongation of root hairs by stimulating auxin production is a promising approach to enlarge root surface area and thereby enhance water and nutrient uptake [73]. Whether this goal can be accomplished without major drawbacks on plant development remains to be shown.

5. Implementation of artificial metabolic pathways to gain novel peroxisomal functions

Besides optimizing peroxisomal metabolism, metabolic engineering can achieve novel peroxisomal functions. The goal is to introduce artificial pathways into plant peroxisomes for either producing novel substances or improving efficiency of peroxisomal pathways degrading toxic compounds.

5.1. Production of biodegradable polymers in plant peroxisomes

Plant peroxisomes are attractive factories for biodegradable polymers, such as polyhydroxyalkanoates (PHA). Renewable bioplastics are sustainable and have the potential to replace conventional mineral oil-based plastics [74].

PHAs are a group of polyesters, which are naturally formed and deposited as inclusion bodies in many bacterial genera. They are not produced in eukaryotes [75]. PHAs can incorporate more than one hundred different hydroxyacids, mainly varying in functional groups of side chains and chain length [76]. Thus, physical properties of PHA range from glues to brittle plastics, depending on the composition [77]. The biosynthesis pathway of the most common type of PHAs, the homopolymer poly-3-hydroxybutyrate (PHB), was discovered first in *Ralstonia eutropha*, where it serves as a carbon sink [78,79]. Its synthesis pathway has been successfully introduced into different microorganisms, which naturally do not produce these polymers [80]. To increase substrate availability for PHA biosynthesis, overproduction of the starting substrate acetyl-CoA was induced, which led to an improved PHA production in these organisms [81].

However, PHA production in microorganisms is not economical because of expensive bacterial feedstock, such as glucose [82]. To address economic inefficiency, plants producing high amounts of PHA were designed. Plants are well suited, as water, light, CO_2, and a few minerals suffice to produce high amounts of biomass. Moreover, plants are unable to degrade PHAs and thus can accumulate these polymers in high amounts. For successful PHA production in plants three prerequisites are needed: (i) the bacterial three-gene pathway consisting of a 3-ketothiolase (*pha*A), an acetoacetyl-CoA reductase (*pha*B) and a PHA synthase (*pha*C), (ii) a large acetyl-CoA pool, and (iii) reducing power [83].

PHA production was first achieved in the cytosol of Arabidopsis and tobacco, because only two additional enzymes had to be introduced, *pha*B and *pha*C, as plants endogenously possess a cytosolic form of *pha*A as part of the mevalonate pathway (Fig. 2A). The production of PHA led to a strong reduction of plant growth, resulting from depletion of cytoplasmic acetyl-CoA, inhibiting

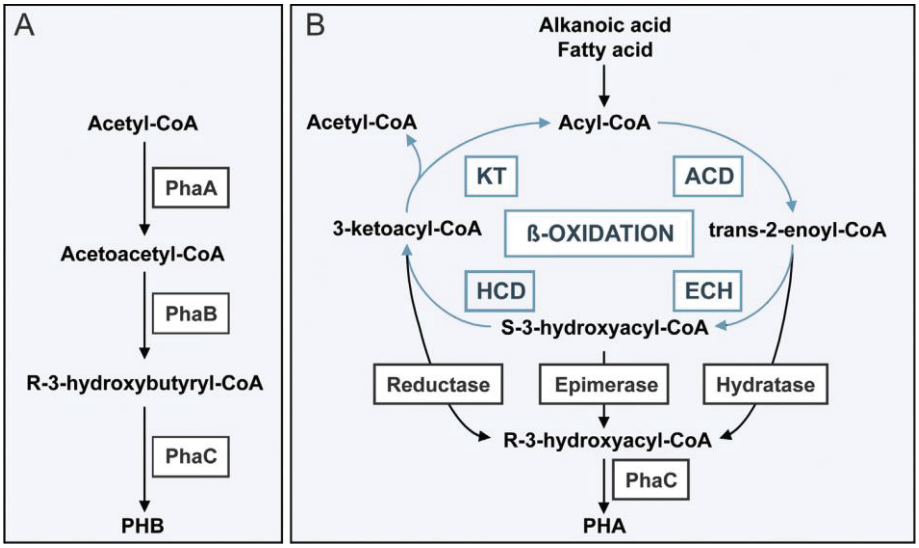

Fig. 2. (A) PHB synthesis in *Ralstonia eutropha*. Bacterial pathway of PHB production in *R. eutropha*. *pha*A, 3-ketothiolase; *pha*B, acetoacetyl-CoA reductase; *pha*C, PHA synthase. (B) PHA synthesis in plants can be implemented into the beta-oxidation cycle. Intermediates of the beta-oxidation can be used for PHA synthesis. Either an epimerase, a hydratase, or a reductase is necessary to convert cycle intermediates into substrates for *pha*C. The beta-oxidation core reactions are depicted in blue. KT, 3-ketothiolase; ACD, acyl-CoA dehydrogenase; ECH, enoyl-CoA hydratase I; HCD, S-3 hydroxyacyl-CoA dehydrogenase.

isoprenoid and flavonoid biosynthesis [75,84]. To achieve higher PHA levels, with less deleterious effects, production was targeted to chloroplasts of numerous plant species. PHA yield was predicted to increase, as plastids have a high flux of acetyl-CoA, which is required for fatty acid biosynthesis. In transgenic plant lines accumulating high amounts of PHA in their chloroplasts, growth was reduced, plants were chlorotic, and sometimes fertility was impacted. The reasons for the strong phenotype have not been clearly determined [85–87].

To minimize plant growth defects, PHA synthesis was targeted to plant peroxisomes (Fig. 2B) exploiting peroxisomal carbon flux through beta-oxidation for synthesis [88–91]. A peroxisomal targeting signal was fused to the bacterial *pha*A, *pha*B, and *pha*C genes. Peroxisomes of PHA-producing plants are significantly enlarged. This reflects that these organelles have the capability to increase their size to accommodate large volumes of PHA granules [91]. Studies with the C4-grass sugarcane, a high biomass crop, showed that peroxisomal PHA biosynthesis significantly contributes to PHA production levels of commercial interest in crop plants, without interfering with plant growth [91].

5.2. Peroxisomal bypass pathways to reduce photorespiration

A central function of plant peroxisomes is their contribution to photorespiration (Fig. 3) [4]. This light-dependent pathway is linked to photosynthesis by the dual function of plastidic RubisCO. Low carbon dioxide concentrations favor the oxygenase reaction of RubisCO leading to an accumulation of toxic 2-phosphoglycolate [92]. This compound is efficiently degraded via the photorespiratory C2 cycle, converting 2-phosphoglycolate to 3-phosphoglycerate, which re-enters the Calvin–Benson cycle. CO_2 and ammonia (NH_3) are released. Substantial energy costs are required for re-assimilation (Fig. 3) [92]. The goal is to optimize plant metabolism and to increase biomass production by minimizing energy losses in photorespiration. As photorespiration is required in all photosynthetic organisms, it cannot be eliminated completely, but bypassed [93]. So far, three reactions have been tested in plants circumventing energy loss from photorespiration [94]. A reduction of the RubisCO oxygenase reaction was attempted by increasing CO_2 levels inside chloroplasts, utilizing carbon derived from 2-phosphogycolate (Fig. 3, blue pathway) [95]. Secondly, an alternative plastidic conversion route for 2-phosphoglycolate has been reported (Fig. 3, red pathway) [96]. Both approaches bypassing the mitochondrial CO_2 release led to an increase in biomass production under ambient CO_2 conditions [95,96].

To avoid mitochondrial NH_3 production a short-circuit pathway of the photorespiratory nitrogen cycle was implemented into peroxisomes [97]. Glyoxylate carboligase (GCL) and hydroxypyruvate isomerase (HYI) from *E. coli* were introduced into peroxisomes of transgenic tobacco leaves resulting in a peroxisomal conversion of glyoxylate to hydroxypyruvate (Fig. 3, green pathway). Unfortunately, this bypass did not show the benefits expected for biomass production [97]. Instead, leaves of transgenic tobacco displayed chlorotic lesions under ambient CO_2 levels. Detailed analyses revealed that the GCL/HYI pathway introduced was not fully operating, due to silencing of the bacterial hydroxypyruvate isomerase gene [97]. Thus, the functionality of this proposed pathway remains to be demonstrated. The use of RNA-silencing tobacco mutants might overcome this obstacle [98]. It might enable further analyses studying peroxisomes as tools to bypass photorespiration [97].

5.3. Peroxisomal degradation pathways for pollutants

Genetically modified plants can help to reduce environmental pollution by degradation of long-persisting chemical compounds in contaminated soil or ground water. The implementation of catabolic pathways from various bacterial and fungal organisms into plants allows detoxification of certain organic pollutants [99].

For example, tobacco plants have been developed which degrade the halogenated aliphatic compound 1,2-dichloroethane, a carcinogenic chemical of high stability. In these plants, two enzymes from *Xanthobacter autotrophicus* were expressed that catabolize 1,2-dichloroethane to glycolate in combination with endogenous enzymes [100]. High accumulation of the resulted end product glycolate is toxic for the plant cell and needs to be directly metabolized. In particular for the root tissue, it might be to ectopically introduce the photorespiratory enzyme glycolate oxidase in root cells for the conversion of glycolate to glyoxylate.

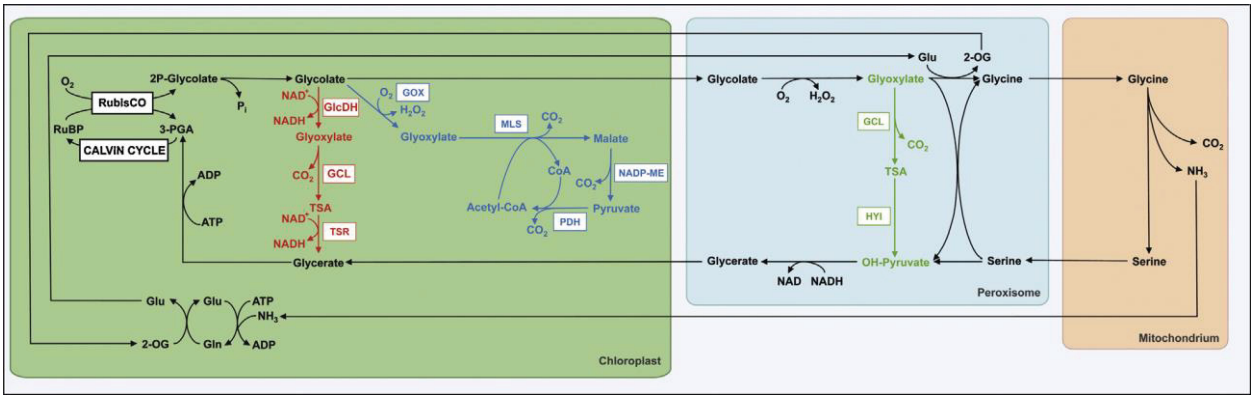

Fig. 3. The loss of ammonia during photorespiration can be bypassed. Ammonia and CO_2 are released in mitochondria during the conversion of glycine to serine. Ammonia can be re-assimilated in chloroplasts. The ammonia-consuming reactions can be bypassed by a photorespiratory short-circuit in peroxisomes (shown in green) by introducing two bacterial enzymes GCL and HYI. The plastidic bypasses introduced by Maier et al. [95] and Kebeish et al. [96] are presented in blue and red, respectively. RuBP, ribulose-1,5-bisphosphate; PGA, phosphoglycerate; Glu, glutamate; Gln, glutamine; 2-OG, 2-oxoglutarate; ATP, adenosine triphosphate; ADP, adenosine diphosphate; NAD(H), nicotinamide adenine dinucleotide; TSA, tartronic semialdehyde; GCL, glyoxylate carbolyase; HYI, hydroxypyruvate isomerase.

Sulfur dioxide is a major air pollutant emitted by industrial processes. SO_2 adversely affects growth and development of crop species, causing chlorosis, necrosis and long-term yield reduction [101–103]. It enters plant tissues as gas, where it is transformed to sulfite. Excess amounts of sulfite are toxic to the plant cell. Peroxisomal catalase activity is sensitive to sulfite, resulting in high H_2O_2 levels upon sulfite stress [104]. The key enzyme to protect plants against sulfite toxicity is the peroxisomal sulfite oxidase, catalyzing the oxidation of sulfite to sulfate. To improve sulfite detoxification, the peroxisomal sulfite oxidase from maize was overexpressed in plants [105,106]. Transgenic lines exhibiting elevated sulfite oxidase levels confer enhanced tolerance to excess sulfite, which is indicated by lower H_2O_2 and higher catalase levels. Hence, the overexpression of sulfite oxidase may protect peroxisomal catalase from inhibition by sulfite [106].

6. Concluding remarks

Besides recent progress in the field of peroxisome engineering, the emerging potential of plant peroxisomes for green biotechnology is described in this review. Strategies are presented which either (i) manipulate peroxisomal pathways to alter oilseed quantity and quality, or (ii) improve tolerance toward abiotic and biotic stresses. Further, approaches are shown which involve (iii) implementing new pathways in peroxisomes, such as the production of biodegradable polymers, (iv) bypassing peroxisomal pathways for a better energy-cost efficiency, and (v) detoxifying pollutants from contaminated soil, water and air.

However, several limitations have to be considered when modifying or introducing pathways to peroxisomes. If fluxes through endogenous peroxisomal pathways are changed, overall cellular metabolism and substrate homeostasis could be negatively influenced. For example, changes in peroxisomal contributions to auxin synthesis or photorespiration were reported to create substantial reductions in fitness [107,108]. In order to estimate the biotechnological potential of plant peroxisomes, it is necessary to understand how peroxisomal metabolism is regulated and coordinated.

When implementing novel pathways, the pH optimum inside peroxisomes needs to be considered, because newly introduced enzymes with a strict cofactor- and pH-dependency might be impaired. The pH of plant peroxisomes has not yet been determined. Reports for other eukaryotic organisms, including yeast and mammals, indicated contradictory results the peroxisomal matrix is either acidic or alkaline [109–112]. In addition, cofactors need to be available in peroxisomes, when implementing certain enzymatic reactions. Peroxisomes are capable of importing fully folded proteins, which have already bound their cofactor in the cytosol [113]. For ATP, NAD and CoA transporters have been identified importing these cofactors into peroxisomes [114–116]. Further, the level of peroxide radicals could interfere with enzyme activities, since peroxisomes exhibit an oxidative metabolism producing ROS.

Successful engineering of plant peroxisomal metabolism requires insights into the complete protein inventory. To date, proteome analyses identified more than 100 peroxisomal proteins in plants. However, further enzymes are necessary to fulfill proposed or described metabolic functions [117]. In this context, a major obstacle is the missing comprehensive knowledge about metabolite transport proteins, mediating the flux of solutes across the peroxisomal membrane [118]. Although many peroxisomal transport steps are hypothesized in plants, the corresponding transporter genes have not yet been assigned. Besides the three cofactor carriers mentioned earlier, only the carrier importing fatty acids has been identified so far [114–116,118–120]. With regard to metabolite transport, biotechnological implementations have to be considered carefully, because the prospective substrates and products need to be shuttled in and out of peroxisomes.

As very little is know about endogenous export from peroxisomes, secretion of substances produced in peroxisomes might even be a favorable trait for biotechnological production, as it is known for algae [121]. Such a process protects the cell from potential toxic effects of compounds created in this organelle. On the other hand, secretion of products can be favorable to avoid expensive downstream processing after biotechnological production. In a process called peroxicretion, subsequent excretion of peroxisomal products from cells was achieved by fusing the soluble domain of a Golgi-derived v-SNARE to a peroxisomal membrane protein used as an anchor. Fusion of peroxisomes with the plasma membrane was induced and products were released into the extracellular space [122]. This artificial secretion pathway, coupled to an inducible promoter controlling the time point of product release, might raise the utility of engineered production in plant peroxisomes for industrial biotechnology.

A long-term goal of engineering plant peroxisomes is the construction of synthetic peroxisomes in plants or other eukaryotic organisms, such as yeast. First steps toward this goal have been taken recently, when in a human cell line two antioxidant enzymes, a Cu/Zn-superoxide dismutase and a catalase isoform, were expressed in polymer vesicles, which have a membrane made

permeable by insertion of channel proteins. In this artificial peroxisome superoxide radicals and H_2O_2 detoxification was functional [123].

Acknowledgements

This work was supported by the DFG-grant 1781/1-1, 1781/2-1 and GRK 1525. The authors thank Andreas P.M. Weber for helpful discussion and P.K. Lundqvist for reading the manuscript.

References

[1] J.M. Hibberd, A.P.M. Weber, Plant metabolism and physiology, Curr. Opin. Plant Biol. 15 (2012) 225–227.
[2] M. Hayashi, M. Nishimura, Entering a new era of research on plant peroxisomes, Curr. Opin. Plant Biol. 6 (2003) 577–582.
[3] R. Erdmann, M. Veenhuis, W.H. Kunau, Peroxisomes: organelles at the crossroads, Trends Cell Biol. 7 (1997) 400–407.
[4] J. Hu, et al., Plant peroxisomes: biogenesis and function, Plant Cell 24 (2012) 2279–2303.
[5] J. Nielsen, Metabolic engineering: techniques for analysis of targets for genetic manipulations, Biotechnol. Bioeng. 58 (1998) 125–132.
[6] J.M. Palma, et al., Antioxidative enzymes from chloroplasts, mitochondria, and peroxisomes during leaf senescence of nodulated pea plants, J. Exp. Bot. 57 (2006) 1747–1758.
[7] S.J. Gould, G.A. Keller, N. Hosken, J. Wilkinson, S. Subramani, A conserved tripeptide sorts proteins to peroxisomes, J. Cell Biol. 108 (1989) 1657–1664.
[8] C. Ma, S. Reumann, Improved prediction of peroxisomal PTS1 proteins from genome sequences based on experimental subcellular targeting analyses as exemplified for protein kinases from Arabidopsis, J. Exp. Bot. 59 (2008) 3767–3779.
[9] B.W. Swinkels, S.J. Gould, A.G. Bodnar, R.A. Rachubinski, S. Subramani, A novel, cleavable peroxisomal targeting signal at the amino-terminus of the rat 3-ketoacyl-CoA thiolase, EMBO J. 10 (1991) 3255–3262.
[10] M.S. Lee, R.T. Mullen, R.N. Trelease, Oilseed isocitrate lyases lacking their essential type 1 peroxisomal targeting signal are piggybacked to glyoxysomes, Plant Cell 9 (1997) 185–197.
[11] T. Meyer, C. Holscher, C. Schwoppe, A. von Schaewen, Alternative targeting of *Arabidopsis* plastidic glucose-6-phosphate dehydrogenase G6PD1 involves cysteine-dependent interaction with G6PD4 in the cytosol, Plant J. 66 (2011) 745–758.
[12] M. Schrader, N.A. Bonekamp, M. Islinger, Fission and proliferation of peroxisomes, Biochim. Biophys. Acta 1822 (2011) 1343–1357.
[13] T. Orth, et al., The PEROXIN11 protein family controls peroxisome proliferation in Arabidopsis, Plant cell 19 (2007) 333–350.
[14] M. Yan, N. Rayapuram, S. Subramani, The control of peroxisome number and size during division and proliferation, Curr. Opin. Cell Biol. 17 (2005) 376–383.
[15] M. Islinger, S. Grille, H.D. Fahimi, M. Schrader, The peroxisome: an update on mysteries, Histochem. Cell Biol. 137 (2012) 547–574.
[16] J.A. Napier, I.A. Graham, Tailoring plant lipid composition: designer oilseeds come of age, Curr. Opin. Plant Biol. 13 (2010) 330–337.
[17] N. Ruiz-Lopez, O. Sayanova, J.A. Napier, R.P. Haslam, Metabolic engineering of the omega-3 long chain polyunsaturated fatty acid biosynthetic pathway into transgenic plants, J. Exp. Bot. 63 (2012) 2397–2410.
[18] J.A. Napier, The production of unusual fatty acids in transgenic plants, Annu. Rev. Plant Biol. 58 (2007) 295–319.
[19] J. Jaworski, E.B. Cahoon, Industrial oils from transgenic plants, Curr. Opin. Plant Biol. 6 (2003) 178–184.
[20] V. Eccleston, J. Ohlrogge, Expression of lauroyl-acyl carrier protein thioesterase in *Brassica napus* seeds induces pathways for both fatty acid oxidation and biosynthesis and implies a set point for triacylglycerol accumulation, Plant Cell 10 (1998) 613–622.
[21] L. Moire, E. Rezzonico, S. Goepfert, Y. Poirier, Impact of unusual fatty acid synthesis on futile cycling through beta-oxidation and on gene expression in transgenic plants, Plant Physiol. 134 (2004) 432–442.
[22] S.P. Slocombe, et al., Oil accumulation in leaves directed by modification of fatty acid breakdown and lipid synthesis pathways, Plant Biotechnol. J. 7 (2009) 694–703.
[23] B. Halliwell, Reactive species and antioxidants. Redox biology is a fundamental theme of aerobic life, Plant Physiol. 141 (2006) 312–322.
[24] R. Mittler, Oxidative stress, antioxidants and stress tolerance, Trends Plant Sci. 7 (2002) 405–410.
[25] W. Wang, B. Vinocur, A. Altman, Plant responses to drought, salinity and extreme temperatures: towards genetic engineering for stress tolerance, Planta 218 (2003) 1–14.
[26] N. Kaur, J. Hu, Dynamics of peroxisome abundance: a tale of division and proliferation, Curr. Opin. Plant Biol. 78 (2009) 781–788.
[27] M. Desai, J. Hu, Light induces peroxisome proliferation in Arabidopsis seedlings through the photoreceptor phytochrome A, the transcription factor HY5 HOMOLOG, and the peroxisomal protein PEROXIN11b, Plant Physiol. 146 (2008) 1117–1127.
[28] M.C. Castillo, L.M. Sandalio, L.A. del Rio, J. Leon, Peroxisome proliferation, wound-activated responses and expression of peroxisome-associated genes are cross-regulated but uncoupled in *Arabidopsis thaliana*, Plant Cell Environ. 31 (2008) 492–505.
[29] E. Lopez-Huertas, W.L. Charlton, B. Johnson, I.A. Graham, A. Baker, Stress induces peroxisome biogenesis genes, EMBO J. 19 (2000) 6770–6777.
[30] D.J. Morre, et al., Peroxisome proliferation in Norway spruce induced by ozone, Protoplasma 155 (1990) 58–65.
[31] J.M. Palma, M. Garrido, M.I. Rodriguez-Garcia, L.A. del Rio, Peroxisome proliferation and oxidative stress mediated by activated oxygen species in plant peroxisomes, Arch Biochem. Biophys. 287 (1991) 68–74.
[32] G.M. Pastori, L.A. del Rio, An activated-oxygen-mediated role for peroxisomes in the mechanism of senescence of *Pisum sativum* leaves, Planta 193 (1994) 385–391.
[33] M.C. Romero-Puertas, et al., Cadmium toxicity and oxidative metabolism of pea leaf peroxisomes, Free Radic. Res. 31 (Suppl) (1999) S25–S31.
[34] A.G. Nila, et al., Expression of a peroxisome proliferator-activated receptor gene (xPPARalpha) from *Xenopus laevis* in tobacco (*Nicotiana tabacum*) plants, Planta 224 (2006) 569–581.
[35] I. Isemann, S. Green, Activation of a member of the steroid hormone receptor superfamily by peroxisome proliferators, Nature 347 (1990) 645–650.
[36] J.H. Valenzuela-Soto, et al., Transformed tobacco (*Nicotiana tabacum*) plants over-expressing a peroxisome proliferator-activated receptor gene from *Xenopus laevis* (xPPARα) show increased susceptibility to infection by virulent *Pseudomonas syringae* pathogens, Planta 233 (2011) 507–521.
[37] S. Mitsuya, et al., Salt stress causes peroxisome proliferation, but inducing peroxisome proliferation does not improve NaCl tolerance in *Arabidopsis thaliana*, PLoS One 5 (2010) e9408.
[38] L.A. del Rio, et al., Reactive oxygen species, antioxidant systems and nitric oxide in peroxisomes, J. Exp. Bot. 53 (2002) 1255–1272.
[39] V. Mittova, M. Guy, M. Tal, M. Volokita, Salinity up-regulates the antioxidative system in root mitochondria and peroxisomes of the wild salt-tolerant tomato species *Lycopersicon pennellii*, J. Exp. Bot. 55 (2004) 1105–1113.
[40] V. Mittova, M. Tal, M. Volokita, M. Guy, Up-regulation of the leaf mitochondrial and peroxisomal antioxidative systems in response to salt-induced oxidative stress in the wild salt-tolerant tomato species *Lycopersicon pennellii*, Plant Cell Environ. 26 (2003) 845–856.
[41] A. Mhamdi, G. Noctor, A. Baker, Plant catalases: peroxisomal redox guardians, Arch. Biochem. Biophys. 61 (2012) 4197–4220.
[42] E.A. Mohamed, et al., Overexpression of bacterial catalase in tomato leaf chloroplasts enhances photo-oxidative stress tolerance, Plant Cell Environ. 26 (2003) 2037–2046.
[43] T. Moriwaki, et al., Overexpression of the *Escherichia coli* catalase gene, katE, enhances tolerance to salinity stress in the transgenic indica rice cultivar, BR5, Plant Biotechnol. Rep. 2 (2008) 41–46.
[44] T. Shikanai, et al., Inhibition of ascorbate peroxidase under oxidative stress in tobacco having bacterial catalase in chloroplasts, FEBS Lett. 428 (1998) 47–51.
[45] Y.-J. Li, R.-L. Hai, X.-H. Du, X.-N. Jiang, H. Lu, Over-expression of a Populus peroxisomal ascorbate peroxidase (PpAPX) gene in tobacco plants enhances stress tolerance, Plant Breeding 128 (2009) 404–410.
[46] J. Wang, H. Zhang, R.D. Allen, Overexpression of an Arabidopsis peroxisomal ascorbate peroxidase gene in tobacco increases protection against oxidative stress, Plant Cell Physiol. 40 (1999) 725–732.
[47] J.C. Waller, P.K. Dhanoa, U. Schumann, R.T. Mullen, W.A. Snedden, Subcellular and tissue localization of NAD kinases from Arabidopsis: compartmentalization of *de novo* NADP biosynthesis, Planta 231 (2010) 305–317.
[48] A.R. Kataya, S. Reumann, Arabidopsis glutathione reductase 1 is dually targeted to peroxisomes and the cytosol, Plant Signal. Behav. 5 (2010).
[49] Z. Chen, T.E. Young, J. Ling, S.C. Chang, D.R. Gallie, Increasing vitamin C content of plants through enhanced ascorbate recycling, Proc. Natl. Acad. Sci. USA 100 (2003) 3525–3530.
[50] C.H. Foyer, et al., Overexpression of glutathione-reductase but not glutathione synthase leads to increases in antioxidant capacity and resistance to photoinhibition in poplar trees, Plant Physiol. 109 (1995) 1047–1057.
[51] I.F. Acosta, E.E. Farmer, Jasmonates, The *Arabidopsis* Book, vol. 8, 2010, pp. e0129.
[52] C. Wasternack, E. Kombrink, Jasmonates: structural requirements for lipid-derived signals active in plant stress responses and development, ACS Chem. Biol. 5 (2010) 63–77.
[53] X. Peng, et al., Constitutive expression of rice WRKY30 gene increases the endogenous jasmonic acid accumulation, PR gene expression and resistance to fungal pathogens in rice, Planta 236 (2012) 1485–1498.
[54] B. Hause, G. Hause, C. Kutter, O. Miersch, C. Wasternack, Enzymes of jasmonate biosynthesis occur in tomato sieve elements, Plant Cell Physiol. 44 (2003) 643–648.
[55] V. Lipka, et al., Pre- and postinvasion defenses both contribute to nonhost resistance in Arabidopsis, Science 310 (2005) 1180–1183.
[56] P. Bednarek, et al., A glucosinolate metabolism pathway in living plant cells mediates broad-spectrum antifungal defense, Science 323 (2009) 101–106.
[57] G. Graser, N.J. Oldham, P.D. Brown, U. Temp, J. Gershenzon, The biosynthesis of benzoic acid glucosinolate esters in *Arabidopsis thaliana*, Phytochemistry 57 (2001) 23–32.
[58] V. Baskar, M.A. Gururani, J.W. Yu, S.W. Park, Engineering glucosinolates in plants: current knowledge and potential uses, Appl. Biochem. Biotechnol. 168 (2012) 1694–1717.

[59] S. Lee, et al., Benzoylation and sinapoylation of glucosinolate R-groups in Arabidopsis, Plant J. 72 (2012) 411–422.
[60] A.V. Qualley, J.R. Widhalm, F. Adebesin, C.M. Kish, N. Dudareva, Completion of the core β-oxidative pathway of benzoic acid biosynthesis in plants, Proc. Natl. Acad. Sci. U.S.A. 109 (2012) 16383–16388.
[61] F. Geu-Flores, C.E. Olsen, B.A. Halkier, Towards engineering glucosinolates into non-cruciferous plants, Planta 229 (2009) 261–270.
[62] M.E. Møldrup, et al., Engineering of benzylglucosinolate in tobacco provides proof-of-concept for dead-end trap crops genetically modified to attract *Plutella xylostella* (diamondback moth), Plant Biotechnol. J. 10 (2012) 435–442.
[63] N. Nesi, R. Delourme, M. Brégeon, C. Falentin, M. Renard, Genetic molecular approaches to improve nutritional value of *Brassica napus* L. seed, C. R. Biol. 331 (2008) 763–771.
[64] W. Wang, B. Vinocur, O. Shoseyov, A. Altman, Role of plant heat-shock proteins and molecular chaperones in the abiotic stress response, Trends Plant Sci. 9 (2004) 244–252.
[65] J.C. Young, J.M. Barral, F. Ulrich Hartl, More than folding: localized functions of cytosolic chaperones, Trends Biochem. Sci. 28 (2003) 541–547.
[66] C. Ma, M. Haslbeck, L. Babujee, O. Jahn, S. Reumann, Identification and characterization of a stress-inducible and a constitutive small heat-shock protein targeted to the matrix of plant peroxisomes, Plant physiol. 141 (2006) 47–60.
[67] H. Chauhan, N. Khurana, A. Nijhavan, J.P. Khurana, P. Khurana, The wheat chloroplastic small heat shock protein (sHSP26) is involved in seed maturation and germination and imparts tolerance to heat stress, Plant Cell Environ. 35 (2012) 1912–1931.
[68] Y. Sato, S. Yokoya, Enhanced tolerance to drought stress in transgenic rice plants overexpressing a small heat-shock protein, sHSP17.7, Plant Cell Rep. 27 (2008) 329–334.
[69] J. Zou, C. Liu, A. Liu, D. Zou, X. Chen, Overexpression of OsHsp17.0 and OsHsp23.7 enhances drought and salt tolerance in rice, J. Plant Physiol. 169 (2012) 628–635.
[70] L.C. Strader, A.H. Culler, J.D. Cohen, B. Bartel, Conversion of endogenous indole-3-butyric acid to indole-3-acetic acid drives cell expansion in Arabidopsis seedlings, Plant Physiol. 153 (2010) 1577–1586.
[71] B.K. Zolman, N. Martinez, A. Millius, A.R. Adham, B. Bartel, Identification and characterization of Arabidopsis indole-3-butyric acid response mutants defective in novel peroxisomal enzymes, Genetics 180 (2008) 237–251.
[72] L.C. Strader, B. Bartel, The Arabidopsis PLEIOTROPIC DRUG RESISTANCE8/ABCG36 ATP binding cassette transporter modulates sensitivity to the auxin precursor indole-3-butyric acid, Plant Cell 21 (2009) 1992–2007.
[73] A.P. Wasson, et al., Traits and selection strategies to improve root systems and water uptake in water-limited wheat crops, J. Exp. Bot. 63 (2012) 3485–3498.
[74] K. Sudesh, H. Abe, Y. Doi, Synthesis, structure and properties of polyhydroxyalkanoates: biological polyesters, Prog. Polym. Sci. 25 (2000) 1503–1555.
[75] Y. Poirier, D.E. Dennis, K. Klomparens, C. Somerville, Polyhydroxybutyrate, a biodegradable thermoplastic, produced in transgenic plants, Science 256 (1992) 520–523.
[76] A. Steinbüchel, et al., Considerations on the structure and biochemistry of bacterial polyhydroxyalkanoic acid inclusions, Can. J. Microbiol. 41 (1995) 94–105.
[77] Q. Ren, N. Sierro, M. Kellerhals, B. Kessler, B. Witholt, Properties of engineered poly-3-hydroxyalkanoates produced in recombinant *Escherichia coli* strains, Appl. Environ. Microbiol. 66 (2000) 1311–1320.
[78] Y. Poirier, Polyhydroxyalknoate synthesis in plants as a tool for biotechnology and basic studies of lipid metabolism, Prog. Lipid Res. 41 (2002) 131–155.
[79] A. Steinbüchel, S. Hein, in: W. Babel, A. Steinbüchel (Eds.), Biopolyesters, vol. 71, Springer, Berlin, Heidelberg, 2001, pp. 81–123.
[80] Y. Poirier, N. Erard, J. MacDonald-Comber Petetot, Synthesis of polyhydroxyalkanoate in the peroxisome of *Pichia pastoris*, FEMS Microbiol. Lett. 207 (2002) 97–102.
[81] K. Kocharin, Y. Chen, V. Siewers, J. Nielsen, Engineering of acetyl-CoA metabolism for the improved production of polyhydroxybutyrate in *Saccharomyces cerevisiae*, AMB Express 2 (2012) 52.
[82] Y. Poirier, Polyhydroxyalkanoate synthesis in plants as a tool for biotechnology and basic studies of lipid metabolism, Prog. Lipid Res. 41 (2002) 131–155.
[83] K. Tilbrook, L. Gebbie, P.M. Schenk, Y. Poirier, S.M. Brumbley, Peroxisomal polyhydroxyalkanoate biosynthesis is a promising strategy for bioplastic production in high biomass crops, Plant Biotechnol. J. 9 (2011) 958–969.
[84] H. Nakashita, et al., Production of biodegradable polyester by a transgenic tobacco, Biosci. Biotechnol. Biochem. 63 (1999) 870–874.
[85] K. Bohmert, et al., Transgenic *Arabidopsis* plants can accumulate polyhydroxybutyrate to up to 4% of their fresh weight, Planta 211 (2000) 841–845.
[86] L.A. Petrasovits, et al., Enhanced polyhydroxybutyrate production in transgenic sugarcane, Plant Biotechnol. J. 10 (2012) 569–578.
[87] Y. Poirier, C. Nawrath, C. Somerville, Production of polyhydroxyalkanoates, a family of biodegradable plastics and elastomers, in bacteria and plants, Biotechnology 13 (1995) 142–150.
[88] Y. Arai, et al., Synthesis of a novel class of polyhydroxyalkanoates in Arabidopsis peroxisomes, and their use in monitoring short-chain-length intermediates of beta-oxidation, Plant Cell Physiol. 43 (2002) 555–562.
[89] J.J. Hahn, A.C. Eschenlauer, U.B. Sleytr, D.A. Somers, F. Srienc, Peroxisomes as sites for synthesis of polyhydroxyalkanoates in transgenic plants, Biotechnol. Prog. 15 (1999) 1053–1057.
[90] V. Mittendorf, et al., Polyhydroxyalkanoate synthesis in transgenic plants as a new tool to study carbon flow through beta-oxidation, Plant J. 20 (1999) 45–55.
[91] V. Mittendorf, et al., Synthesis of medium-chain-length polyhydroxyalkanoates in *Arabidopsis thaliana* using intermediates of peroxisomal fatty acid beta-oxidation, Proc. Natl. Acad. Sci. USA 95 (1998) 13397–13402.
[92] S. Reumann, A.P. Weber, Plant peroxisomes respire in the light: some gaps of the photorespiratory C2 cycle have become filled – others remain, Biochim. Biophys. Acta 1763 (2006) 1496–1510.
[93] V.G. Maurino, C. Peterhansel, Photorespiration: current status and approaches for metabolic engineering, Curr. Opin. Plant Biol. 2010 (2010) 23.
[94] C. Peterhansel, C. Blume, S. Offermann, Photorespiratory bypasses: how can they work? J. Exp. Bot. 64 (2013) 709–715.
[95] A. Maier, et al., Transgenic introduction of a glycolate oxidative cycle into *A. thaliana* chloroplasts leads to growth improvement, Front. Plant Sci. 3 (2012) 38.
[96] R. Kebeish, et al., Chloroplastic photorespiratory bypass increases photosynthesis and biomass production in *Arabidopsis thaliana*, Nat. Biotechnol. 25 (2007) 593–599.
[97] J.d.F.C. Carvalho, et al., An engineered pathway for glyoxylate metabolism in tobacco plants aimed to avoid the release of ammonia in photorespiration, BMC Biotechnol. 11 (2011) 111.
[98] O. Voinnet, S. Rivas, P. Mestre, D. Baulcombe, An enhanced transient expression system in plants based on suppression of gene silencing by the p19 protein of tomato bushy stunt virus, Plant J. 33 (2003) 949–956.
[99] B. Van Aken, Transgenic plants for phytoremediation: helping nature to clean up environmental pollution, Trends Biotechnol. 26 (2008) 225–227.
[100] G.L. Mena-Benitez, et al., Engineering a catabolic pathway in plants for the degradation of 1,2-dichloroethane, Plant Physiol. 147 (2008) 1192–1198.
[101] H.A. Menser, H. He, Ozone and sulfur dioxide synergism—injury to tobacco plants, Science 153 (1966) 424–425.
[102] M. Noji, et al., Cysteine synthase overexpression in tobacco confers tolerance to sulfur-containing environmental pollutants, Plant Physiol. 126 (2001) 973–980.
[103] T. van der Kooij, L.J. DeKok, S. Haneklaus, E. Schnug, Uptake and metabolism of sulphur dioxide by *Arabidopsis thaliana*, New Phytol. 135 (1997) 101–107.
[104] S. Veljovic-Jovanovic, L. Milovanovic, T. Oniki, U. Takahama, Inhibition of catalase by sulfite and oxidation of sulfite by H_2O_2 cooperating with ascorbic acid, Free Radic. Res. 31 (Suppl) (1999) S51–S57.
[105] G. Brychkova, et al., Sulfite oxidase protects plants against sulfur dioxide toxicity, Plant J. 50 (2007) 696–709.
[106] Z. Xia, et al., Overexpression of a maize sulfite oxidase gene in tobacco enhances tolerance to sulfite stress via sulfite oxidation and CAT-mediated H_2O_2 scavenging, PLoS ONE 7 (2012) e37383.
[107] D. Igarashi, et al., Identification of photorespiratory glutamate:glyoxylate aminotransferase (GGAT) gene in Arabidopsis, Plant J. 33 (2003) 975–987.
[108] B.K. Zolman, A. Yoder, B. Bartel, Genetic analysis of indole-3-butyric acid responses in *Arabidopsis thaliana* reveals four mutant classes, Genetics 156 (2000) 1323–1337.
[109] T.B. Dansen, K.W. Wirtz, R.J. Wanders, E.H. Pap, Peroxisomes in human fibroblasts have a basic pH, Nat. Cell Biol. 2 (2000) 51–53.
[110] A. Jankowski, et al., In situ measurements of the pH of mammalian peroxisomes using the fluorescent protein pHluorin, J. Biol. Chem. 276 (2001) 48748–48753.
[111] F.M. Lasorsa, et al., The yeast peroxisomal adenine nucleotide transporter: characterization of two transport modes and involvement in deltapH formation across peroxisomal membranes, Biochem J. 381 (2004) 581–585.
[112] C.W. van Roermund, et al., The peroxisomal lumen in *Saccharomyces cerevisiae* is alkaline, J Cell Sci. 117 (2004) 4231–4237.
[113] T. Lanyon-Hogg, S.L. Warriner, A. Baker, Getting a camel through the eye of a needle: the import of folded proteins by peroxisomes, Biol. Cell 102 (2010) 245–263.
[114] Y. Arai, M. Hayashi, M. Nishimura, Proteomic identification and characterization of a novel peroxisomal adenine nucleotide transporter supplying ATP for fatty acid beta-oxidation in soybean and Arabidopsis, Plant Cell 20 (2008) 3227–3240.
[115] K. Bernhardt, S. Wilkinson, A.P.M. Weber, N. Linka, A peroxisomal carrier delivers NAD(+) and contributes to optimal fatty acid degradation during storage oil mobilization, Plant J. 69 (2012) 1–13.
[116] N. Linka, et al., Peroxisomal ATP import is essential for seedling development in *Arabidopsis thaliana*, Plant Cell 20 (2008) 3241–3257.
[117] S. Reumann, Toward a definition of the complete proteome of plant peroxisomes: Where experimental proteomics must be complemented by bioinformatics, Proteomics 11 (2011) 1764–1779.
[118] N. Linka, C. Esser, Transport proteins regulate the flux of metabolites and cofactors across the membrane of plant peroxisomes, Front. Plant Sci. 3 (2012) 3.
[119] S. Footitt, et al., Control of germination and lipid mobilization by COMATOSE, the Arabidopsis homologue of human ALDP, EMBO J. 21 (2002) 2912–2922.

[120] M. Hayashi, et al., Ped3p is a peroxisomal ATP-binding cassette transporter that might supply substrates for fatty acid beta-oxidation, Plant Cell Physiol. 43 (2002) 1–11.
[121] R. Radakovits, R.E. Jinkerson, A. Darzins, M.C. Posewitz, Genetic engineering of algae for enhanced biofuel production, Eukaryot. Cell 9 (2010) 486–501.
[122] C.M. Sagt, et al., Peroxicretion: a novel secretion pathway in the eukaryotic cell, BMC Biotechnol. 9 (2009) 48.
[123] P. Tanner, V. Balasubramanian, C.G. Palivan, Aiding nature's organelles: artificial peroxisomes play their role, Nano Lett. (2013), http://dx.doi.org/10.1021/nl401215n.

AUTHOR CONTRIBUTIONS

Martin G. Schroers, Sarah K. Kessel-Vigelius, Jan Wiese, and Thomas J. Wrobel wrote the manuscript as co-authors with equal contribution. Nicole Linka assisted in drafting and submitting this manuscript. Florian Hahn assisted with figure layouts.

VII. Acknowledgements

Ich danke von Herzen:

PD Dr. Nicole Linka für die hervorragende Betreuung während der Promotionszeit. Du standest mir immer mit Rat und Tat zur Seite ohne dabei einengend zu werden. Unvergessen sind auch die tollen privaten Abende mit der Peroxisomengruppe bei Dir zu Hause oder unterwegs. Bleib wie Du bist!

Prof. Dr. Andreas Weber für die Möglichkeit zur Promotion in seinem Institut. Sie haben mich stets unterstützt und mir mit Anregungen weiter geholfen.

Apl. Prof. Dr. Peter Jahns für die Übernahme des Korreferats.

Dr. Carlo van Roermund für eine gelungene Kooperation und stets unterhaltsame gemeinsame Arbeit im Labor.

Meinem ehemaligen Tischnachbarn im „Schlauch“, **Dr. Jan Wiese,** für die tolle Zeit, besonders bei der gemeinsamen Arbeit an *Manuscript 3*, sowie für die Unterstützung beim Schreiben dieser Dissertation – sei es durch Anregungen oder Korrekturlesen.

Dr. Kristin Bernhardt dafür, dass Du jede noch so nervige Frage zu deinem *alten* Projekt bei der Übergabe und in den drei darauf folgenden Jahren stets beantwortet hast.

Sarah Keßel-Vigelius, **Jan Wiese**, **Christian Bordych**, **Manuel Sommer**, **Thea Pick**, **Dominik Brilhaus**, **Nadine Hocken**, **Ali Denton**, **Simon Schliesky**, **Canan Külahoglu**, **Thomas Wrobel**, **Sam Kurz**, **Lisa Leson**, **Florian Hahn**, **Fabio Facchinelli**, **Lennart Charton**, **Angelo Agossou Yao**, **Fabian Brandenburg** und **Nils Jaspert** für die tolle Zeit und die spaßigen Pausen. Ihr wart super Kollegen und ich werde Euch vermissen!

Den aktuellen und ehemaligen Mitgliedern **der Peroxisomengruppe** für tolle Zeiten – sei es auf der Arbeit oder privat.

Dem **Weberlab** für eine schöne Zeit. Ihr seid die Besten.

Allen, die an meinen Manuskripten beteiligt waren und jenen, die ich an dieser Stelle vergessen habe.

Natascha Schroers, die mich als Freundin, Verlobte und Frau mit viel Unterstützung und Verständnis durch Studium und Promotion begleitet hat.

Meinen Eltern, meiner Familie und meinen Schwiegereltern für die Unterstützung während des Studiums und der Promotion.

Der **Deutschen Forschungsgemeinschaft** für die Finanzierung dieser Arbeit und **Nicole Linka** für den fairen Umgang mit den bewilligten Mitteln.